THE QUARK BAG MODEL

P. HASENFRATZ and J. KUTI

Central Research Institute for Physics, 1525 Budapest, p.f. 49, Hungary

NORTH-HOLLAND PUBLISHING COMPANY - AMSTERDAM

PHYSICS REPORTS (Section C of Physics Letters) 40, No. 2 (1978) 75–179. NORTH-HOLLAND PUBLISHING COMPANY

THE QUARK BAG MODEL

Peter HASENFRATZ and Julius KUTI

Central Research Institute for Physics, 1525 Budapest, p.f. 49, Hungary

Received 6 May 1977

Contents:

Abstract:

The quark bag model is reviewed here with particular emphasis on spectroscopic applications and the discussion of exotic objects as baryonium, gluonium, and the quark phase of matter. The physical vacuum is pictured in the model as a two-phase medium. In normal phase of the vacuum, outside hadrons, the propagation of quark and gluon fields is forbidden. When small bubbles in a second phase are created in the medium of the normal phase with a characteristic size of one fermi, the hadron constituent fields may propagate inside the bubbles in normal manner. The bubble (bag) is stabilized against the pressure of the confined hadron constituent fields by vacuum pressure and surface tension. Inside the bag the colored quarks and gluons are governed by the equations of quantum chromodynamics.

1. Introduction

The purpose of the present paper is to discuss recent work on the quark bag model and its applications to hadron spectroscopy and some high-energy phenomena.

It has become widely accepted that hadrons are composite objects with fractionally charged quark constituents. Hadron spectroscopy may be explained then in terms of the excitations of valence quarks inside composite hadrons. Perhaps even more strikingly, under powerful electron and neutrino microscopes, the elementary quark degrees of freedom (quark-partons) have been resolved in deep inelastic lepton–nucleon scattering.

Nevertheless, quarks as ordinary elementary particles have never been isolated from composite hadrons. This negative experimental result motivates the idea of quark confinement and accordingly, quarks are assumed to be permanently bound inside strongly interacting particles.

The final microscopic theory for describing this strange situation in hadron physics is not known yet. The quark bag model is a recent attempt to approach the problem of quark confinement from the phenomenological side.

1.1. The quark bag model

Motivated by recent field theoretical investigations we shall assume that the physical vacuum is characterized by some microscopic structure which in "normal phase", outside hadrons, cannot support the propagation of quark and gluon fields. The vacuum acts like a strange medium against hadronic constituent fields, though Lorentz invariance will be maintained.

Now, by concentration of energy, a small domain of a different phase may be created in the "medium" of the physical vacuum. It is like boiling the vacuum and creating small bubbles with a characteristic size of one fermi. Inside the bubble (the hadron phase) quark and gluon fields can propagate in the ordinary manner.

We picture the hadron then as a small domain in the new phase with quark and gluon constituents. This is the bag. The boundary surface of the bag between the two phases is impermeable against the vector gluon fields, so that they cannot penetrate into the "normal phase" of the vacuum (see fig. 1.1).

The impermeability of the surface is expressed in the form of boundary conditions for the gluon fields. The gluon electric fields $\boldsymbol{E}_i$ ($i = 1, 2 \ldots, 8$) in an octet of eight colors are tangential whereas the gluon induction fields $\boldsymbol{B}_i$ are normal to the surface in the instantaneous rest frame of the surface element. As a consequence, there is no gluon field energy or momentum flux through the surface.

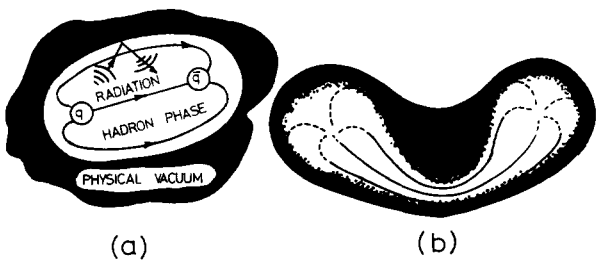

Fig. 1.1. The two different phases of the vacuum are separated in (a) by the boundary of the bag in hadron phase. The gluon radiation emitted by a moving quark is totally reflected on the bag surface and the color electric flux lines are confined to the hadron phase when the bag tries to fission into color non-singlet parts in (b).

The dynamics of the quark and gluon fields inside the bag is governed locally by the field equations of quantum chromodynamics (q.c.d.). This is why we introduced eight gluon fields in the explicitly gauge invariant boundary conditions. Gluons are confined inside the hadron phase and quarks become also confined, as we shall see, because of the gluon gauge fields they always drag along.

Now we come to the important point why the bag being embedded in the physical vacuum as a small droplet of hadron phase is stable in its time evolution. We assume that to create a vacuum bubble in hadron phase takes an amount of energy B per unit volume, and an amount of energy σ per unit surface. B may be associated with the vacuum pressure exerted on the bubble: the energy required to increase the volume of the bubble by an amount δV is $B\delta V$. The surface tension σ is associated with the surface energy on the boundary between the hadron phase and the "normal" vacuum phase.

The pressure exerted by the gluon fields on the boundary of the hadron is balanced out by the volume energy B per unit volume (vacuum pressure) and surface energy σ per unit surface.

The quark bag model is the invention of the ingenious M.I.T. group who have introduced volume tension (or vacuum pressure) to stabilize hadrons. The surface energy σ per unit surface was introduced by the Budapest group upon dynamical and physical considerations.

It is important to note that a closed hadron domain in space is always colorless in the terminology of quantum chromodynamics. This follows from the boundary conditions and accordingly, the color electric flux of the gluon fields is always zero across the surface. As a consequence, the triality quantum number of a closed hadron domain is always zero in the quark bag model.

The boundary of the bag is transparent against leptons and the mediators of the electromagnetic and weak interactions. These particles (or fields) can propagate in both phases of the vacuum in the normal manner. The two-phase picture of the vacuum in the bag model is a strong interaction phenomenon.

We do not attempt to derive σ or B from some microscopic structure of the physical vacuum in gauge theories, though it did not escape our attention that the above discussed physical picture may be related to instantons in q.c.d., or to other vacuum phenomena.

For illustration, we shall briefly discuss a simple field theoretical model in the spirit of the quark bag theory.

1.2. Soft bag in gauge field theory

The Lagrangian of 't Hooft, and Kogut and Susskind which we shall study is not renormalizable, though it deviates from a renormalizable one only for small values of some field with the dimension of mass. Therefore, the deviation from a renormalizable theory occurs only in the infra-red region.

The Lagrangian is an effective one in the sense that higher order quantum corrections from massless gluons in quantum chromodynamics may give rise effectively to similar modifications.

We shall forget about the non-Abelian character of q.c.d. and simplify the calculations with an effective Abelian gauge field. The charged particles in their coupling to the gauge field will be represented by an external source function $J_\mu(x)$. Let us consider first the Lagrangian

$$\mathscr{L}(x) = -\tfrac{1}{4} Z F_{\mu\nu}(x) F^{\mu\nu}(x) - J_\mu(x) A^\mu(x),$$

where

$$F_{\mu\nu} = \partial_\mu A_\nu - \partial_\nu A_\mu.$$

Our metric throughout the paper is $(+---)$. We set $\hbar = c = 1$ everywhere, except when $\hbar$ and c are written out explicitly, for pedagogical purposes.

If Z were a constant as in electrodynamics, one could take it out from the kinetic energy term:

$$A_\mu \longrightarrow Z^{-1/2} A_\mu,$$

$$\mathscr{L} \longrightarrow -\tfrac{1}{4} F_{\mu\nu} F^{\mu\nu} - Z^{-1/2} J_\mu A^\mu.$$

One notes, therefore, that the interaction is proportional to Z^{-1}. We want to describe the so-called infra-red effect that for vanishing momentum transfer, the effective coupling Z^{-1} between the charges becomes infinite. Now if Z were momentum dependent then a non-local Lagrangian would be required.

Instead, Z will be allowed to be some function of an auxiliary scalar field φ with the dimension of a mass. It is required that $Z(\varphi) \to 0$ when $\varphi \to 0$.

The complete Lagrangian is defined then as follows:

$$\mathscr{L}(x) = -\tfrac{1}{4} Z(\varphi) F_{\mu\nu} F^{\mu\nu} + \tfrac{1}{2} \partial_\mu \varphi \partial^\mu \varphi - V(\varphi) - J_\mu A^\mu. \tag{1.1}$$

We shall assume that $V(\varphi) > 0$ when $\varphi \neq 0$, and $V(0) = 0$. For calculations one can take

$$V(\varphi) = \tfrac{1}{2} m^2 \varphi^2 + \lambda \varphi^4.$$

The infra-red effect is incorporated by requiring $Z(\varphi) \to 0$ for $\varphi \to 0$, and $Z(\varphi) \to 1$ for large $|\varphi|$ as it is shown in fig. 1.2.

One notes that the Lagrangian (1.1) is gauge invariant, since $\varphi(x)$ is a neutral scalar field, and only $A_\mu(x)$ is transformed under the gauge transformation $A_\mu(x) \to A_\mu(x) + \partial_\mu \chi(x)$.

We shall study now Coulomb's law in the model. The Lagrangian (1.1) yields the Euler–Lagrange equations

$$\partial^\mu D_{\mu\nu} = J_\nu,$$

where $D_{\mu\nu}$ is the "induction field"

$$D_{\mu\nu} = Z F_{\mu\nu}.$$

The function $Z(\varphi)$ describes the electric and magnetic polarizabilities of the vacuum as a physical medium. This polarizability against the gluon field $A_\mu(x)$ is controlled by the neutral, scalar field $\varphi(x)$. For static field configurations, $Z(\varphi)$ corresponds to the dielectric constant ϵ, and $Z^{-1}(\varphi)$ is associated with the magnetic permeability μ:

$$\epsilon(\varphi) = Z(\varphi), \qquad \mu(\varphi) = Z^{-1}(\varphi). \tag{1.2}$$

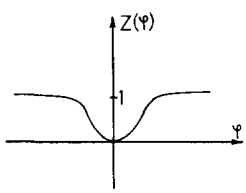

Fig. 1.2. The dielectric constant $Z(\varphi)$ as a function of the auxiliary field φ.

When the charged particles are fixed sources we are interested in the following static solution:

$$J_i = 0, \qquad J_0 = \rho(\boldsymbol{x}),$$
$$D_{ij} = 0, \qquad D_{0i} = D_i, \qquad i, j = 1, 2, 3.$$

The energy density is given by

$$\mathcal{H}(\boldsymbol{x}) = \tfrac{1}{2}\epsilon^{-1}\boldsymbol{D}^2 + \tfrac{1}{2}(\nabla\varphi)^2 + V(\varphi). \tag{1.3}$$

To specify $Z(\varphi)$ at small values of $\varphi(\boldsymbol{x})$ we shall assume that for $\varphi(\boldsymbol{x}) \to 0$, $Z(\varphi) \approx \text{const} \cdot \varphi^4$. The static solution which emerges from a qualitative calculation is shown in fig. 1.3.

An electric vortex develops between two point charges of opposite sign at large distances. The gauge field around the charged point particles drives the scalar field $\varphi(\boldsymbol{x})$ to be non-zero, and it is non-vanishing along the whole electric vortex. Farther away from the vortex configuration $\varphi(\boldsymbol{x})$ drops to zero, and the gauge field vanishes there.

The vacuum may exist in two phases in this model. In the absence of charges the scalar field $\varphi(\boldsymbol{x})$ vanishes and the gauge field cannot penetrate there. This is the gauge field non-supporting "normal phase" of the vacuum. In a domain of space, however, where charged particles are present the gauge field of the particles drives φ to be non-zero and the domain becomes an ordinary polarizable medium. It is the gauge field supporting hadron phase.

The induction field $\boldsymbol{D}$ becomes confined in a vortex tube of definite width and arbitrary length when the distance between the point charges is increasing. This electric vortex is similar to the dual string; the potential energy between the charged particles is proportional to the distance between them:

$$V(r) \approx \text{const} \cdot r.$$

The repulsion of the gluon field from the "normal phase" of the vacuum can be understood as an exercise from electrostatics.

We consider a point charge Q embedded in a semi-infinite dielectric ϵ_1 a distance d away from a plane interface which separates the first medium from another semi-infinite dielectric ϵ_2. The surface is taken as the plane $z = 0$, as shown in fig. 1.4.

The solution of the problem is given by the method of image charges. The electric field $\boldsymbol{E}$ is derivable from a potential ϕ which is given for $z \gtrless 0$ by the formula

$$\phi = \frac{1}{4\pi\epsilon_1}\left(\frac{Q}{R_1} + \frac{Q'}{R_2}\right), \qquad z > 0$$

$$\phi = \frac{1}{4\pi\epsilon_2}\frac{Q''}{R_3}, \qquad z < 0$$

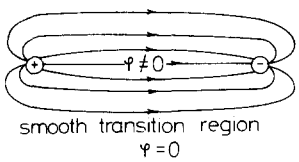

Fig. 1.3. The electric vortex tube connecting opposite charges in 't Hooft's model.

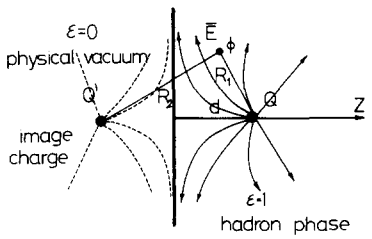

Fig. 1.4. The static electric field of a point charge Q embedded in a semi-infinite dielectric slab.

where the image charge Q' is located at the symmetrical position with respect to Q,

$$Q' = \frac{\epsilon_1 - \epsilon_2}{\epsilon_1 + \epsilon_2} Q,$$

while Q'' is the charge at the position of the physical charge Q as it is seen from the semi-infinite dielectric ϵ_2

$$Q'' = \frac{2\epsilon_2}{\epsilon_1 + \epsilon_2} Q.$$

The semi-infinite slab of dielectric ϵ_1 corresponds in our terminology to the "hadron phase" of the vacuum, if $\epsilon = 1$ is taken, for instance. The semi-infinite slab of dielectric ϵ_2 may be associated with the "normal phase" when $\epsilon_2 \to 0$. In this limit the induction vector $\boldsymbol{D}$ vanishes in the left half-space and it becomes tangential to the surface in the "hadron phase" (fig. 1.4).

Something very similar happens between the two phases in the above discussed field theoretical model. The difference is that the gradient term $(\nabla\varphi)^2$ in (1.3) makes the transition smooth between the two phases and, of course, the shape of the surface is determined dynamically.

There is a similar situation in the presence of magnetic fields. Since the permeability μ of the "normal phase" is infinite according to (1.2), the magnetic field $\boldsymbol{H}$ becomes perpendicular to the surface in the "hadron phase": the boundary condition on the magnetic field $\boldsymbol{H}$ at the surface of a very high-permeability material is the same as for the electric field at the surface of a conductor. Therefore, the magnetic field $\boldsymbol{H}$ cannot penetrate into the "normal phase", similarly to the induction vector in the electrostatic case.

The reflection coefficient R on the surface between the two phases, for electromagnetic waves of the gluon field propagating in the "hadron phase", is given by

$$R = \left(\frac{1 - \epsilon_2}{1 + \epsilon_2}\right)^2, \qquad \epsilon_1 = 1.$$

When $\epsilon_2 \to 0$ there is total reflection on the surface. The gluon field becomes confined to the "hadron phase".

Charged point particles are also confined to the "hadron phase" because of the gluon gauge field they always drag along.

The field theoretical model which we have presented here describes a soft bag with smeared boundary surface between the two phases of the vacuum. We would get a "hard" bag by neglecting the kinetic term $(\partial_\mu\varphi)^2$ for φ in the Lagrangian (1.1), and requiring $Z(\varphi)$ to be a step function. In that particular limit the boundary becomes sharp as in the phenomenological quark bag model which is the subject-matter of the present paper.

1.3. Gauge field inside the bag and q.c.d.

We shall imagine that there is a bubble in hadron phase moving in the physical vacuum in a Lorentz invariant manner. The bubble is filled with an Abelian gauge field $A_\mu(x)$, for the sake of simplicity.

The relativistic action W for this simple bag is written as

$$W = -\tfrac{1}{4}\int \mathrm{d}t \int_{\text{bag}} \mathrm{d}^3x F_{\mu\nu}F^{\mu\nu} - \sigma \int \mathrm{d}t \int_{\text{surf}} \mathrm{d}^2s \sqrt{1 - V_\mathrm{T}^2} - B \int \mathrm{d}t \int_{\text{bag}} \mathrm{d}^3x, \tag{1.4}$$

where $F_{\mu\nu} = \partial_\mu A_\nu - \partial_\nu A_\mu$. The first double integral in (1.4) is extended over the interior points of the bag, for a given instant of time t. There is no gauge field outside the bag. The second term describes the action for the surface of the bag where d^2S is the infinitesimal surface area and V_T is the velocity of the surface element along the normal vector of the surface at a given point. In other words, the second double integral in (1.4) is the three-dimensional area of the hypersurface swept out by the surface of the bag in Minkowski space–time. The strength of surface tension is set by the constant σ with dimension energy/area, or length^{-3}.

The last term in (1.4) is proportional to the four-dimensional volume swept out by the bag as a whole in Minkowski space–time. For a given instant of time it is proportional to the three-dimensional volume of the bag. The constant B has the dimension of energy/volume, or length^{-4}. This term describes the vacuum pressure against the bubble from the outside.

The action W is Lorentz invariant, since it is defined in a geometrical manner.

Variation of the gauge field inside the bag yields Maxwell's equations in the interior points

$$\partial^\mu F_{\mu\nu} = 0.$$

Variation of $A_\mu(x)$ on the surface gives the boundary conditions for the gauge field

$$\boldsymbol{n} \cdot \boldsymbol{E} = 0, \qquad n_0 \boldsymbol{E} + \boldsymbol{n} \times \boldsymbol{B} = 0, \tag{1.5}$$

where $\boldsymbol{n}$ is the exterior, normal three-vector to the surface at a given point, and n_0 is the velocity of the surface element along $\boldsymbol{n}$. The boundary conditions (1.5) require the gluon $\boldsymbol{E}$-field to be tangential and the $\boldsymbol{B}$-field to be normal to the surface in the instantaneous rest frame of the surface element.

Variation of the surface elements in the action principle $\delta W = 0$ determines the dynamical equation for the time evolution of the bubble's shape:

$$\tfrac{1}{2}(\boldsymbol{E}^2 - \boldsymbol{B}^2)|_s = 2\sigma\kappa + B. \tag{1.6}$$

In eq. (1.6), κ denotes the mean curvature of the surface at a given point in Minkowski space.

κ is a dynamical quantity which measures the curvature of the hypersurface as embedded in the four-dimentional space–time. It contains the transverse velocity and acceleration of the surface element with a forthcoming discussion in the following section.

For a static surface there is great simplification in eq. (1.6):

$$\tfrac{1}{2}(\boldsymbol{E}^2 - \boldsymbol{B}^2)|_s = \sigma(1/R_1 + 1/R_2) + B, \tag{1.7}$$

where $1/R_1$ and $1/R_2$ are the principal curvatures of the surface at a given point.

The static surface is a solution of classical bag dynamics, if fixed external sources are coupled to the gauge field $A_\mu(\boldsymbol{x})$ inside the bag.

Equation (1.7) has a transparent physical interpretation. It describes the balance of forces in equilibrium. The first term on the right-hand side of (1.7) describes the surface tension of the boundary between the two phases like for an air bubble embedded in liquid phase. The second term B acts like vacuum pressure against the bubble. The left-hand side of eq. (1.7) can be interpreted as the gluon "field pressure" on the boundary from the inside of the bag. It is balanced out in equilibrium by surface tension and vacuum pressure. This is the content of eq. (1.7).

The bag without quarks may be pictured as a gluon gas bubble moving in the otherwise undetectable medium of the physical vacuum. There is no qualitative change in the picture when quarks are coupled to the gluon field inside the bag.

The negative sign of the magnetic "field pressure" requires some explanation. The right-hand side

of (1.7) is Lorentz invariant, since it is of geometrical origin. The left-hand side must be also Lorentz invariant as guaranteed by the relation

$$-\tfrac{1}{4} F_{\mu\nu}F^{\mu\nu} = \tfrac{1}{2}(\boldsymbol{E}^2 - \boldsymbol{B}^2),$$

so that the electric field $\boldsymbol{E}^2$ and the magnetic field $\boldsymbol{B}^2$ act with opposite sign on the boundary.

Physically, the repulsive force exerted by the electric field on the walls of the bag can be understood from the simple model of subsection 1.2. There is a polarization surface-charge density on the plane at $z = 0$ between the two semi-infinite slabs as given by

$$\sigma_{\text{pol}} = \frac{Q}{2\pi} \frac{\epsilon_1 - \epsilon_2}{\epsilon_1(\epsilon_2 + \epsilon_2)} \frac{d}{(\rho^2 + d^2)^{3/2}},$$

where ρ is the distance from the origin on the plane $z = 0$. Instead of using the image charges we can describe the fields in terms of the polarization charge density σ_{pol}. When $\epsilon = 1$ and $\epsilon_2 \to 0$, the polarization charge is of the same sign as Q. Therefore the force between the charge and the surface is repulsive.

The situation is the opposite when a magnetic field is created by, say, a magnetic monopole g whose polarization effect will induce a magnetic surface charge density of opposite sign, so that the force between the source of the field and the surface becomes attractive.

The electric induction vector $\boldsymbol{D}$ of charge Q cannot penetrate into the semi-infinite slab of dielectric ϵ_2 because of the shielding effect of the polarization charge on the surface.

The electric field $\boldsymbol{E}$ goes over into dielectric ϵ_2 smoothly and it is non-vanishing there. However, the energy density $\frac{1}{2}\boldsymbol{E} \cdot \boldsymbol{D}$ vanishes in the semi-infinite slab ϵ_2 when $\epsilon_2 \to 0$.

In the bag model we make the outside region completely forbidden for the gauge field A_μ which is not even defined there.

The action W in (1.4) can be easily extended to include non-Abelian gauge fields and colored quarks. This will be done in the forthcoming sections. Apart from the two terms of surface tension σ and vacuum pressure $\boldsymbol{B}$, the action W becomes identical to that of q.c.d. in the interior points of the bag.

Quantum chromodynamics became popular among many theorists for the following reasons:

(1) it explains scaling in deep inelastic lepton–nucleon scattering in terms of asymptotic freedom;

(2) it allows for a spatially symmetric ground state of the nucleon in the terminology of the static quark model;

(3) it gives a total cross section of electron–positron annihilation into hadrons which is three times larger than without color, in approximate agreement with the data;

(4) there is a hope that only color singlet states are observable in the theory with a possible explanation for quark confinement.

The last point is only a conjecture and there are serious doubts about its validity.

The field theoretic model with the effective Lagrangian (1.1) illustrates what we would like to get out from q.c.d. phenomenologically as a physical picture for hadrons.

There is now more direct indication that the structure of the physical vacuum in a gauge theory as q.c.d. may play an important role. The so-called pseudoparticles, or instantons, may be responsible for the structure of the vacuum in close relation to the problem of quark confinement.

The vacuum in the presence of pseudoparticles acts like a shielding plasma for electric flux lines in a $2+1$ dimensional gauge model. This shielding effect generates the confinement force between quarks in the model. The implications of instantons on hadron structure are being intensively explored in quantum chromodynamics.

There is a hope in q.c.d. that as a result of detailed and ingenious "microscopic" calculations the additional binding terms σ and B turn out to be unnecessary in the action W of eq. (1.4). In that case quantum chromodynamics in itself would be able to bind quarks and gluons inside hadrons.

The quark bag model, on the other hand, is a phenomenological device which may be a reasonable description for hadrons even if the final microscopic theory is quite different from anything what we are guessing today.

We shall bring up an interesting example from the history of nuclear physics which is somewhat analogous to our model-building philosophy of the quark bag model.

1.4. The liquid drop model and single particle spectra

A heavy nucleus is best described in telegraphic style as a bag of nucleons.

In a more sophisticated manner, the close packing of the nucleons in the nucleus and the existence of a relatively sharp nuclear boundary have led to the comparison of the nucleus with a liquid drop. The empirical binding energies can be interpreted then as a sum of surface energy, volume energy, and electrostatic energy of the nuclear droplet. The treatment of the nucleus as a deformable droplet is quite successful in the theory of nuclear fission.

According to the liquid drop model, the fundamental modes of nuclear excitations correspond to collective types of motion, such as surface oscillations and elastic vibrations.

New progress in the theory of nuclear spectra was obtained through the development of the so-called single particle model. This model assumes that nuclear stationary states, like electron configurations in atoms, can be approximately described in terms of the motion of the individual particles in an average field of force.

The single particle model explains the stability of certain nuclei, those which possess closed shells of protons and neutrons. The model is also successful in accounting for the spins of nuclear ground states and nuclear magnetic moments.

The liquid drop model and the single particle model represent opposite approaches to the problem of nuclear structure. Each refers to essential aspects of nuclear structure, and it is expected that a synthesis is necessary for a detailed description of nuclear properties.

The necessity of this synthesis is clearly indicated by the observed behaviour of nuclear quadrupole moments. Though the quadrupole moments of nuclear ground states give definite evidence of the shell structure, for many nuclei, the magnitude of the quadrupole moments is too large in comparison with the predictions of the single particle model. This suggests that the equilibrium shape of those nuclei deviates from spherical symmetry.

A simple explanation arises if one considers the motion of the individual particles in a deformable nucleus. The centrifugal pressure exerted by the particles on the walls of the nucleus may lead to a considerable deformation. The quadrupole moments associated with those deformations are in accordance with observations.

An instructive scheme to demonstrate this idea is that where the nuclear energy levels are treated as due to a filling-up of individual particle levels for nucleons in a spherical box with infinite walls. It is assumed here that the strong interaction of each nucleon with all other nucleons in the nucleus can be approximated as a roughly constant interaction potential over the nuclear volume so that the nucleons form a "self-consistent" box (or bag).

This bag is deformable, and there are dynamical degrees of freedom associated with the surface deformations. When an even number of protons or neutrons are present they pair off to give zero spin

and moments. We shall assume that for closed shell nuclei the nucleus is treated as an incompressible droplet of constant density μ and only the surface and Coulomb energy terms are considered.

For odd A nuclei great success is obtained by associating the spin and moments of the nucleus with the odd valence nucleon alone, outside the core. The valence nucleon is coupled to the core through the collective variables of the droplet. This coupling arises from the boundary condition for the valence nucleon's wave function at the surface of the nucleus.

The description of odd A nuclei in terms of the dynamical variables of the valence nucleons outside the core, together with the collective variables of the nuclear droplet may be called the bag model of the nucleus, in our terminology. The model is quite successful in describing the single particle excitation spectra of odd A nuclei.

The analogy with the quark bag model is almost self-explanatory. The valence quarks of hadrons are similar to the valence nucleons of nuclei, and the dynamical variables of the bag (hadron droplet) are analogous to the collective variables of the nuclear droplet. The volume energy of the nucleus is like the volume energy BV of the bag.

In both models, the surface energy is an essential part of the droplet's dynamics.

Let the surface of the nucleus in polar coordinates be given by $\rho(\vartheta, \varphi)$. We expand ρ in spherical harmonics writing

$$\rho(\vartheta, \varphi) = \rho_0\Big(1 + \sum_{l,m} \rho_{lm} Y_{lm}(\vartheta, \varphi)\Big), \tag{1.8}$$

where ρ_0 is the radius of the nucleus in its original equilibrium shape for spherically symmetric closed shell nuclei. The function Y_{lm} is the normalized spherical harmonic of the order l, m. The expansion parameters ρ_{lm} are the coordinates which describe the deformation of the nuclear surface.

The idea of a continu us surface does not apply if we consider surface elements of linear dimensions comparable with the distance between the nucleons. The quantities ρ_{lm} therefore lose their meaning if l becomes of the order of, or larger than, $A^{1/3}$.

This remark is relevant perhaps when we deal with the quantum fluctuations of the hadron droplet in the quark bag model. Since the bag is a phenomenological model to some unknown microscopic dynamics, there is a hope that a physical cut-off is provided by the microscopic structure for short wave-length fluctuations of the surface. We may feel released therefore from the burden of including an infinite set of collective bag coordinates in practical considerations.

If the coefficients ρ_{lm} are small in (1.8), the potential energy of the deformations takes the form

$$V = \tfrac{1}{2} \sum_{l,m} c_l \rho^*_{lm} \rho_{lm}. \tag{1.9}$$

The associated kinetic energy is given by

$$K = \tfrac{1}{2} \sum_{l,m} B_l \dot{\rho}^*_{lm} \dot{\rho}_{lm}. \tag{1.10}$$

For an incompressible nucleus of constant density μ, one finds

$$B_l = \mu \rho_0^5 / l, \tag{1.11}$$

assuming nuclear matter to have irrotational flow. If the charge of the nucleus $Z \cdot e$ is uniformly distributed over its volume, one obtains

$$c_l = (l-1)(l+2)\rho_0^2 \sigma - \frac{3}{2\pi} \frac{l-1}{2l+1} \frac{Z^2 e^2}{\rho_0}, \tag{1.12}$$

where σ is the surface tension. As an approximate estimate of σ we may use the average value

$$4\pi\rho_0^2\sigma = 15.4A^{2/3}\,\text{MeV} \tag{1.13}$$

deduced from nuclear binding energies.

The surface dynamics is determined by eqs. (1.9–1.12). The Hamiltonian of the nuclear surface takes the form

$$H_{\text{surf}} = K + V = \sum_{l,m}\left\{\frac{1}{2B_l}\Pi_{lm}^*\Pi_{lm} + \tfrac{1}{2}c_l\rho_{lm}^*\rho_{lm}\right\}, \tag{1.14}$$

where Π_{lm} is the momentum conjugate to ρ_{lm}. The surface oscillations may thus be considered as a system of harmonic oscillators with frequencies

$$\omega_l = \sqrt{c_l/B_l}, \tag{1.15}$$

and mass coefficients B_l.

It is clear from eq. (1.8) and eq. (1.10) that only internal motions of the surface transverse to its extension in space are dynamical. That is, the kinetic energy K depends only on the transverse velocities of the surface elements. The longitudinal expansion or shrinkage of the surface is also physical but it is somehow associated with "potential energy" and not kinetic energy.

There is a similar situation in the surface dynamics of the bag model formulated in a relativistic manner.

For spheroidal deformations the surface and Coulomb energy terms of the nucleus partly cancel and give an increased energy proportional to ϵ^2 on distortion from the spherical shape, where $\epsilon = (b-a)/\rho_0$ (a and b are the semi-axes of the ellipsoid) is proportional to the distortion

$$\Delta E_{\text{surf}} + \Delta E_{\text{Cb}} = \epsilon^2(2.74A^{2/3} - 0.054Z^2A^{-1/3}). \tag{1.16}$$

The energy levels of the spheroidal bag can be specified by the same notation as for the spherical box. The degeneracy of eigenvalues with respect to m for a given value of l is removed and there is a splitting which is linear in ϵ and depends on l and m^2. Distortion to oblate disk shape lowers the kinetic energy for $|m| \approx l$ and increases it for $m^2 \ll l^2$. One notes that l is not a strict angular momentum quantum number in this problem.

The expected effect of these considerations on the nuclear shape is that for closed shells $\Delta E \approx \text{const}\cdot\epsilon^2$, so $\epsilon = 0$ is most stable. Secondly, for a valence nucleon outside a closed shell, $\Delta E \approx c_1\epsilon^2 - c_2\epsilon$ if ϵ is chosen positive for the oblate case. Then $\epsilon = c_2/2c_1$ gives the stable shape for minimum energy.

The linear term can be easily understood by noting that the kinetic energy $K = E - V$ is proportional to $\hbar^2/M\rho_0^2$ and, for a Bohr orbit with $m = l$, the particle goes around the equator. Therefore ρ_0 is replaced by $b > \rho_0$ and one finds $\Delta K = -\frac{2}{3}\epsilon K_0$ for ab^2 fixed and $m = l \gg 1$. This asymptotic result for large l works quite well down to $l = 4$.

Similarly to these nuclear deformations we expect cigar-like bag shapes for high angular momentum excitations of hadrons.

Since the nucleons cannot penetrate through the nuclear potential wall, a coupling arises between the particles and the surface. This coupling between the single particle motion and the nuclear deformation gives rise to a certain sharing of angular momentum between the particle and the surface (see fig. 1.5).

The angular momentum structure of the stationary states may therefore deviate essentially from the case of the pure single particle model. While the latter model may be called quasi-atomic model,

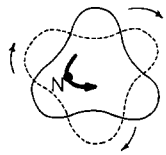

Fig. 1.5. The schematic picture of a nucleus whose core is described by the collective variables of an incompressible liquid droplet in octuple excitation. The odd valence nucleon's motion is coupled to the octuple surface vibration. The arrows indicate that the vibration of the surface carries angular momentum.

the combined "bag model" is somewhat analogous to molecular structures, where there is an interaction between electronic and nuclear motion.

This "bag model" for the nucleus is a clever phenomenological device which describes the main features of nuclear spectra for odd A nuclei without being involved in the microscopic dynamics of A protons and neutrons. The microscopic dynamics is ultimately governed by complicated forces between protons and neutrons.

In the next section we shall review the first extended particle model of the geometrical variety. It proves to be a most useful introduction to quark bag dynamics.

2. Dirac's electron bag model

In 1962 Dirac made a proposal for an extended electron model. He was mainly motivated by the existence of the muon. The muon was interpreted in his model as the first radial excitation of the electron at the bottom of an excitation spectrum for extended leptons.

As far as we know Dirac's Lagrangian model was the first one to describe extended objects in four-dimensional relativistic picture abandoning conventional non-linear field theory.

It is instructive to see how the electron gets stabilized by a tension type force in the Dirac model, as a useful introduction to the bag model of quark confinement.

The concept of an electron of finite size is an old one, first proposed by Abraham and Lorentz. Dirac has introduced special Poincaré stresses to stabilize the extended Abraham–Lorentz electron in a fully relativistic manner.

The electron is assumed to have a charged conducting surface. Outside the surface Maxwell's equations hold. Inside the surface there is no field. The electron is stabilized against the Coulomb repulsion of its surface charge by a non-Maxwellian force of the type of surface tension, or Poincaré stresses. It may be pictured as a bubble in the electromagnetic field whose energy expression, in addition to the electromagnetic field energy, contains a positive term proportional to the surface of the particle.

Dirac's bubble may be called the bag model of the electron, though this bag is empty inside. The picture is just opposite to what we advocated for hadrons: the gauge field is "confined" to the exterior of the electron bag.

2.1. The action principle

In a four-dimensional relativistic picture the surface of the extended electron appears as a tube with a three-dimensional hypersurface. The action W is written as

$$W = W_0 + W_s,$$

where

$$W_0 = -\frac{1}{4} \int_{x^1>1} J g^{\mu\rho} g^{\nu\sigma} F_{\mu\nu} F_{\rho\sigma} \, \mathrm{d}^4 x \tag{2.1}$$

is a four-dimensional integral extended over the Minkowski space–time outside the tube.

We shall work with general curvilinear coordinates x^μ. The surface of the extended electron is described by $x^1 = 1$ in the curvilinear coordinate system, though any other specification would be allowed.

For reference, we introduce a rectilinear and orthogonal system $y^\Lambda(x)$. The functions $y^\Lambda(x)$ describe the x coordinate system in terms of the y coordinate system, with the metric

$$g_{\mu\nu} = y_{\Lambda,\mu} y^{\Lambda}_{,\nu}$$

in the x system. $y_{\Lambda,\mu}$ denotes $\partial y_\Lambda / \partial x^\mu$ and Greek capital suffixes will always refer to the y coordinate system. J^2 is the determinant of $-g_{\mu\nu}$ in eq. (2.1).

We take now as general coordinates of the extended particle the gauge field potential $A_\mu(x)$, and $y^\Lambda(x)$ for all values of x^μ with $x^1 \geqslant 1$. No general coordinates are associated with the interior points of the bubble.

The general coordinates together with the fixed function $x^1 = 1$ determine the surface of the electron, and the electromagnetic field relative to the y system. A physically unimportant curvilinear system of coordinates outside the electron's surface is also determined by the general coordinates.

The action for the surface is written as

$$W_s = -\sigma \int_{x^1=1} M \, \mathrm{d}x^0 \, \mathrm{d}x^2 \, \mathrm{d}x^3, \tag{2.2}$$

where M^2 is the determinant of g_{ab} (a, b take on the values of 0, 2, 3 here, and later on). W_s is proportional to the three-dimensional area of the tube swept out by the surface through its motion in Minkowski space–time.

The strength of surface tension, and therefore the equilibrium size and mass of the electron, is determined by the positive constant σ of dimension energy/area, or length^{-3}.

We have to stress here the importance of the curvilinear coordinate system x^μ. In rectilinear and orthogonal coordinates y^Λ the action for the electromagnetic field,

$$W_0 = -\tfrac{1}{4} \int_{\text{outside}} \mathrm{d}^4 y F_{\Lambda\Lambda'} F^{\Lambda\Lambda'},$$

and the action for the surface,

$$W_s = -\sigma \int_{\text{surf}} \mathrm{d}^3 S(y)$$

are not appropriate for deriving the Euler–Lagrange equations of motion.

Namely, to have a correct action principle, we must express the action W in terms of variables q which describe the physical system for all space and time under the condition that, when small variations are performed in all the q's, δW is a linear function of the δq's.

To describe the surface of the tube, one may introduce parameters u_1, u_2, u_3 to specify a general point on it and then the four coordinates $y^\Lambda(u)$ of the point are taken as the variables q for the surface. The four-potential $A_\Lambda(y)$ throughout space–time outside the surface is also taken as general coordinate q. However, δW is not a linear function of the variations δq's.

If one makes a variation $\delta y^\Lambda(u)$ describing the surface being pulled out infinitesimally, δW will not be minus the δW for $-\delta y^\Lambda(u)$, corresponding to the surface being pushed in infinitesimally, since the field inside the surface is kept zero identically. The other problem with the coordinates y is that the dynamical variables $A_\Lambda(y)$ defined only when y is outside the surface require a time-dependent definition for a moving surface making the canonical formalism impossible.

The difficulties can be circumvented by working in an appropriate curvilinear coordinate system as introduced above.

In the variational process we do not change the equation $x^1 = 1$ for the surface. An arbitrary variation of the electron's surface comes from varying the coordinate system:

$$y^\Lambda(x) \to y^\Lambda(x) + \delta y^\Lambda(x).$$

After an arbitrary variation $\delta A_\mu(x)$, $\delta y^\Lambda(x)$ we find

$$\begin{aligned}\delta W = &- \int_{x^1>1} \{(JF^{\rho\sigma})_{,\sigma}\delta A_\rho + [J(F_\mu{}^\alpha F^{\mu\beta} - \tfrac{1}{4}F_{\mu\nu}F^{\mu\nu}g^{\alpha\beta})y_{\Lambda,\alpha}]_{,\beta}\delta y^\Lambda\}\,\mathrm{d}^4x \\ &- \int_{x^1=1} JF^{\rho 1}\delta A_\rho\,\mathrm{d}x^0\,\mathrm{d}x^2\,\mathrm{d}x^3 \\ &- \int_{x^1=1} \{J(F_\mu{}^\alpha F^{\mu 1} - \tfrac{1}{4}F_{\mu\nu}F^{\mu\nu}g^{\alpha 1})y_{\Lambda,\alpha} - \sigma(Mc^{ab}y_{\Lambda,a})_{,b}\}\delta y^\Lambda\,\mathrm{d}x^0\,\mathrm{d}x^2\,\mathrm{d}x^3, \qquad (2.3)\end{aligned}$$

where c^{ab} is the reciprocal matrix to g_{ab}.

From the first line of eq. (2.3) we get the Maxwell equations in curvilinear coordinates

$$(JF^{\mu\nu})_{,\nu} = 0. \qquad (2.4)$$

The second term in square bracket in the first line of eq. (2.3) vanishes as a consequence of the Maxwell equations (2.4). This is expected, since there is no Euler–Lagrange equation describing the arbitrary motion of the curvilinear system of coordinates outside the electron's surface.

Dirac requires $A_\mu(x) = 0$ on the surface of the electron and this constraint is preserved during the variational process. Therefore, the second line of eq. (2.3) vanishes automatically. The constraint $A_\mu(x) = 0$ for the gauge field on the surface implies the relation $F_{ab} = 0$ which can be written in a covariant manner:

$$n_\mu \tilde{F}^{\mu\nu} = 0, \qquad (2.5)$$

where n_μ is a unit normal to the surface $f(x) = 1$,

$$n_\mu = -f_{,\mu}(-g^{\rho\tau}f_{,\rho}f_{,\tau})^{-1/2}.$$

In our case $f(x) = x^1$ and n_μ takes the form

$$n_\mu = -\frac{1}{\sqrt{-g^{11}}}(0, 1, 0, 0).$$

To establish a convention we choose $\boldsymbol{n}$ to be the exterior normal to the surface.

The dual field strength tensor $\tilde{F}_{\mu\nu} = \frac{1}{2}\epsilon_{\mu\nu\rho\sigma}F^{\rho\sigma}$ appears in eq. (2.5). Written out in the y coordinate system

$$\boldsymbol{n} \cdot \boldsymbol{B} = 0,$$

and (2.6)

$$\boldsymbol{n} \times \boldsymbol{E} - n_0 \boldsymbol{B} = 0, \qquad \text{at } x^1 = 1,$$

where $\boldsymbol{n}$ is the three-dimensional normal vector to the surface at a given point and n_0 is the velocity of the surface element along $\boldsymbol{n}$.

The boundary conditions in eq. (2.6) are the familiar ones for a conducting surface, namely, the tangential components of the electric field and the normal component of the magnetic field are zero in the instantaneous rest frame of the surface element.

The third line of eq. (2.3) gives the equation of motion for the surface of the extended electron

$$-\tfrac{1}{4}F_{\mu\nu}F^{\mu\nu} = \sigma J^{-1}\,(Mg^{1\mu}/g^{11})_{,\mu}, \qquad \text{for } x^1 = 1, \tag{2.7}$$

or in covariant notation

$$-\tfrac{1}{4}F_{\mu\nu}F^{\mu\nu} = -\sigma J^{-1}(Jn^{\mu})_{,\mu}. \tag{2.8}$$

Apart from a factor 2σ the right-hand side of eq. (2.8) is the mean curvature of the electron's hypersurface in Minkowski space. This is not unexpected, since the electron's hypersurface in space–time without coupling to the electromagnetic field would correspond to a minimal surface as a consequence of the geometrical action W_s. The mean curvature vanishes in each point of a minimal surface.

2.2. The spectrum of radial vibrations

As we have discussed previously the motion of the external points in the curvilinear coordinate system is not physical, which is reflected in a certain "gauge" freedom in choosing the mapping $y^{\wedge}(x)$. We shall choose a "Coulomb-type gauge", that is a mapping which is described by the physically important surface variables only.

For a spherically symmetric electron whose centre is at rest $\rho(t)$ designates the radius of the surface. In curvilinear polar coordinates

$$\begin{aligned} y^0 &= x^0 (= t), \\ y^1 &= x^1 \rho(t) \sin x^2 \cos x^3, \\ y^2 &= x^1 \rho(t) \sin x^2 \sin x^3, \\ y^3 &= x^1 \rho(t) \cos x^2, \end{aligned}$$

where the polar angles ϑ and φ are identified with x^2 and x^3, respectively. The mean curvature of the vibrating surface is given then by the following expression

$$\frac{1}{2}J^{-1}\left(\frac{Mg^{1\mu}}{g^{11}}\right)_{,\mu} = \frac{1}{2}\frac{\mathrm{d}}{\mathrm{d}t}\frac{\dot{\rho}}{(1-\dot{\rho}^2)^{1/2}} + \frac{1}{\rho(1-\dot{\rho}^2)^{1/2}}. \tag{2.9}$$

Since there is no electric monopole radiation in Maxwell's theory, outside the surface the

electromagnetic field is simply the static Coulomb field of a sphere with radius $\rho(t)$. Then the relation

$$-\tfrac{1}{4}F_{\mu\nu}F^{\mu\nu} = \frac{\alpha}{8\pi\rho^4(t)}, \qquad \alpha = \frac{e^2}{4\pi}, \tag{2.10}$$

follows, and the equation of motion for $\rho(t)$ is given by

$$\frac{\alpha}{2\rho^4} = 4\pi\sigma\left(\frac{\mathrm{d}}{\mathrm{d}t}\frac{\dot\rho}{(1-\dot\rho^2)^{1/2}} + \frac{2}{\rho(1-\dot\rho^2)^{1/2}}\right). \tag{2.11}$$

The latter is a consequence of eqs. (2.7, 2.9, 2.10).

The equilibrium radius a of the electron is calculated by taking $\dot\rho = 0$ in eq. (2.11):

$$a^3 = \alpha/16\pi\sigma. \tag{2.12}$$

In static equilibrium the Coulomb repulsion of the surface charge is balanced by the surface tension of the bubble

$$\tfrac{1}{2}E^2 = \sigma((1/\rho) + (1/\rho)).$$

Equation (2.11) can be interpreted as the Euler–Lagrange equation derived from the Lagrangian

$$L = -\sigma 4\pi\rho^2(1-\dot\rho^2)^{1/2} - \alpha/2\rho,$$

where $\rho(t)$ is the dynamical variable.

The energy of the oscillating electron is a conserved quantity. It is given by

$$E = \sigma(4\pi\rho^2/(1-\dot\rho^2)^{1/2}) + \alpha/2\rho. \tag{2.13}$$

The first term in eq. (2.13) is the surface energy with an expected relativistic factor $(1-\dot\rho^2)^{1/2}$ in the denominator. It is just σ-times the surface area when the surface is instantaneously at rest. The second term in eq. (2.13) is recognized as the Coulomb energy of the extended electron. In static equilibrium it is twice as much as surface energy.

For a given value of E the surface performs non-linear oscillations around the equilibrium radius a. The classical turning points of the oscillatory motion are ρ_1 and ρ_2 as shown in fig. 2.1.

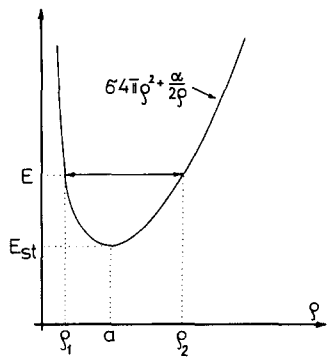

Fig. 2.1. The sum of the Coulomb energy and surface energy without the kinetic term is shown here. At a given energy there is a non-linear oscillation between the two turning points.

The static energy in equilibrium is

$$E_{st} = \tfrac{3}{4}\alpha/a, \tag{2.14}$$

whose one-third is surface energy.

Around the equilibrium radius $\rho = a$ the surface can perform harmonic small oscillations with a frequency

$$2\pi\nu = \sqrt{6}/a.$$

The energy of one quantum with this frequency is

$$h\nu = \tfrac{4}{3}\sqrt{6}E_{st}/\alpha, \tag{2.15}$$

which is approximately $448E_{st}$. The corresponding classical amplitude is a large one and the energy spectrum of the extended electron cannot be calculated from a simple harmonic approximation around the static equilibrium.

Therefore, we turn now to the Hamiltonian formulation of spherical vibrations.

Introducing the canonical momentum η conjugate to ρ,

$$\eta = \partial L/\partial\dot{\rho},$$

the Hamiltonian of the spherically vibrating electron is given by

$$H = (\eta^2 + 16\pi^2\sigma^2\rho^4)^{1/2} + \alpha/2\rho. \tag{2.16}$$

The classical Poisson bracket relation

$$\{\rho, \eta\}_P = 1 \tag{2.17}$$

is valid between the canonically conjugate variables ρ and η.

The semi-classical quantization procedure gives a first idea about the spectrum of spherical excitations in analytic form. The Bohr–Sommerfeld quantization condition is

$$2\int_{\rho_1}^{\rho_2} \eta(\rho)\,\mathrm{d}\rho = 2\pi\hbar(n + \tfrac{3}{4}), \qquad n = 0, 1, 2, \ldots, \tag{2.18}$$

where $\eta(\rho)$ is expressed from the relation

$$E = (\eta^2 + 16\pi^2\sigma^2\rho^4)^{1/2} + \alpha/2\rho. \tag{2.19}$$

The constant $\frac{3}{4}$ on the right-hand side of eq. (2.18) comes from the contribution of the turning points ρ_1 and ρ_2 to the semi-classical approximation. The value $\frac{1}{2}$ is correct for smooth potentials, and the Coulomb term $\alpha/2\rho$ in the limit $\alpha \to 0$ requires a modified number because it acts like a rigid wall at $\rho = 0$. Only the theoretical foundation of eq. (2.18) based on the Schrödinger equation of the system can finally justify this intuitive procedure.

The first few energy levels as determined from eqs. (2.18, 2.19) are given below in units of $(4\pi\sigma)^{1/3}$

$$(4\pi\sigma)^{-1/3} \cdot \begin{cases} E_0 = 1.94 \\ E_1 = 3.41 \\ E_2 = 4.61 \\ E_3 = 5.66. \end{cases} \tag{2.20}$$

For large n we find asymptotically

$$E_n \sim 53 E_{st} n^{2/3}, \tag{2.21}$$

where E_{st} is the classical energy of the static bubble in equilibrium. The spectrum is not equidistant as in the case of a harmonic oscillator.

For large excitations the Coulomb term acts like a rigid wall at $\rho = 0$ and the spectrum becomes similar to that of the square root Hamiltonian for a non-linear oscillator with potential energy $\sigma^2(4\pi\rho^2)^2$ solved in the region $\rho \in (0, \infty)$. The non-linear oscillator spectrum goes asymptotically as $E_n \sim n^{4/3}$ hence the power $\frac{2}{3}$ in the "square rooted" spectrum of eq. (2.21).

We note from eqs. (2.14) and (2.20) that the ground state energy $E_0 = 43.3 E_{st}$ is much larger than the classical energy of the static bubble. The surface oscillations of the Bohr–Sommerfeld orbits are large and strongly anharmonic.

The rigorous quantization of spherical vibrations starts from eqs. (2.16) and (2.17). There we replace the Poisson bracket with the quantum mechanical commutator

$$[\rho, \eta] = i\hbar.$$

In coordinate representation the surface of the extended electron is described by the quantum mechanical wave function $\psi(\rho)$, and the kinetic energy operator is represented by

$$\eta^2 \to -\hbar^2(d^2/d\rho^2).$$

In order to define η^2 as a Hermitian operator on the interval $\rho \in (0, \infty)$, we require the wave function $\psi(\rho)$ to vanish at $\rho = 0$.

The Hamiltonian in eq. (2.16) acts upon $\psi(\rho)$ as a non-local integral operator. The stationary Schrödinger equation

$$[(\eta^2 + \sigma^2(4\pi\rho^2)^2)^{1/2} + (\alpha/2\rho)]\psi(\rho) = E\psi(\rho) \tag{2.22}$$

gives the level spectrum of the extended "electron bag" in spherical approximation. The Coulomb barrier $\alpha/2\rho$ in eq. (2.22) requires the wave function $\psi(\rho)$ to vanish at $\rho = 0$ as ρ^λ where

$$\alpha = -2\lambda \operatorname{ctg} \tfrac{1}{2}\pi\lambda.$$

The mathematical interpretation of the square root operator on the left-hand side of the Schrödinger equation is as follows. First, we choose a complete orthonormal set of vectors in the Hilbert space as the solutions of the eigenvalue equation

$$\left[-\frac{d^2}{d\rho^2} + V(\rho)\right]\varphi_n(\rho) = \epsilon_n \varphi_n(\rho), \tag{2.23}$$

where

$$V(\rho) = \sigma^2(4\pi\rho^2)^2.$$

The boundary condition $\varphi_n(0) = 0$ is required for the solutions of eq. (2.23).

Since the square root operator $[\eta^2 + \sigma^2(4\pi\rho^2)^2]^{1/2}$ is diagonal in the above defined matrix represen-

tation, it can be written as a non-local integral operator

$$[\eta^2+\sigma^2(4\pi\rho^2)^2]^{1/2}|\psi\rangle \to \int_0^\infty d\rho' K(\rho,\rho')\psi(\rho'),$$

$$K(\rho,\rho') = \sum_n \epsilon_n^{1/2}\varphi_n(\rho)\varphi_n^*(\rho') \tag{2.24}$$

acting upon the state vectors of the Hilbert space.

The Schrödinger equation of the extended electron's eigenfunctions becomes then

$$\int_0^\infty d\rho' K(\rho,\rho')\psi(\rho') + \frac{\alpha}{2\rho}\psi(\rho) = E\psi(\rho). \tag{2.25}$$

This integral equation can be solved by numerical methods. The kernel K can be approximated as

$$K \sim K_N(\rho,\rho') = \sum_{n=1}^{N} \epsilon_n^{1/2}\varphi_n(\rho)\varphi_n^*(\rho'), \tag{2.26}$$

where ϵ_n and $\varphi_n(\rho)$ are obtained from eq. (2.23) numerically.

Given the approximate expression of eq. (2.26) for the kernel K, the Schrödinger equation (2.25) can be written in matrix representation, with the expansion

$$\psi(\rho) = \sum_{n=1}^{N} b_n\varphi_n(\rho)$$

for the eigenfunctions of Dirac's bubble. From the solution of the matrix equation we get the energy spectrum and the wave functions.

On a large basis with $N = 40$ we get very accurate solutions for the first few energy levels and eigenfunctions:

$$(4\pi\sigma)^{-1/3}\begin{cases} E_0 = 1.95 \\ E_1 = 3.42 \\ E_2 = 4.61 \\ E_3 = 5.67. \end{cases} \tag{2.27}$$

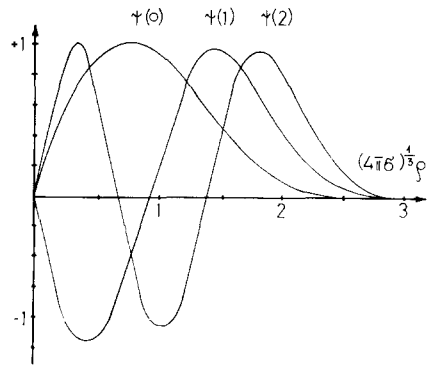

Fig. 2.2. The quantum mechanical wave functions of the surface are shown for the ground state and the first and second excited states.

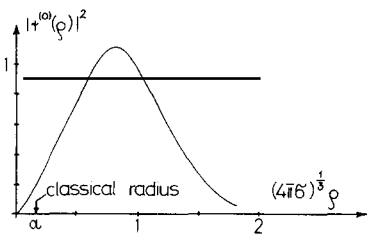

Fig. 2.3. The probability density is given for finding the extended electron with radius ρ in its ground state.

One notes the good agreement with the preliminary results of the semi-classical approximation as given by eq. (2.20).

The corresponding eigenfunctions are shown in fig. 2.2. The ground state is nodeless as expected, and each eigenfunction has one more node than that corresponding to the next lowest eigenvalue. Figure 2.3 shows the probability distribution $|\psi_0(\rho)|^2$ for finding the bubble in its ground state with a radius between ρ and $\rho + d\rho$. It is peaked far from the value of the extended electron's classical radius, due to the large quantum fluctuations of the surface.

The center of mass coordinate of Dirac's electron may be treated in the quantization process along the line of general methods available for extended objects. Lorentz invariance is, however, an interesting feature of the model already at the classical level.

2.3. *The energy-momentum tensor*

Dirac's extended electron has correct Lorentz transformation properties in contrast with the Abraham–Lorentz electron model. The special Poincaré stresses introduced by Dirac compensate for the Maxwell stresses making the total self-stress vanish in the rest frame.

In the Abraham–Lorentz model the self-stress does not vanish. In fact, it can be shown that its contribution to the momentum is just one-third of the contribution from the self-energy, leading to the famous and troublesome factor of $\frac{4}{3}$ in the inertia of electromagnetic energy, even for non-relativistic velocities.

We shall see now that it is impossible to break up the rest mass of the Dirac electron into an electromagnetic contribution and surface energy in a Lorentz invariant manner. The separate parts behave differently under Lorentz transformations, only the total energy (or mass) has correct transformation properties.

The energy-momentum tensor of the "electron bag" is calculated in the y coordinate system. So far we have kept the y coordinate system rectilinear and orthogonal. Now we shall vary the y coordinates around the rectilinear and orthogonal coordinate lines. The metric tensor of the y system will be designated by $\gamma_{\Lambda K}$.

The energy-momentum tensor $T^{\Lambda K}(y)$ in rectilinear and orthogonal coordinates is defined in terms of the variation of the action W as

$$\delta W = -\tfrac{1}{2}\int d^4y(-\det \gamma_{MN})^{1/2} T^{\Lambda K}(y)\delta\gamma_{\Lambda K}(y), \tag{2.28}$$

where $\delta\gamma_{\Lambda K}(y)$ corresponds to an infinitesimal variation of the rectilinear and orthogonal coordinates. The expression for δW in eq. (2.28) is the change of the action W for this variation.

The action of the extended electron, as we have seen, is $W = W_0 + W_s$. Variation of the electromagnetic part W_0 with respect to the rectilinear and orthogonal coordinates determines the well-known energy-momentum tensor of the electromagnetic field outside the bubble.

We shall calculate here the contribution of the surface to the total energy-momentum tensor of the extended particle. First, one notes that W_s may be written in the following form

$$W_s = -\sigma \int \cdots \int dx^0\, dx^2\, dx^3\, d^4y\delta^4(y - y(x^0, x^2, x^3))\sqrt{\det g_{ab}}, \tag{2.29}$$

where

$$y^{\wedge}(x^0, x^2, x^3) = y^{\wedge}(x^0, x^1 = 1, x^2, x^3),$$

and

$$g_{ab} = y^{\Lambda}_{,a} y^{K}_{,b} \gamma_{\Lambda K}$$

is the metric tensor on the surface ($a, b = 0, 2, 3$).

Variation of g_{ab} yields

$$\delta M = \tfrac{1}{2} M c^{ab} y^{\Lambda}_{,a} y^{K}_{,b} \delta \gamma_{\Lambda K}, \tag{2.30}$$

where $M = \sqrt{\det g_{ab}}$ was defined before, and c^{ab} is the reciprocal matrix to g_{ab}. Variation of W_s in eq. (2.29) together with the relation of eq. (2.30) determines the energy-momentum density $T_s^{\Lambda K}(y)$ of the surface:

$$T_s^{\Lambda K}(y) = \sigma \int \mathrm{d}x^0\, \mathrm{d}x^2\, \mathrm{d}x^3 \delta^4(y - y(x^0, x^2, x^3)) M c^{ab} y^{\Lambda}_{,a} y^{K}_{,b}. \tag{2.31}$$

It vanishes outside the surface, as expected.

The total four-momentum associated with the surface of the extended electron is defined by

$$P_s^{\Lambda} = \int T^{0\Lambda}\, \mathrm{d}^3 y,$$

with the choice $x^0 = y^0$, one writes

$$P_s^{\Lambda} = \sigma \int \mathrm{d}x^2\, \mathrm{d}x^3 M c^{0b} y^{\Lambda}_{,b}(x^0, x^2, x^3). \tag{2.32}$$

The energy-momentum four-density p_s^{Λ}, as generated by surface tension in a given point (x^0, x^2, x^3) of the surface, follows from eq. (2.3):

$$p_s^{\Lambda} = \sigma M c^{0b} y^{\Lambda}_{,b}.$$

After similar considerations we find the angular momentum tensor $M_s^{K\Lambda}$ of the surface,

$$M_s^{K\Lambda} = \int \mathrm{d}x^2\, \mathrm{d}x^3 (y^K p_s^{\Lambda} - y^{\Lambda} p_s^K).$$

For illustration of the formula in eq. (2.32) we shall calculate the energy carried by the closed surface of the bubble. The surface is described in polar coordinates by $\rho(\vartheta, \varphi, t)$. M in eq. (2.32) can be expressed in terms of $\rho(\vartheta, \varphi, t)$ and its derivatives,

$$M = \rho^2 \sin\vartheta \left(1 - \dot{\rho}^2 + \frac{1}{\rho^2}\rho^2_{,\vartheta} + \frac{1}{\rho^2 \sin^2\vartheta}\rho^2_{,\varphi}\right)^{1/2}.$$

The surface energy P_s^0 is calculated from eq. (2.32):

$$P_s^0 = \sigma \int \mathrm{d}\varphi \int \mathrm{d}(\cos\vartheta) \rho^2 \left(1 + \frac{1}{\rho^2}\rho^2_{,\vartheta} + \frac{1}{\rho^2 \sin^2\vartheta}\rho^2_{,\varphi}\right) \Big/ \left(1 - \dot{\rho}^2 + \frac{1}{\rho^2}\rho^2_{,\vartheta} + \frac{1}{\rho^2 \sin^2\vartheta}\rho^2_{,\varphi}\right)^{1/2}. \tag{2.33}$$

When a surface element is at rest instantaneously ($\dot{\rho} = 0$), its contribution to the surface energy P_s^0 becomes proportional to the surface area $\mathrm{d}f$

$$\mathrm{d}p_s^0 = \sigma\, \mathrm{d}\varphi\, \mathrm{d}(\cos\vartheta) \rho^2 \left(1 + \frac{1}{\rho^2}\rho^2_{,\vartheta} + \frac{1}{\rho^2 \sin^2\vartheta}\rho^2_{,\varphi}\right)^{1/2} = \sigma\, \mathrm{d}f,$$

as expected for surface tension.

For non-relativistic motion of the surface we may approximate P_s^0 in eq. (2.33) by using $\dot{\rho}^2 \ll 1$,

$$P_s^0 = \sigma \int \mathrm{d}f\{1 + \tfrac{1}{2}\dot{\rho}^2 \cos^2 \epsilon + \mathrm{O}(\dot{\rho}^4)\}. \tag{2.34}$$

In eq. (2.34), ϵ is the angle between the normal vector $\boldsymbol{n}$ of the surface element and the position vector of the surface point. One notes that only the projection of the velocity vector $\boldsymbol{v}$ along $\boldsymbol{n}$ appears in the expression for P_s^0.

Surface tension σ multiplied by the surface area $\mathrm{d}f$

$$\mathrm{d}\mu = \sigma\, \mathrm{d}f$$

may be identified in eq. (2.34) with the inertial mass of the surface element $\mathrm{d}f$. By inspection of eq. (2.32) one finds that the three-momentum density $\mathrm{d}\boldsymbol{p}_s$ of a surface element is always normal to the surface and its magnitude is $\mathrm{d}\mu\dot{\rho}\cos\epsilon$ in the non-relativistic limit.

Reparametrization invariance of the geometrical action W_s explains why we have found no three-momentum density associated with the longitudinal motion of the surface element $\mathrm{d}f$. The action W_s is invariant under any continuous transformation of the surface points which can be simply described as the reparametrization of the coordinate lines on the surface.

The longitudinal motion of a surface element in the surface can always be described as reparametrization of the coordinate lines. This motion is, therefore, not physical and there is no three-momentum associated with it.

We shall return now to the Lorentz transformation properties of Dirac's extended electron. The exact static solution is

$$\rho(\vartheta, \varphi, t) = a,$$

and the electric field strength

$$\boldsymbol{E} = \frac{e}{4\pi r^2}\frac{\boldsymbol{r}}{r}$$

describes Coulomb's law. There is no magnetic field $\boldsymbol{B}$ in the rest frame of the bubble.

The electrostatic field energy $M_{\mathrm{EM}} = \alpha/2a$ is interpreted as the electromagnetic rest mass of the extended electron. The rest mass of the surface $M_s = \sigma 4\pi a^2$ is given by the static surface energy. The relation

$$M_{\mathrm{EM}} = 2M_s$$

is valid in static equilibrium.

We shall perform a boost on the particle along the third axis with boost velocity v. The electromagnetic energy after the boost is

$$P_{\mathrm{EM}}^0 = \tfrac{1}{2}\int (\boldsymbol{E}^2 + \boldsymbol{B}^2)\, \mathrm{d}^3y = M_{\mathrm{EM}}(1 + \tfrac{1}{3}v^2)/(1 - v^2)^{1/2}. \tag{2.35}$$

The surface energy of the boosted electron is determined from eq. (2.33):

$$P_{\mathrm{surf}}^0 = M_s(1 - \tfrac{2}{3}v^2)/(1 - v^2)^{1/2}. \tag{2.36}$$

One notes from eqs. (2.35) and (2.36) that only the sum of the electromagnetic energy and surface

energy transforms as the zeroth component of a Lorentz vector,

$$P^0_{\rm EM} + P^0_{\rm surf} = (M_{\rm EM} + M_{\rm surf})/(1 - v^2)^{1/2},$$

where $M_{\rm EM} + M_{\rm surf} = 3\alpha/4a$ is the static energy of the extended electron at rest.

The third component of the surface momentum vector is calculated from eq. (2.32),

$$P^3_{\rm surf} = \tfrac{1}{3}M_s v/(1 - v^2)^{1/2}.$$

The momentum $P^3_{\rm surf}$ is only one-third of what is naively expected, since the motion of the surface elements under the boost is mainly longitudinal along the surface.

The third component of the electromagnetic field momentum is the same as in the Abraham–Lorentz electron model:

$$P^3_{\rm EM} = \tfrac{4}{3}M_{\rm EM} v/(1 - v^2)^{1/2}.$$

However, the sum of the surface momentum and field momentum has correct transformation properties,

$$P^3_{\rm surf} + P^3_{\rm EM} = (M_s + M_{\rm EM})v/(1 - v^2)^{1/2}. \tag{2.37}$$

The relation $M_{\rm EM} = 2M_s$ which is the balance of surface tension and Coulomb repulsion in static equilibrium is used in the derivation of eq. (2.37).

2.4. Instability

Dirac's extended bubble is not a realistic electron model yet. He interpreted the muon–electron mass difference as a rather successful application of the model, in the following sense. The mass of the electron was identified with the static, classical energy of the bubble at rest, as given by eq. (2.14). The muon energy, as the first radial quantum excitation of the classical ground state in Dirac's interpretation, was calculated by putting $n = 1$ in the Bohr–Sommerfeld quantum condition of (2.18) and ignoring the factor $\frac{3}{4}$ for zero-point fluctuations. Accordingly, the mass ratio is

$$m_\mu/m_e \sim 53, \tag{2.38}$$

not very far from the experimental value.

However, there is no justification for ignoring the effects of the zero-point fluctuations on the spectrum of the extended electron. We observe from eq. (2.27) that the ratio is different

$$E_1/E_0 \sim \mathrm{O}(1),$$

as compared with (2.38), when the large quantum fluctuations of the ground state and the first radial excitation are taken into account. We shall return to the discussion of the zero-point fluctuations in subsection 6.4.

The other problem with Dirac's electron model is that it does not carry the half-integer spin of the physical electron. This defect may be eliminated in the future by introducing a spinning surface in the extended model.

Nevertheless, even with correct half-integer spin, there is no selection rule between the muon and the electron in the model because the muon may decay into the ground state electron plus photons,

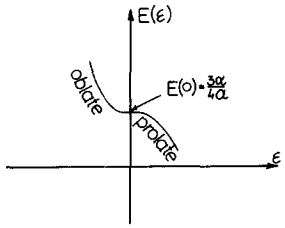

Fig. 2.4. The static energy is shown as a function of the deformation parameter ϵ (eccentricity).

electromagnetically. Only a miracle might suppress the decay rate of

$$\mu \to \mathrm{e} + \text{photons}$$

below the experimental upper bound.

Perhaps the most serious difficulty with Dirac's extended electron is its instability in classical, static equilibrium. To demonstrate this, let us consider small deformations of the elliptical type around the static equilibrium.

For a prolate ellipsoid, we take the minor semi-axis to be the static radius a from (2.12a). The total energy of the ellipsoid is then

$$E = \sigma S + E_{\mathrm{Cb}}, \tag{2.39}$$

where

$$S = 2\pi\left(a^2 + \frac{ab}{\epsilon}\sin^{-1}\epsilon\right), \qquad \epsilon = \sqrt{1 - a^2/b^2},$$

is the surface area, and ϵ is the eccentricity. The electrostatic energy E_{Cb} may be calculated from the capacitance C of our conducting prolate ellipsoid,

$$C = \frac{\sqrt{b^2 - a^2}}{\mathrm{Arch}(b/a)}.$$

There are similar formulae for the oblate case, too. There the major semi-axis is taken as the classical radius a.

The total energy from (2.39) is shown in fig. 2.4 as the function of the only parameter ϵ. One notes that the static sphere is in a neutral position energetically, with an inflection point at $\epsilon = 0$. For prolate shapes the static energy decreases and the extended electron is unstable. What happens is that the increase of the surface energy for prolate deformations cannot compensate the decrease of the Coulomb energy.

It remains an interesting and open question in which manner the electron gets stabilized due to the quantum fluctuations of the surface.

3. Bagged quantum chromodynamics

3.1. Quantum chromodynamics

Many theorists believe today in q.c.d. as the microscopic dynamics of quarks and gluons providing a key understanding of hadron structure. This field theoretical model is very elegant and simple in its formulation.

We shall designate the quark fields by $q_{i\alpha}$ where the first index $i = 1, 2, 3$ refers to the color gauge group of SU(3). Quarks belong to the triplet representation of color SU(3). The second index α refers to the flavor group of SU(4) as the approximate hadronic symmetry:

quark species	up	down	strange	charmed
red	q_{11}	q_{12}	q_{13}	q_{14}
yellow	q_{21}	q_{22}	q_{23}	q_{24}
blue	q_{31}	q_{32}	q_{33}	q_{34}

If there are more flavors in Nature, the flavor group can be enlarged and the forthcoming discussion remains unaffected.

The vector gluon fields are designated by $A_{i\mu}$ where the first index i refers to color. Gluons belong to an octet representation of the color gauge group SU(3), and the eight colors are labelled with $i = 1, 2, \ldots 8$. These vector particles are flavor singlets under the hadronic symmetry group SU(4).

The action W is invariant under the color gauge group SU(3) and we shall write for it

$$W = \int \mathrm{d}^4x\{-\tfrac{1}{4}F_{i\mu\nu}F_i^{\mu\nu} + \tfrac{1}{2}\mathrm{i}\bar{q}\gamma^\mu \overleftrightarrow{\partial}_\mu q - g\bar{q}\tfrac{1}{2}\lambda_i\gamma^\mu q A_{i\mu}\}, \tag{3.1}$$

where the flavor and color indices of the quark fields $q_{i\alpha}$ are not written out explicitly. Terms without some indices are understood to be summed over those omitted indices here, and later on.

The non-Abelian field-strength tensor in eq. (3.1) is given by

$$F_i^{\mu\nu} = \partial^\mu A_i^\nu - \partial^\nu A_i^\mu + g f_{ijk} A_j^\mu A_k^\nu.$$

The structure constants of the color gauge group SU(3) are denoted as f_{ijk} and g is the small, fundamental quark–gluon coupling constant in the theory. The eight Gell-Mann matrices λ_i act in color space.

The action W in eq. (3.1) is invariant under the hadronic symmetry group SU(4), though a symmetry breaking quark mass term can always be trivially added to W.

It is not difficult to obtain the following set of Euler–Lagrange field equations from the action principle $\delta W = 0$

$$D_{ij}^\mu F_{j\mu\nu} = g\bar{q}\tfrac{1}{2}\lambda_i\gamma_\nu q, \tag{3.2}$$

$$-\mathrm{i}\partial_\mu\gamma^\mu q_{i\alpha} + g(\tfrac{1}{2}\lambda_j A_{j\mu})_{ik}\gamma^\mu q_{k\alpha} = 0. \tag{3.3}$$

In eq. (3.2) we have introduced the gauge covariant derivative

$$D_{ij}^\mu = \delta_{ij}\partial^\mu - g f_{ijk} A_k^\mu.$$

There are eight conserved color currents $J_i^\mu(x)$ in the theory, and they are given by

$$gJ_i^\mu(x) = g\{\bar{q}\tfrac{1}{2}\lambda_i\gamma^\mu q + f_{ijk}F_j^{\nu\mu}A_{k\nu}\}. \tag{3.4}$$

The two terms in eq. (3.4) are the contributions to the color currents from quarks and gluons, respectively.

The eight color generators of the model are determined from the color currents as

$$Q_i = \int \mathrm{d}^3x J_i^0(x), \qquad i = 1, 2, \ldots, 8. \tag{3.5}$$

They are constants of motion and measure the color charges of the hadronic system with colored quark and gluon constituents.

There is a conjecture in certain theoretical circles that the color non-singlet degrees of freedom can not be excited in the theory, and only color singlet hadrons are physically observable. This means that the color generators Q_i of eq. (3.5) would all vanish when applied upon the physically observable state vectors of the theory.

We shall avoid here any discussion about the validity of this conjecture. Instead, we shall introduce a phenomenological structure for the vacuum with "collective variables" to implement quark and gluon confinement as the initial dynamical assumption of the quark bag model. The existence of an approximate bag-like structure may, or may not follow from quantum chromodynamics without additional assumptions.

3.2. The action principle in the quark bag model

Following the considerations of the Introduction, the bag is pictured here as a bubble in hadron phase embedded in the field non-supporting physical vacuum in a Lorentz invariant manner. The bubble is filled with colored quark fields and the non-Abelian gauge fields of gluons in mutual interaction. The pressure of quarks and gluons exerted on the surface of the bubble is balanced by surface tension and vacuum pressure.

The relativistic action W for the bag is a generalization of eq. (1.4) for the case of quantum chromodynamics. As we have discussed in section 2 the action is properly defined in a curvilinear coordinate system, where the surface of the bag is fixed.

We shall introduce again the general curvilinear coordinates x^μ. The surface of the bag is described by coordinate lines with $x^1 = 1$. The interior of the bag is mapped into the region $x^1 \in (0, 1)$.

For reference, we also introduce a second rectilinear and orthogonal coordinate system y^Λ, similarly to the discussion of section 2. The functions $y^\Lambda(x)$ describe the x coordinate system in terms of the y coordinate system, with the metric

$$g_{\mu\nu} = y_{\Lambda,\mu} y^{\Lambda}_{,\nu}$$

in the x system. The four covariant vectors

$$\tau^{\Lambda}_{\mu} = \partial y^\Lambda / \partial x^\mu, \qquad \text{for } \Lambda = 0, 1, 2, 3,$$

are known as a tetrad, or vierbein. They transform as Lorentz vectors in their Λ indices under the Lorentz transformations of the y coordinate system.

The general coordinates of the extended hadron are designated in the quark bag model by $A_{i\mu}(x)$ for the non-Abelian gluon fields, $q_{i\alpha}(x)$ for the quark fields, and $y^\Lambda(x)$ for the "collective variables" of the bag. The general coordinates are defined for those values of x^μ where $x^1 \in (0, 1)$; there are no general coordinates outside the bag.

The action W is written in curvilinear coordinates as

$$W = \int_{x^1 \in (0,1)} \mathrm{d}^4x J \{ -\tfrac{1}{4} g^{\mu\rho} g^{\nu\sigma} F_{i\mu\nu} F_{i\rho\sigma} + \tfrac{1}{2}\mathrm{i}(\bar{q}\gamma^\Lambda \tau^{\mu}_{\Lambda} \partial_\mu q - \partial_\mu \bar{q}\gamma^\Lambda \tau^{\mu}_{\Lambda} q)$$
$$- g\bar{q}\tfrac{1}{2}\lambda_i \gamma^\Lambda \tau^{\mu}_{\Lambda} A_{i\mu} \} - \sigma \int_{x^1=1} M \, \mathrm{d}x^0 \, \mathrm{d}x^2 \, \mathrm{d}x^3 - B \int_{x^1 \in (0,1)} \mathrm{d}^4x, \tag{3.6}$$

where $J = \sqrt{-\det g_{\mu\nu}}$ is the Jacobian, $M = \sqrt{\det g_{ab}}$, $(a, b = 0, 2, 3)$.

The first term on the right-hand side of eq. (3.6) is recognized as the action of q.c.d. as restricted to the interior points of the bag. Hence the terminology: bagged quantum chromodynamics. The second and third terms describe surface tension and vacuum pressure, respectively, as it was discussed in subsections 1.3 and 2.1; the action for the surface is σ times the three-dimensional area of the tube swept out by the surface of the bag in the four-dimensional Minkowski space, whereas the last term is proportional to the four-dimensional volume of the tube with the proportionality factor B.

Our variational process for the bag is similar in its spirit to the derivation of the equation of motion for Dirac's electron in subsection 2.1. From the terms in δW which are proportional to $\delta A_{i\mu}(x)$ and $\delta q_{i\alpha}(x)$ inside the bag we get the well-known non-Abelian field equations for quarks and gluons in curvilinear coordinates. They are identical with eqs. (3.2) and (3.3) for the interior points of the bag in the y coordinate system.

Variation of $A_{i\mu}$ on the surface leads to the linear boundary conditions

$$F_i^{\rho\mu} n_\mu = 0, \qquad i = 1, 2, \ldots, 8 \tag{3.7}$$

for the gluon fields at $x^1 = 1$. In eq. (3.7) n_μ is the unit normal four-vector to the surface $x^1 = 1$:

$$n_\mu = -\frac{1}{\sqrt{-g^{11}}}(0, 1, 0, 0).$$

To establish a convention we take $\boldsymbol{n}$ to be the exterior normal to the surface.

When eq. (3.7) is written in the y coordinate system, one finds

$$\boldsymbol{n} \cdot \boldsymbol{E}_i = 0, \tag{3.8}$$

$$n_0 \boldsymbol{E}_i + \boldsymbol{n} \times \boldsymbol{B}_i = 0, \tag{3.9}$$

so that the normal components of the gluon electric fields $\boldsymbol{E}_i$ and the tangential components of the gluon magnetic fields $\boldsymbol{B}_i$ all vanish on the boundary of the bag in the instantaneous rest frame of the surface element.

The color electric fields $\boldsymbol{E}_i$ and the color magnetic fields $\boldsymbol{B}_i$ are defined as the time–space and space–space components of the field strength tensor $F_{i\mu\nu}$, respectively.

It follows from eq. (3.8) that there is no color electric flux through the surface of the bag. As a consequence of Gauss's theorem, the total color charges Q_i for $i = 1, 2, \ldots, 8$ must vanish in the bag model for an extended hadron with closed boundary:

$$Q_i = \int_{\text{bag}} \mathrm{d}^3 y J_i^0(y) = -\int_{\text{surf}} \mathrm{d}f n_\mu F_i^{0\mu} = 0.$$

Similarly, there is no gluon field energy or momentum flow across the surface of the bag. The boundary conditions of eq. (3.7) render the walls of extended hadrons impermeable against the colored vector gluon fields.

Nothing has been said so far about the boundary conditions for the colored quark fields. We have seen that the colored gluon fields are confined to small closed domains of space (bags), and only color singlet states are allowed. Since the colored quarks are always coupled to colored gluons, we may expect that they become confined inside colorless, (white) bags.

As we shall see in subsection 4.1, the boundary condition

$$q_{i\alpha}(x) = 0, \qquad x^1 = 1, \qquad i = 1, 2, 3, \qquad \alpha = 1, 2, 3, 4, \tag{3.10}$$

for the colored quark fields is motivated on the quantum mechanical level. The physical content of eq. (3.10) may be explained as follows.

The point-like colored quark always drags along a color electric field which is subject to the boundary condition in eq. (3.7). This field generates a repulsive potential barrier between the quark and the surface of the bag, so that the quantum mechanical wave function of the point-like quark becomes repelled from the immediate vicinity of the boundary.

This picture is consistent with the mathematical requirement that all the quark wave functions vanish on the surface in the presence of gluon interaction. Equation (3.10) may be generalized to be imposed on the interacting quantized quark fields as an operator equation, and we shall also accept it in the classical theory.

Equation (3.10) is different from the boundary condition imposed on the quark fields by the MIT group. The relation between the different boundary conditions and the arguments which favor eq. (3.10) will be discussed in detail in subsection 4.1.

Returning to the action principle $\delta W = 0$ we are left with variations of $y^{\Lambda}(x)$. Variation of $y^{\Lambda}(x)$ inside the bag is just an identity when the field equations (3.2) and (3.3) are used. We get nothing, since the variation of curvilinear coordinate lines inside the bag is without physical significance.

However, variation of $y^{\Lambda}(x)$ on the surface when $x^1 = 1$ is maintained leads to the equation of motion for the boundary of the extended hadron:

$$-\tfrac{1}{4}F_i^{\mu\nu}F_{i\mu\nu} = -\sigma J^{-1}\partial_\mu(Jn^\mu) + B, \qquad x^1 = 1. \tag{3.11}$$

The first term on the right-hand side of eq. (3.11) is 2σ times the mean curvature of the surface in Minkowski space. The second term B describes the vacuum pressure. The boundary conditions of eqs. (3.7) and (3.10) are applied in the derivation of eq. (3.11).

The mean curvature depends on the acceleration of the corresponding surface point, therefore eq. (3.11) is a real equation of motion for the surface. In the absence of surface tension eq. (3.11) is only a relation between the coordinates and velocities.

We picture then the classical bag theory as follows:

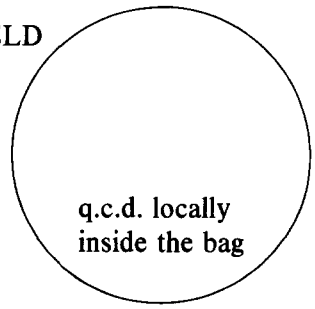

BUBBLE AND FIELD DYNAMICS

field equations of q.c.d. (see eqs. (3.3) and (3.4))

bubble dynamics
$-\tfrac{1}{4}F_{i\mu\nu}F_i^{\mu\nu} = -\sigma J^{-1}\partial_\mu(Jn^\mu) + B$

BOUNDARY CONDITIONS

gauge fields
$F_i^{\rho\mu}n_\mu = 0$

quark fields
$q_{i\alpha}(x) = 0$

The energy-momentum tensor density $T^{\Lambda K}(y)$ of the quark bag model is calculated in the rectilinear and orthogonal coordinate system y. Essentially, the method which was applied to Dirac's extended electron in subsection 2.3 may be copied here.

$T^{\Lambda K}(y)$ receives contributions from three independent parts of the action W:

$$T^{\Lambda K}(y) = T_0^{\Lambda K}(y) + T_\sigma^{\Lambda K}(y) + T_B^{\Lambda K}(y). \tag{3.12}$$

In eq. (3.12) the term $T_0^{\Lambda K}$ is the same as in ordinary chromodynamics. The energy-momentum density $T_\sigma^{\Lambda K}$ of the surface agrees with the formula in eq. (2.31). $T_B^{\Lambda K}$ is a new piece in $T^{\Lambda K}$, since there was no volume energy in the electron model:

$$\delta W_B = -\tfrac{1}{2}\int \mathrm{d}^4 y \sqrt{-\det \gamma_{\Lambda' K'}}\, T_B^{\Lambda K} \delta \gamma_{\Lambda K}(y). \tag{3.13}$$

After the variations are performed in eq. (3.13), one finds

$$T_B^{\Lambda K}(y) = B \int \mathrm{d}^4 x \delta^4(y - y(x)) \gamma^{\Lambda K}(y).$$

The total four-momentum of the bubble which is not of chromodynamical origin is given by

$$P^{\Lambda}_{\mathrm{bag}} = \int (T_\sigma^{0\Lambda}(y) + T_B^{0\Lambda}(y))\, \mathrm{d}^3 y.$$

One notes that there is no three-momentum associated with the second term $T_B^{0\Lambda}(y)$. Only the surface carries three-momentum as independent dynamical entity.

To get a feeling about the confinement force between colored quarks, we shall study a simplified model, first. The classical bag equations will be solved for infinitely heavy colored point quarks surrounded by bagged color gauge fields.

3.3. Static bag with point-like colored quarks

Let us consider a pair of point-like colored particles coupled to the non-Abelian gluon fields inside the bag. When the particles are infinitely heavy, they become nailed down to fixed points in space. They are characterized by fixed sources with color spin $\frac{1}{2}\lambda_i^{(1)}$ and $\frac{1}{2}\lambda_i^{(2)}$.

Since the color generators are not commuting, color as an independent degree of freedom bears some resemblance to spin in quantum mechanics. The quarks in triplet representation are unambiguously characterized by the color generators Q_3 and Q_8.

	Quarks			Antiquarks		
	red	yellow	blue	green	violet	orange
Q_3	1	−1	0	−1	1	0
Q_8	1/3	1/3	−2/3	−1/3	−1/3	2/3

There is a limit when the complexities of the non-Abelian structure can be avoided. Solving the problem in the lowest order of the small coupling constant g, we get eight sets of Abelian equations with the charge density j_i^0 on the right-hand side:

$$j_i^0 = g\tfrac{1}{2}\lambda_i^{(1)}\delta^3(\boldsymbol{r} - \boldsymbol{r}_1) + g\tfrac{1}{2}\lambda_i^{(2)}\delta^3(\boldsymbol{r} - \boldsymbol{r}_2), \qquad i = 1, 2, \ldots, 8.$$

In this limit the Lagrangian (or energy) is quadratic in the gauge fields and the combination

$$g^2 \sum_{i=1}^{8} (\tfrac{1}{2}\lambda_i^{(n)})^2, \qquad n = 1, 2, \tag{3.14}$$

occurs in the self-interaction, while the interaction term is proportional to

$$g^2 \sum_{i=1}^{8} \tfrac{1}{2}\lambda_i^{(1)} \tfrac{1}{2}\lambda_i^{(2)}.$$

The term in eq. (3.14) is proportional to a Casimir operator which has the value $\frac{4}{3}g^2$ in triplet representation. In a singlet state

$$\tfrac{1}{2}\lambda_i^{(1)} + \tfrac{1}{2}\lambda_i^{(2)} = 0,$$

which gives $-\frac{4}{3}g^2$ for the second expression. So the problem is equivalent to that of an Abelian field coupled to a quark and antiquark with charges $\pm\sqrt{\frac{4}{3}}g = \pm g'$ respectively.

Consider, therefore, the Abelian problem. We have to solve a rather peculiar exercise from electrostatics: given two fixed (color) charges at positions $\boldsymbol{r}_1$ and $\boldsymbol{r}_2$ with opposite signs for their charges, find the shape of a domain (gluon bag) inside which the Maxwell equations are valid for the gluon field,

$$\begin{aligned} &\operatorname{curl} \boldsymbol{E} = \operatorname{curl} \boldsymbol{B} = 0, \\ &\operatorname{div} \boldsymbol{B} = 0, \\ &\operatorname{div} \boldsymbol{E} = g'[\delta^3(\boldsymbol{r} - \boldsymbol{r}_1) - \delta^3(\boldsymbol{r} - \boldsymbol{r}_2)]. \end{aligned} \tag{3.15}$$

The color magnetic moments are ignored here, and $\boldsymbol{B} = 0$ is assumed in the solution of eq. (3.15).

On the static surface of the bag we have the following linear boundary condition

$$\boldsymbol{n} \cdot \boldsymbol{E} = 0, \tag{3.16}$$

where $\boldsymbol{n}$ is the normal vector to the static surface.

The equation of motion for the bag's shape becomes now a static relation between the electric field pressure and the sum of the surface tension and vacuum pressure. From eq. (3.11) we find

$$\tfrac{1}{2}\boldsymbol{E}^2|_s = \sigma((1/R_1) + (1/R_2)) + B, \tag{3.17}$$

where $1/R_1$ and $1/R_2$ are the principal curvatures in two orthogonal directions at a given point of the static surface.

If the surface is characterized by the function $\rho(\vartheta)$ in polar coordinates, the sum of the principal curvatures is given by

$$\frac{1}{R_1} + \frac{1}{R_2} = \frac{1}{(\rho^2 + \rho_{,\vartheta}^2)^{1/2}}\left[2 - \frac{\rho_{,\vartheta}}{\rho}\operatorname{ctg}\vartheta + \frac{\rho_{,\vartheta}^2 - \rho\rho_{,\vartheta\vartheta}}{\rho^2 + \rho_{,\vartheta}^2}\right]$$

for axial-symmetric surface.

Numerical solution

Introducing the scalar potential $\phi(\boldsymbol{r})$ for the color electric field $\boldsymbol{E}$ by the definition

$$\boldsymbol{E} = -\operatorname{grad}\phi,$$

we write the static Lagrangian of the bag as

$$L = \tfrac{1}{2}\int_{\text{bag}} \mathrm{d}^3 r (\operatorname{grad}\phi)^2 - \int_{\text{bag}} \mathrm{d}^3 r \phi j_0 - \sigma F - BV. \tag{3.18}$$

The static charge distribution in eq. (3.18) is

$$j_0(r) = g'\{\delta^3(r - r_1) - \delta^3(r - r_2)\},$$

F is the surface area and V is the volume of the bag.

The field equations and the boundary condition together with the bag's dynamical equation for static equilibrium can be derived from the Lagrangian of eq. (3.18) by the variation of the potential and the surface of the bag.

A numerical solution is available for the problem using the variational method $\delta L = 0$ with respect to ϕ and $\rho(\vartheta, \varphi)$. Since the bag has cylindrical symmetry around the axis defined by the $q\bar{q}$ pair, we shall write the expansion

$$\rho(\vartheta) = \sum_l \beta_l P_{2l}(\cos\vartheta) \tag{3.19}$$

for the surface with unknown coefficients β_l, to be determined from the variational principle.

The color Coulomb potentials of the point charges are separated from $\phi(r)$:

$$\phi(r) = \frac{g'}{4\pi|r - r_1|} - \frac{g'}{4\pi|r - r_2|} + \sum_i c_i \left(\frac{r}{\rho_{\max}}\right)^{2i} P_{2i}(\cos\vartheta), \tag{3.20}$$

where we have to determine the expansion coefficients c_i.

The equation $\Delta\phi(r) = -j_0$ inside the bag is satisfied by the Ansatz of eq. (3.20) automatically. The variational solution for the expansion coefficients β_l and c_i determines the shape of the bag in terms of $\rho(\vartheta)$, together with the field potential $\phi(r, \vartheta)$ inside.

The boundary condition

$$\partial\phi/\partial n = 0$$

on the surface of the bag, and the equation of the static equilibrium

$$\tfrac{1}{2}(\text{grad}\,\phi)^2 = \sigma((1/R_1) + (1/R_2)) + B$$

are satisfied as a consequence of the variational equations.

The numerical method where a finite number of expansion parameters is used gives rapid convergence and satisfactory results. To illustrate the rapid convergence of the method we shall give here a numerical solution with five parameters in the expansion of $\rho(\vartheta)$ and $\phi(r, \vartheta)$ respectively.

For a first orientation, the strength of the quark–gluon coupling was set at the value

$$g'^2/4\pi = 0.2. \tag{3.21}$$

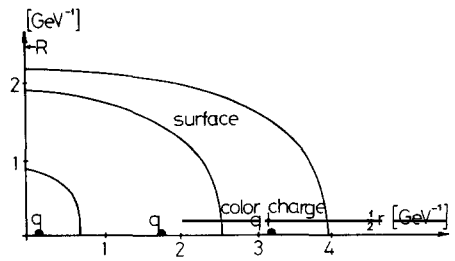

Fig. 3.1. The shape of one quadrant of the bag in longitudinal section for different q–$\bar{q}$ separations is shown. The arrow indicates the radius of an ideal cylindrical vortex tube.

The strength of surface energy is

$$\sigma = 216\ \text{MeV/fermi}^2 \tag{3.22}$$

in the numerical example, and $B = 0$ is chosen for simplicity.

The shape of the bag is shown in fig. 3.1 for different values of the distance between the point-like quark and antiquark. We estimate the error in the calculation as due to the cut-off in the expansions of eqs. (3.19) and (3.20) at five parameters to be within ten percent.

The computer calculation confirms our intuitive picture about the static confinement force for colored quarks separated at large distances: a color electric vortex develops between the color charges for large separation.

The color electric vortex

We shall imagine a fictive geometrical configuration where the color charges of the quark and antiquark are smeared uniformly on two parallel disks at a distance r. The radius of the two disks is chosen to be

$$R = (g'^2/2\pi^2\sigma)^{1/3}. \tag{3.23}$$

There is an exact static solution of the bag equations to this geometry.

The color electric field $\boldsymbol{E}$ forms a homogeneous vortex of radius R with a cylindrical surface between the color charges. Since $\boldsymbol{E}$ is tangential at the surface, the boundary condition of eq. (3.16) is satisfied on the cylindrical surface of the static vortex-like bag.

It follows from eq. (3.17) that

$$\tfrac{1}{2}\boldsymbol{E}^2 = \sigma/R \tag{3.24}$$

is valid on the cylindrical surface. From Gauss's law,

$$g' = |\boldsymbol{E}|R^2\pi,$$

the radius R of the vortex can be expressed with the help of eq. (3.24) and it agrees with the value which we have chosen in eq. (3.23).

The static energy U_c stored in the color electric field,

$$U_c = \lambda_c r,$$

is proportional to the length of the vortex, with the proportionality factor

$$\lambda_c = \tfrac{1}{2}(4\pi\sigma^2 g'^2)^{1/3}. \tag{3.25}$$

The surface energy

$$U_s = \lambda_s r$$

is also proportional to r, with

$$\lambda_s = (4\pi\sigma^2 g'^2)^{1/3}. \tag{3.26}$$

A similar vortex develops between two point-like color charges at large separation. Only at the ends of the cigar-like bag are the field $\boldsymbol{E}$ and the shape of the bag modified when compared with the exact cylindrical vortex.

The potential energy $V(r)$ of the $q\bar{q}$-pair for the numerical solution with five parameters β_l, $l = 0, 1, \ldots, 4$ and c_i, $i = 0, 1, \ldots, 4$ is shown in fig. 3.2. A divergent Coulomb self-energy for the point-like color charges which is independent of the distance r is subtracted from $V(r)$.

The potential energy $V(r)$ is well approximated by

$$V(r) \approx -\frac{g'^2}{4\pi}\frac{1}{r}$$

at small distances where a dominant Coulomb-like interaction energy is expected between the color charges. At large distances $V(r)$ is proportional to r,

$$V(r) \approx \lambda r,$$

and the proportionality factor λ is guessed from the exact vortex solution to be

$$\lambda = \tfrac{3}{2}(4\pi\sigma^2 g'^2)^{1/3}.$$

With the parameters of eqs. (3.21) and (3.22) the numerical value of λ is one GeV/fermi, well-tailored for charmonium calculations. The color electric vortex solution with linearly rising potential energy sets in at rather small distances around $r = 0.5$ fermi.

The surface energy is also shown in fig. 3.2. It is linear as expected for a vortex between color charges, and the relation

$$\lambda_s = 2\lambda_c,$$

which follows from eqs. (3.25) and (3.26) is well approximated by the numerical solution. The slope of the surface energy is twice of the slope for the gluon field energy in fig. 3.2.

The radius of the ideal vortex can be calculated from eq. (3.23) with the previously fixed values of $g'^2/4\pi$ and σ

$$2R \approx 1 \text{ fermi}.$$

This value of R is shown in fig. 3.1 indicating the rapid convergence of the bag's width to that of the exact color vortex with increasing values of r.

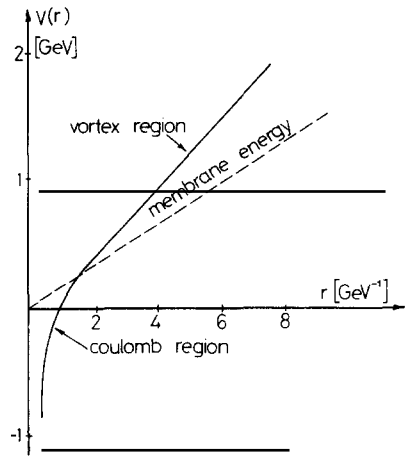

Fig. 3.2. The static energy of the $q\bar{q}$-system.

Fig. 3.3. Quark–diquark configuration.

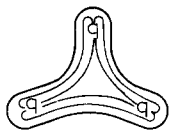

Fig. 3.4. Three quarks at large separation.

The static configuration of three colored point quarks is more complicated. Though no computer calculations are available, we may conjecture the qualitative picture using the approximate notion of the previously discussed quark valencies as follows:

When the red, yellow, and blue quarks are lined up as a chain molecule type configuration, the color electric flux lines of E_3 and E_8 are shown in fig. 3.3. Two quarks at the end of the chain always attract each other (diquark).

For example, the attractive force between a red quark and a yellow quark due to their color charge Q_3 is stronger then the repulsive force generated by the color charge Q_8. This observation motivates the quark–diquark model of baryons in certain theoretical circles.

If one quark is pulled out from the chain, we get three vortices with a junction in the middle, fig. 3.4. This is probably the energetically most favorable arrangement for three quarks which are not lined up along a chain. The conjectured configuration motivates some string models for baryons with three quarks at the ends.

In the numerical example we have set the strength of vacuum pressure B to be zero. This condition can be easily removed in the calculation which works for any combination of surface tension σ and vacuum pressure B.

There may occur, however, a rather peculiar singularity on the surface of the bag for $\sigma = 0$ which requires some caution. The color electric field $\boldsymbol{E}$ is tangential at each point of the surface. For $B = 0$ this is realized in such a way that the surface becomes flat in two opposite points on the axis connecting the $q\bar{q}$-pair. Since the mean curvature of the surface is zero in these points $\boldsymbol{E}$ vanishes there.

In the other extreme case when $\sigma = 0$, the equation of static equilibrium is

$$\tfrac{1}{2}\boldsymbol{E}^2|_s = B,$$

and the color electric field strength must be constant on the surface. The normal component of $\boldsymbol{E}$ is, of course, zero in each point of the surface. It turns out that the shape of the bag develops a singularity on the surface in two opposite points where the surface was flat previously in the presence of surface tension. The singular shape is shown in fig. 3.5 for a cross section of the cylindrically symmetric bag. The singularity of the surface is smoothed out in the presence of surface tension.

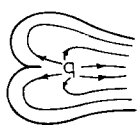

Fig. 3.5. The static surface of the bag with pure volume tension near to a point color charge.

4. Quark boundary condition and surface dynamics

4.1. Quark boundary condition

In the previous section we studied the extreme example where the quarks were fixed in space surrounded by a bagged gluon field. It gave us a feeling about the nature of the confinement force between point-like static quarks when they were separated at large distances.

Here we shall study the confinement mechanism for quarks when they can move inside the bag. Our purpose is a better understanding of the quark boundary condition on the surface of a hadron in the bag model.

First, let us consider a free quark field $q_i(x)$ confined to the interior of the bag without being coupled to gauge fields. The suffices $i = 1, 2, 3$ stand for color. The local flux of color in the interior is

$$J^{\mu}_{ik}(x) = \bar{q}_i(x)\gamma^{\mu}q_k(x).$$

If the quantum numbers associated with the currents are not to be lost through the surface, then it is necessary that

$$n_{\mu}J^{\mu}_{ik} = \bar{q}_i n \cdot \gamma q_k = 0$$

on the surface.

Now, $(in\gamma)^2 = 1$, so that $in\gamma$ has eigenvalues ± 1. Following the M.I.T. group, let us assume that

$$-in\gamma q_{k\alpha} = q_{k\alpha}, \qquad k = 1, 2, 3, \qquad \alpha = 1, 2, 3, 4 \tag{4.1}$$

is satisfied on the surface as the quark boundary condition when we approach from interior points. In eq. (4.1) the flavor index α of SU(4) is also written out explicitly. Then it follows from eq. (4.1) that

$$n_{\mu}J^{\mu}_{\alpha i,\beta k} = 0,$$

and

$$\bar{q}_{\alpha i}q_{\beta k} = 0$$

are valid on the boundary of the bag.

The stress tensor for the quark fields which describes momentum and energy flow inside the bag is

$$T^{\mu\nu}_{\text{quark}} = \sum_{i,\alpha}\left\{\tfrac{1}{2}i\bar{q}_{i\alpha}\gamma^{\mu}\frac{\partial}{\partial x^{\nu}}q_{i\alpha} - \tfrac{1}{2}i\frac{\partial\bar{q}_{i\alpha}}{\partial x^{\nu}}\gamma^{\mu}q_{i\alpha}\right\},$$

and

$$\partial_{\mu}T^{\mu\nu}_{\text{q}} = 0.$$

The momentum and energy flow through the surface is given by evaluating $n_{\mu}T^{\mu\nu}_{\text{q}}$ on the surface:

$$n_{\mu}T^{\mu\nu}_{\text{q}} = \frac{1}{2}\frac{\partial}{\partial x_{\nu}}\sum_{i,\alpha}\bar{q}_{i\alpha}q_{i\alpha}. \tag{4.2}$$

The boundary condition in eq. (4.1) is used in the derivation of eq. (4.2). We have found before that $\bar{q}_{i\alpha}q_{i\alpha} = 0$ on the surface, hence its derivative points along the normal,

$$\frac{\partial}{\partial x^{\nu}}\sum_{i,\alpha}\bar{q}_{i\alpha}q_{i\alpha} = 2n_{\nu}p_{\text{q}}.$$

Therefore, we find that

$$n_\mu T_q^{\mu\nu} = n^\nu p_q,$$

and p_q is interpreted as a "pressure" on the surface, since in the instantaneous rest frame of the surface element the momentum flow is normal to the surface and is given by p_q. We may call p_q the quark pressure. It is balanced by surface tension σ and vacuum pressure B.

In the M.I.T. model, where $\sigma = 0$, the total energy-momentum tensor for hadrons is

$$T^{\mu\nu}_{\text{hadron}} = \begin{cases} T_q^{\mu\nu} + Bg^{\mu\nu}, & \text{inside the bag} \\ 0 & \text{outside,} \end{cases}$$

in the absence of gluon fields. The balance of quark pressure and vacuum pressure on the surface leads to the non-linear boundary condition:

$$p_q = B \to B = \tfrac{1}{2} n^\mu \frac{\partial}{\partial x^\mu} \sum_{i,\alpha} \bar{q}_{i\alpha} q_{i\alpha}. \tag{4.3}$$

Since the surface variables do not appear with second time derivatives in eq. (4.3), the surface variables are not new dynamical degrees of freedom in the M.I.T. version. The surface variables are simply given there as functions of the interior fields $q_{i\alpha}(x)$. This feature remains valid in the presence of quark–gluon coupling.

The boundary condition in eq. (4.1) may be interpreted physically as follows. Outside the bag the physical vacuum generates a large (eventually infinite) effective mass for quarks, so that they cannot propagate there with finite energy. The outside vacuum acts as a scalar confinement potential with infinite walls maintaining Lorentz invariance in the formulation of the model. It can be shown that such a scalar potential requires the boundary condition of eq. (4.1).

We shall argue now that the quark boundary condition in the presence of quark–gluon coupling, at least for slowly moving quarks in adiabatic approximation, becomes

$$q_{i\alpha}(x) = 0. \tag{4.4}$$

Let us consider a fixed infinite plane at $z = 0$ with its normal vector $\boldsymbol{n}$ along the z-axis. Let the plane be a reflecting dielectric mirror against an Abelian gauge field $A_\mu(x)$ with the linear boundary conditions of eq. (1.5). One notes that this is the semi-infinite dielectric slab of section 1.2 with $\epsilon_1 = 1$ for $z > 0$, and $\epsilon_2 = 0$ for $z < 0$.

Let the gauge field A_μ be coupled to a quark spinor field $q(x)$ which is not restricted by the boundary condition of eq. (4.1) on the surface. The plane at $z = 0$ is transparent against free quarks in the absence of quark–gluon coupling. Nevertheless, as we shall see, quarks cannot get through the dielectric mirror because of the gauge field A_μ dragged along by the quark color charge. The simple example motivates the boundary condition in eq. (4.4).

The motion of a charged point quark will be studied in the region $z > 0$. There is an instantaneous Coulomb interaction between the quark and the dielectric. The instantaneous color electric field which is tangential on the plane at $z = 0$ is calculated by introducing the image charge of the quark at $r^{\text{im}} = (x, y, -z)$ as shown in fig. 4.1. The position of the quark is denoted by $r = (x, y, z)$.

The potential $\phi(r')$ of the color electric field is given by

$$\phi(r') = \frac{g}{4\pi} \frac{1}{|r - r'|} + \frac{g}{4\pi} \frac{1}{|r^{\text{im}} - r'|}, \tag{4.5}$$

where r' is an arbitrary point in the region $z > 0$.

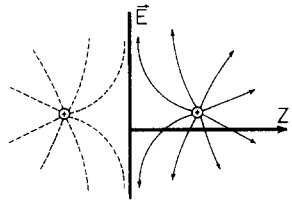

Fig. 4.1. The static color-electric field of a point-like color charge in a semi-infinite dielectric slab.

The first term in eq. (4.5) gives the divergent Coulomb self-energy of the point-like quark when evaluated at the point $r' = r$. It is independent of r and can be absorbed in the mass of the quark.

The second term, however, gives a z-dependent finite additional mass term in the one-particle Dirac equation. This mass term is identical with the potential energy between the dielectric and the quark. The force between the dielectric mirror and the charged particle is repulsive for both the point quark and its antiparticle.

The Dirac equation of the point quark with the scalar self-mass term $\alpha/4z$ is written as

$$\left\{-\mathrm{i}\begin{bmatrix} 0 & \sigma_z \\ \sigma_z & 0 \end{bmatrix}\frac{\mathrm{d}}{\mathrm{d}z} + \left(m + \frac{\alpha}{4z}\right)\begin{bmatrix} 1 & 0 \\ 0 & -1 \end{bmatrix}\right\} q(z) = Eq(z), \tag{4.6}$$

where $q(z)$ is the spinor wave function. The x and y dependence of the Dirac spinor can be separated in cylindrical coordinates. Here we consider only those solutions with vanishing azimuthal quantum number without x and y dependence. The conclusion remains the same for all partial waves.

Since the third component of the spin operator Σ_z commutes with the Dirac Hamilton operator H_D, the Ansatz

$$q(z) = \begin{bmatrix} f(z)\varphi \\ g(z)\chi \end{bmatrix}, \qquad \mathrm{i}\chi = \sigma_z\varphi \tag{4.7}$$

is required to be common eigenfunction of Σ_z and H_D. In eq. (4.7) φ and χ are two-component spinors, and

$$\varphi = \begin{bmatrix} 1 \\ 0 \end{bmatrix}$$

describes a quark state with the third component of the spin along the positive z-axis.

From the Dirac equation (4.6) we find the first order differential equations,

$$\begin{aligned} Ef &= -g' + (m + (\alpha/4z))f \\ Eg &= f' - (m + (\alpha/4z))g. \end{aligned} \tag{4.8}$$

For any value of the energy $E = \sqrt{p^2 + m^2}$, there is a solution to (4.8) which is regular at $z = 0$, with

$$f(z) \sim \text{const} \cdot z^{\alpha/4}, \qquad g(z) \sim \text{const} \cdot z^{\alpha/4}$$

for small values of z. There is also a singular solution with

$$f(z) \sim \text{const} \cdot z^{-\alpha/4}, \qquad g(z) \sim \text{const} \cdot z^{-\alpha/4}$$

when z goes to zero.

The exact solution of eq. (4.8) are calculated as follows. After the substitutions

$$g = \mathrm{i}\frac{p}{m}\mathrm{e}^{-\mathrm{i}pz}[F_1(2\mathrm{i}pz) - F_2(2\mathrm{i}pz)], \tag{4.9}$$

$$f = \sqrt{1+\frac{E}{m}}\,\mathrm{e}^{-\mathrm{i}pz}[F_1(2\mathrm{i}pz) + F_2(2\mathrm{i}pz)] \tag{4.10}$$

we find the second order equations for F_1 and F_2:

$$\xi F_1''(\xi) + (1-\xi)F_1' - \left(1 + \frac{\alpha m}{4\mathrm{i}p} + \frac{\alpha^2}{16\xi}\right)F_1 = 0,$$

$$\xi F_2''(\xi) + (1-\xi)F_2' - \left(\frac{\alpha^2}{16\xi} + \frac{\alpha m}{4\mathrm{i}p}\right)F_2 = 0,$$

where $\xi = 2\mathrm{i}pz$.

Now the function G_2 with

$$G_2(\xi) = \xi^{-\alpha/4}F_2(\xi)$$

satisfies the confluent hypergeometric equation which has a regular solution

$$G_2(2\mathrm{i}pz) = M\left(\frac{\alpha}{4} + \frac{\alpha m}{4\mathrm{i}p}, \frac{\alpha}{2} + 1, 2\mathrm{i}pz\right) \tag{4.11}$$

in terms of the Kummer function M. There is also a well-known irregular solution with $M \to U$. The most general solution of the confluent hypergeometric equation is an arbitrary linear combination of the M and U functions.

The function F_1 can be calculated from F_2 using the relation

$$F_1(\xi) = -4\frac{\mathrm{i}p}{\alpha E}\xi F_2'(\xi) - \frac{m}{E}F_2(\xi).$$

Since $M(a, b, z)$ behaves for small z as $M \sim 1 + \mathrm{O}(z)$ the choice (4.11) for the function G_2 defines the regular solution of the Dirac equation for f and g in eqs. (4.8) and (4.9). The small z behavior of $U(a, b, z)$ is $U \sim z^{-\alpha/2}(1 + \mathrm{O}(z))$ so this choice corresponds to the irregular solution of the Dirac equation for f and g.

Let us consider first the regular solution of the Dirac equation. From the large z behavior of M

$$M(a, b, \xi) \xrightarrow[z\to\infty]{} \frac{\Gamma(b)}{\Gamma(a)}\xi^{a-b}\,\mathrm{e}^{\xi},$$

we find asymptotically

$$f_{\mathrm{reg}}(z) \sim \mathrm{const}\,\sqrt{1+\frac{E}{m}}\,\sin\left(pz - \frac{\alpha m}{4p}\ln 2pz + \delta\right),$$

$$g_{\mathrm{reg}}(z) \sim \mathrm{const}\,\sqrt{\frac{E}{m} - 1}\,\cos\left(pz - \frac{\alpha m}{4p}\ln 2pz + \delta\right),$$

where the phase δ is defined as

$$\delta = \eta - \frac{\alpha\pi}{8} + \arg\Gamma\left(\frac{\alpha}{4} + 1 + \mathrm{i}\frac{\alpha m}{4p}\right), \qquad \mathrm{e}^{2\mathrm{i}\eta} = \mathrm{i}\frac{p}{E} + \frac{m}{E}. \tag{4.1'}$$

The regular solutions may be interpreted as scattering states with total reflection on the scalar potential barrier $\alpha/4z$ in the following sense. One defines a cut-off potential

$$\begin{aligned} V(z) &= \alpha/4z, && \epsilon < z < \infty \\ &= \alpha/4\epsilon, && 0 < z < \epsilon \\ &= 0, && -\infty < z < 0 \end{aligned} \tag{4.13}$$

with the cut-off at $z = \epsilon$. The scattering states of the Dirac equation for incoming waves from the right are calculated by matching a linear combination of the M and U functions to the solution for $0 < z < \epsilon$. There is a similar procedure at $z = 0$. In the limit $\epsilon \to 0$ the reflection coefficient of the potential barrier (4.13) goes to one, and the quarks or antiquarks cannot penetrate through the plane $z = 0$ into the left half-space.

Quite apart from the cut-off procedure, the regular solutions f_{reg} and g_{reg} form a complete system for $z > 0$ which is selected from the most general solutions of the differential equation (4.6) by imposing the boundary condition

$$q(z) = 0 \tag{4.14}$$

at $z = 0$.

We may conjecture that (4.14) will be maintained for the quark field operators in the quantum field theory of the model.

Apparently, there seems to be a contradiction between the M.I.T. boundary condition (4.1) and $q = 0$. However, one notes that for any fixed, and positive z

$$f = \sqrt{1 + \frac{E}{m}} \sin(pz + \eta), \qquad g = \sqrt{\frac{E}{m} - 1} \cos(pz + \eta), \tag{4.15}$$

in the $\alpha \to 0$ limit. Now the standing waves of (4.15) are exactly the same as if the M.I.T. boundary condition (4.1) were imposed on the solutions of the free Dirac equation in the right half-space.

For small values of the quark–gluon coupling α, f_{reg} and g_{reg} approximately agree with the M.I.T. solutions of the free Dirac equation inside the bag, though there is a difference in a thin skin close to the boundary of the bag. Here f_{reg} and g_{reg} vanish in the $z \to 0$ limit.

The difference is understandable in potential language. In the absence of quark–gluon coupling the free quarks are confined by an infinite scalar potential well in the M.I.T. interpretation. There is a direct quark pressure p_q exerted on the boundary of the bag, as it was discussed before in this subsection. However, in the presence of quark–gluon coupling an effective quark self-mass is generated due to gluon confinement as shown in fig. 4.2. This potential barrier motivates the boundary condition (4.14). There is no direct quark pressure on the surface of the bag then, it is the gauge field

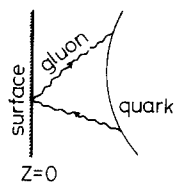

ey diagram of the quark in the semi-infinite dielectric slab. The gluon propagator may have reflections on the surface at

pressure which is balanced by surface tension and vacuum pressure in the quark bag model with quark–gluon coupling.

4.2. Surface tension versus vacuum pressure

Dirac has introduced in 1962 an extended electron model in which the electron's surface is described as the continuum limit of a two-dimensional sequence of geometrical points connected in a Lorentz invariant manner.

The relativistically invariant action W_s of eq. (2.2) for a closed surface can be viewed as a generalization of the action

$$W_{\text{point}} = -m \int \mathrm{d}t \sqrt{1-v^2}$$

for a point particle. W_{point} is associated with the world line of a geometrical point, where v is the velocity, and m is the rest mass of the point.

The relativistic string is a sequence of geometrical points connected in a linear chain in the continuum limit. The associated geometrical action is

$$W_{\text{string}} = -\tau \int \mathrm{d}t \int \mathrm{d}s \sqrt{1-v_\perp^2}, \tag{4.16}$$

where $\mathrm{d}s$ is the length of the line element and $v_\perp$ is the velocity of the line element in the transverse direction. The constant τ has a dimension of energy/length, or length^{-2}.

Nambu has noticed in 1969 that the spectrum of the dual resonance model may be interpreted as the stationary quantum states of a relativistic string defined by (4.16). τ^{-1} is proportional then to $\alpha'(0)$ which is the universal slope of the linear Regge trajectories in the dual resonance model.

It is clear from (4.16) that only internal motions of the string transverse to its extension in space are dynamical. That is, the action W_{string} depends only on the transverse velocity associated with transverse motions. The longitudinal expansion or shrinkage of the line elements is also physical but it is somehow associated with "potential energy" and not kinetic energy.

The relativistic action for a closed surface (or membrane) associated with a geometrical surface is

$$W_{\text{surf}} = -\sigma \int \mathrm{d}t \int \mathrm{d}^2 S \sqrt{1-v_\perp^2},$$

where $\mathrm{d}^2 S$ is the area of the surface element and $v_\perp$ is the velocity of the surface element in the transverse direction.

Again, only internal motions of the surface elements transverse to their extension in space are dynamical in the sense that the action W_{surf} depends only on the transverse velocities associated with transverse motions.

Now, the action

$$W_{\text{vac}} = -B \int \mathrm{d}t \int \mathrm{d}^3 r \tag{4.17}$$

for vacuum pressure contains no transverse velocity. The factor $\sqrt{1-v_\perp^2}$ was forced upon us by Lorentz invariance in the description of the string or the membrane. However, $\mathrm{d}t\,\mathrm{d}^3 r$ itself is an invariant four-dimensional volume element under the Lorentz group, and no factor $\sqrt{1-v_\perp^2}$ is allowed.

Since the action (4.17) does not depend on velocities, it cannot describe dynamical motions. W_{vac} acts as some generalized potential energy when other dynamical degrees of freedom are present in the system.

Let us consider, for example, a bubble with surface tension on the boundary under vacuum pressure from outside. The action is

$$W_{\text{bag}} = -\sigma \int \mathrm{d}t \int \mathrm{d}^2 S \sqrt{1 - v_\perp^2} - B \int \mathrm{d}t \int \mathrm{d}^3 r, \tag{4.18}$$

which describes an "empty bag". The motion of the surface describes the dynamical evolution of the bag, and the vacuum pressure acts as a potential in the equations of motion.

We note that the limit $\sigma \to 0$ in the Hamiltonian associated with the action of eq. (4.18) still describes a dynamical bag whose surface becomes massless. However, the limit $\sigma \to 0$ in the action itself does not describe a dynamical system.

In contrast, the limit $B \to 0$ in the Hamiltonian formulation is the same as in the Lagrangian formulation, since only a potential term is made vanishing for the dynamical bubble.

These limits are illustrated on a simple example in one space – one time dimension as shown in fig. 4.3. In the simplified one-dimensional world we shall write the action for the empty bag as

$$W = -\sigma \int \mathrm{d}t \sqrt{1 - \dot{z}_1^2} - \sigma \int \mathrm{d}t \sqrt{1 - \dot{z}_2^2} - B \int \mathrm{d}t \int_{z_1}^{z_2} \mathrm{d}z. \tag{4.19}$$

The Hamiltonian which is derived from the action (4.19) is

$$H = \sqrt{\sigma^2 + p_1^2} + \sqrt{\sigma^2 + p_2^2} + B|z_2 - z_1|. \tag{4.20}$$

In our illustration the surface under tension corresponds to the sum of two point particles with mass σ, and the vacuum pressure in the Hamiltonian (4.20) acts as a potential. This potential corresponds to a relativistically covariant, long range interaction between the two surface points. As $\sigma \to 0$ we still have a dynamical system in Hamiltonian form where the two end-points are associated with massless particles:

$$H = |p_1| + |p_2| + B|z_2 - z_1|.$$

There is no dynamics, however, if $\sigma \to 0$ is taken in (4.19), that is in the Lagrangian formulation.

The limit $B \to 0$ can be taken both in the action (4.19) and the Hamiltonian (4.20), and we are left with the sum of two point particles of mass σ in this limit.

In three dimension we would get a relativistic bubble of the Dirac variety in the same limit, since the surface points are connected there, in contrast with the disjoint end points of the one-dimensional example.

Vacuum pressure as described by (4.17) may serve as the potential energy term of quark bag dynamics without introducing surface tension. The dynamical quark and gluon fields of the interior make the bag a constrained dynamical system which requires a particular treatment in the Hamiltonian formulation with the stumbling-block of non-linear second class constraints in Dirac's

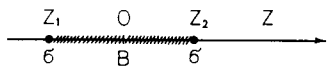

Fig. 4.3. One-dimensional model where volume energy acts between the points of mass σ.

terminology. This model construction was chosen by the M.I.T. group in the original formulation of the quark bag model.

For illustration of the highly constrained M.I.T. Hamiltonian, let us consider the one-dimensional model where a neutral scalar field $\phi(z, t)$ is confined between a fixed wall at $z = 0$ and a moving point $z = \xi(t)$ which is the substitute for the surface of the bag in one dimension (fig. 4.4). The inside of the bag corresponds to the region $0 < z < \xi$.

The Lagrangian is defined as

$$L = \int_0^{\xi(t)} \mathrm{d}z\{\tfrac{1}{2}\phi_{,t}^2 - \tfrac{1}{2}\phi_{,z}^2 - B\} - \sigma\sqrt{1-\dot{\xi}^2}, \tag{4.21}$$

with the boundary condition

$$\phi(0, t) = \phi(z = \xi(t), t) = 0 \tag{4.22}$$

on the confined field $\phi(z, t)$. $\phi_{,t}$ and $\phi_{,z}$ stand for the derivatives with respect to t and z.

Vacuum pressure in eq. (4.21) represents a linear potential $B\xi$ for the surface point ξ. The surface point carries kinetic energy as a relativistic particle of mass σ.

The dynamical coordinates of the model are $\phi(z, t)$ for $0 < z < \xi(t)$ and $\xi(t)$. In curvilinear coordinates x, τ,

$$z = \xi(t)x, \qquad x \in [0, 1]$$

$$t = \tau,$$

the number of dynamical degrees of freedom becomes fixed, for our convenience. The Lagrangian in curvilinear coordinates is given by

$$L = \int_0^1 \mathrm{d}x\{\tfrac{1}{2}\xi\phi_{,\tau}^2 - x\dot{\xi}\phi_{,\tau}\phi_{,x} + \frac{1}{2\xi}(x^2\dot{\xi}^2 - 1)\phi_{,x}^2\} - B\xi - \sigma\sqrt{1-\dot{\xi}^2}.$$

In the Hamiltonian formulation the canonical momenta are defined as

$$\pi = \delta L/\delta\phi_{,\tau} = \xi\phi_{,\tau} - x\dot{\xi}\phi_{,x}, \tag{4.23}$$

$$p = \delta L/\delta\dot{\xi} = -\frac{1}{\xi}\int_0^1 \mathrm{d}x x\pi\phi_{,x} + \frac{\sigma\dot{\xi}}{\sqrt{1-\dot{\xi}^2}}. \tag{4.24}$$

The velocities can be expressed from eqs. (4.23) and (4.24) in terms of the canonical variables ξ, p and

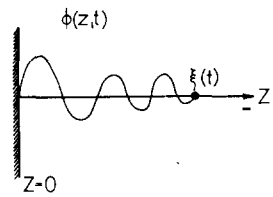

Fig. 4.4. One-dimensional scalar field confined between a rigid wall and a moving point of mass σ.

ϕ, π. We find the following Hamiltonian:

$$H = \frac{1}{\xi}\int_0^1 \mathrm{d}x(\tfrac{1}{2}\pi^2 + \tfrac{1}{2}\phi_{,x}^2) + B\xi + \left[\sigma^2 + \left(p + \frac{1}{\xi}\int_0^1 \mathrm{d}x x\pi\phi_{,x}\right)^2\right]^{1/2}.$$

The Poisson brackets

$$\{\xi, p\}_{\mathrm{P}} = 1,$$

and

$$\{\phi(x,\tau), \pi(x',\tau)\}_{\mathrm{P}} = \delta(x - x')$$

are valid between canonically conjugate variables.

In the Hamiltonian formulation it is understood that the dynamical coordinates $\phi(x = 0, \tau)$ and $\phi(x = 1, \tau)$ are eliminated from the problem as required by eq. (4.22). They are kept zero in any expansion of the field $\phi(x, \tau)$.

The quantum theory of the model is best described in field-diagonal representation. The states of the system are characterized by functionals $\Psi[\xi, \phi(x)]$, and the canonical momenta may be represented as differential operators acting upon the wave functional $\Psi[\xi, \phi(x)]$. We recall from free field theory that the representation

$$p = \frac{\hbar}{\mathrm{i}}\frac{\partial}{\partial\xi}, \pi \to \frac{\hbar}{\mathrm{i}}\frac{\delta}{\delta\phi(x)}$$

is applied there. The time independent Schrödinger equation

$$H\Psi = E\Psi$$

becomes a functional integro-differential equation.

Now we come to the important point. If there is no kinetic energy associated with the surface point, and $\sigma = 0$ is set in the Lagrangian (4.21), confinement is provided by vacuum pressure alone, in accordance with the M.I.T. strategy. The defining equation for p (eq. (4.24)) becomes a constraint then,

$$p + \frac{1}{\xi}\int_0^1 \mathrm{d}x x\pi\phi_{,x} = 0, \tag{4.25}$$

since it does not contain the velocity $\dot{\xi}$. Equation (4.25) is a constraint among the canonical variables in Dirac's terminology expressing the fact that not all of them are independent. The origin of the constraint is that the Lagrangian (4.21) with $\sigma = 0$ does not contain the surface velocity, so that there is no independent canonical momentum belonging to the end point ξ.

As we shall see in the next section, further secondary constraints are generated in the system from consistency requirements. At the end, the second class constraints of Dirac may be used to eliminate the redundant dynamical variables ξ and p, and the Poisson brackets are replaced by Dirac brackets in the canonical formulation of the quantum theory.

Since the constraints are non-linear, the procedure is very difficult to carry out in an explicit way. There is no similar difficulty when surface tension is present with kinetic energy in the Lagrangian.

5. Hamiltonian formulation and quantization

5.1. Quantization with constraints

The main difficulty with the quantization of the bag model with quark and gluon constituents lies in the fact that it is a constrained canonical system. For some reasons such systems occur frequently among the physically interesting theories. If it were the only criterion of building up a successful theory, the bag model would be certainly unbeatable:

a) constraints arise due to the physically unimportant curvilinear system of coordinates inside the bag's surface;

b) the gluon field theory is constrained in itself;

c) in the bag model with pure volume pressure the surface variables are not independent degrees of freedom which leads to additional constraints.

As we have seen, constraints type a) can be avoided by choosing an appropriate parametrization for the curvilinear coordinate system, while the gluon field brings in no new problem relative to the conventional theory, as far as constraints are concerned. The constraints type c) represent the real obstacle in quantizing the MIT bag model.

Although a general formalism is available for the quantization of singular systems of this type, the application of the method is problematic. The first steps have been made by Shalloway, then Rebbi and Johnson proposed a method which may bring the quantization of the bag under vacuum pressure attainable in $3+1$ dimension.

As a simple illustration of this method, we shall consider the $1+1$ dimensional model of subsection 4.2. The quantization procedure in the presence of surface tension will be demonstrated on a model with point-like quarks coupled to gauge fields.

Both cases (vacuum pressure versus surface tension) will be further examplified by discussing the approximation of small oscillations.

Before turning to the main body of this section let us summarize briefly Dirac's theory of singular dynamical systems.

Dirac's theory of singular dynamical systems

A dynamical system is called singular if the expressions $p_i = \partial L(q, \dot{q})/\partial \dot{q}_i$ do not determine unambiguously the velocities $\dot{q}_i$ as functions of the momenta p_i. Dirac has worked out the general framework for the canonical quantization of these systems. We give here a very brief summary of the method and try to clarify the necessary details in the subsequent applications, later on.

In a singular theory the expression $\partial L(q, \dot{q})/\partial \dot{q}_i$ and the coordinates q_i satisfy a number of identities and, therefore, the momenta are subject to the so-called primary constraints $\chi_1^l(q, p) = 0$. Consequently, the Hamiltonian is determined only up to a linear combination of these constraints with arbitrary coefficients. $\chi_1^l(q, p)$ must be zero at any time, which gives the consistency condition

$$\{\chi_1^l(q, p), H\}_P = 0,$$

leading usually to a number of secondary constraints $\chi_2^l(q, p) = 0$ and/or fixing some of the unknown coefficients in the Hamiltonian. The secondary constraints may generate new constraints, and so on.

At the end, the constraints fall into two important classes. In the first class are those whose Poisson brackets with any of the constraints are zero or equal to the linear combination of the constraints. All the others belong to the second class.

In quantizing the theory, the first class constraints are imposed on the state vectors as subsidiary conditions $\chi|\psi\rangle = 0$. We cannot proceed similarly with the second class constraints because acting with their commutator on a state vector we would run into an inconsistency. In the quantized theory the second class constraints are imposed as operator equations. In this case the commutation relations of the dynamical variables must be modified in such a way that the second class constraints commute with any expression of the variables. As a solution, Dirac has proposed the following method:

First, we define in the classical theory modified brackets (Dirac brackets) for the dynamical variables:

$$\{A, B\}_{\mathrm{D}} = \{A, B\}_{\mathrm{P}} - \{A, \chi_i\}_{\mathrm{P}}(\Delta^{-1})_{ik}\{\chi_k, B\}_{\mathrm{P}}$$

where

$$\Delta_{ik} = \{\chi_i, \chi_k\}_{\mathrm{P}}.$$

In the quantization procedure the Dirac bracket is replaced by the quantum mechanical commutator for operators, in the usual manner.

It can be shown that the equations of motion remain the same with the newly defined commutators, and

$$[\chi_i, A]_- = 0$$

is valid for any A, as required for consistency. Now, the dependent variables can be eliminated from the operator equations $\chi_i = 0$ and the problem is defined finally in terms of the independent variables alone. Unfortunately, the new commutation relations for the remaining variables are often very complicated and difficult to represent by operators in Hilbert space.

In certain cases there are methods to circumvent the introduction of Dirac brackets with the help of a suitable transformation of the variables. This is the way followed by Rebbi and Johnson, as we shall see in the next subsection.

5.2. Quantization of the bag model with pure volume tension

As we have indicated previously, the quantization of the bag model when vacuum pressure alone provides for the binding effects is a difficult task. Though in one space – one time dimension, where the solutions are explicitly known, the quantization can be carried out in light-cone variables, this method has not been proved to be applicable so far in higher dimensions.

Rebbi and Johnson have proposed a method first which may bring the quantization of the bag under vacuum pressure attainable in $3+1$ dimension. Johnson formulates the problem in his own language, nevertheless the proposed procedure is in accordance with Dirac's general formalism. We shall use Dirac's terminology.

As a simple illustration of the method, let us consider the $1+1$ dimensional model of subsection 4.2. A neutral scalar field ϕ is confined between a fixed wall and a moving point $\xi(t)$. The action for $\sigma = 0$ is

$$W = \int \mathrm{d}t \int_0^{\xi(t)} \mathrm{d}z \{\tfrac{1}{2}\phi_{,t}^2 - \tfrac{1}{2}\phi_{,z}^2 - B\}$$

with the Dirichlet boundary condition

$$\phi(0, t) = \phi(\xi(t), t) = 0. \tag{5.1}$$

As we have seen, in curvilinear coordinates x, τ,

$$z = \xi(t)x, \qquad x \in [0, 1]$$
$$t = \tau,$$

the canonical momenta are

$$\Pi(x) = \xi\phi_{,\tau} - x\dot{\xi}\phi_{,x}, \tag{5.2}$$

$$p = -\frac{1}{\xi}\int_0^1 \mathrm{d}x x\Pi\phi_{,x}. \tag{5.3}$$

From eqs. (5.2) and (5.3) the velocities cannot be expressed in terms of the canonical coordinates and momenta because (5.3) is only a relation between the coordinates and momenta. Therefore, there is a primary constraint in the theory

$$\chi_1 \equiv p + \frac{1}{\xi}\int_0^1 \mathrm{d}x x\Pi\phi_{,x} = 0. \tag{5.4}$$

Consequently, the Hamiltonian

$$\int_0^1 \mathrm{d}x\Pi\phi_{,\tau} + p\dot{\xi} - L$$

is not unique:

$$H = \frac{1}{\xi}\int_0^1 \mathrm{d}x(\tfrac{1}{2}\Pi^2 + \tfrac{1}{2}\phi_{,x}^2) + B\xi + c\chi_1. \tag{5.5}$$

In eq. (5.5) the multiplicator c is an arbitrary function of the dynamical variables. The constraint (5.4) must be valid at any time, so that

$$\{\chi_1, H\}_{\mathrm{P}} = 0$$

is necessary. A secondary constraint is generated

$$\chi_2 = \frac{1}{2\xi^2}(\phi_{,x}^2 - \Pi^2)|_{x=1} - B,$$

which is recognized as the non-linear boundary condition of the MIT model,

$$\tfrac{1}{2}\partial_\mu\phi\partial^\mu\phi + B = 0.$$

The Poisson bracket of the constraints χ_1 and χ_2 does not vanish,

$$\{\chi_1, \chi_2\}_{\mathrm{P}} \neq 0,$$

so that χ_1 and χ_2 are second class constraints. Therefore, the consistency condition for χ_2 does not generate a new constraint, instead, the multiplicator becomes fixed by

$$\dot{\chi}_2 = \{\chi_2, H\}_P = 0.$$

This leads to a unique Hamiltonian. In the quantized theory the constraints $\chi_i = 0$, $i = 1, 2$ are imposed as operator equations. The coordinate ξ and the momentum p of the bag's end point can be eliminated from the theory, so the problem is defined finally in terms of the field variables alone. For consistency, however, we have to use modified commutators and to remove the associated difficulties.

The method of Johnson gets around the above procedure with the help of a suitable transformation of the dynamical variables in such a way that the Poisson brackets of the new field variables with, say, the constraint χ_1 vanish. Then the Dirac brackets among the new field variables coincide with the Poisson brackets. Therefore, the usual commutation relations become applicable in the quantized theory.

Following Johnson first we write an expansion for the field operators which automatically satisfies the Dirichlet boundary conditions (5.1):

$$\phi(x, t) = (1 - x^2) \sum_{k=1}^{\infty} q_k(t) \frac{\mathrm{d}}{\mathrm{d}x} P_{2k}(x) \frac{4k+1}{2k(2k+1)}, \tag{5.6}$$

$$\Pi(x, t) = \sum_{k=1}^{\infty} \Pi_k(t) \frac{\mathrm{d}}{\mathrm{d}x} P_{2k}(x). \tag{5.7}$$

In the expansions (5.6) and (5.7) the functions $\{\mathrm{d}P_{2k}(x)/\mathrm{d}x\}$ form a complete system in the interval $x \in (0, 1)$ with respect to the weight $1 - x^2$.

The Hamilton function and the constraints can be expressed in terms of the expansion coefficients q and Π of eqs. (5.6) and (5.7). After elementary calculations one finds

$$H = \frac{1}{\xi}\left(\tfrac{1}{2}\Pi \frac{1}{M} \Pi + \tfrac{1}{2} q V q\right) + B\xi,$$

$$\chi_1 = p + \frac{1}{2\xi}(\Pi S q + q S^{\mathrm{T}} \Pi),$$

$$\chi_2 = \frac{1}{2\xi^2}(qAq + \Pi B \Pi) - C,$$

where the matrices $1/M, V, \ldots, C$ are defined as simple integrals of the Legendre polynomials:

$$\left(\frac{1}{M}\right)_{kl} = \int_0^1 \mathrm{d}x \frac{\mathrm{d}}{\mathrm{d}x} P_{2k} \frac{\mathrm{d}}{\mathrm{d}x} P_{2l},$$

$$V_{kl} = \delta_{kl}(4k + 1), \text{ etc.}$$

Now, let us consider the following transformation of the variables:

$$\bar{q} = \exp\left\{-\ln \frac{\xi}{\xi_0} S\right\} q, \qquad \bar{\Pi} = \exp\left\{\ln \frac{\xi}{\xi_0} S^{\mathrm{T}}\right\} \Pi. \tag{5.8}$$

We can check by direct calculation that

$$\{\bar{q}_i, \chi_1\}_P = 0, \qquad i = 1, 2, \ldots$$

$$\{\bar{\Pi}_i, \chi_1\}_P = 0, \qquad i = 1, 2, \ldots$$

and therefore

$$\{\bar{q}_i, \bar{\Pi}_j\}_D = \{\bar{q}_i, \bar{\Pi}_j\}_P = \{q_i, \Pi_j\}_P = \delta_{ij}. \tag{5.9}$$

At the end we can eliminate ξ and p with the help of the constraints χ_1 and χ_2. Therefore, the Hamiltonian will be given as a function of the variables $\bar{q}$ and $\bar{\Pi}$, and the usual canonical commutation relations (5.9) are valid for $\bar{q}$ and $\bar{\Pi}$. The price we pay is that the Hamiltonian becomes a complicated function of the variables $\bar{q}$ and $\bar{\Pi}$, but the problem is at least well defined.

In practice we may try the truncation of the expansions (5.6) and (5.7) retaining only a few modes. Even this problem is rather involved and no explicit solution exists so far. There are, however, interesting results in the approximation of small oscillations around a classical solution, which we shall discuss in the next subsection.

5.3. Small oscillation approximation

In the previous quantization procedure an important point was the transformation (5.8) by which introduction of Dirac brackets has been circumvented.

There are other methods to achieve the same goal. Suppose we have two second class constraints (the number of second class constraints is always even),

$$\chi_1 = p_1 = 0, \tag{5.10}$$

$$\chi_2 = f(q_1, q_2, \ldots, p_1, p_2, \ldots) = 0, \tag{5.11}$$

where p_i is the momentum conjugate to q_i. We can eliminate the first degree of freedom, if we solve the second equation for q_1 and substitute q_1 with this solution into the Hamiltonian, and into all the other expressions. At the same time, we can retain the usual Poisson brackets for q_k, p_k, $k = 2, 3, \ldots$.

So we can try to transform the primary constraints into the form of eq. (5.10). Rebbi has noticed that in the case of small oscillation approximation there was a linear canonical transformation which could be found and performed easily to implement the idea.

To illustrate Rebbi's method, we consider the case of a complex scalar field subject to Dirichlet boundary conditions.

The equations of motion follow from the Lagrangian

$$L = \int_{\text{bag}} \mathrm{d}^3 y \{\partial_\Lambda \phi \partial^\Lambda \phi^* - B\},$$

and the non-linear boundary condition has the form:

$$\partial_\Lambda \phi \partial^\Lambda \phi^* = -B. \tag{5.12}$$

It is easy to find exact solutions where the bag is a static sphere. Let us choose the lowest energy solution

$$\phi = \frac{\sqrt{B} R_0^2}{\pi} \frac{\sin \pi(|y|/R_0)}{|y|} \exp\left\{-\mathrm{i}\pi \frac{t}{R_0}\right\},$$

and consider the quantization of the small oscillations about this static cavity solution.

We follow the usual path: an appropriate curvilinear coordinate system will be introduced, then the form of the primary constraints and the Hamiltonian has to be found.

Rebbi found the mapping

$$y^0 = x^0$$

$$y_i = Rx_i + \sum_{l,m} b_{l,m}\partial_i^x (x^l Y_m^l(\vartheta, \varphi))$$

particularly useful. Here x, ϑ, φ are the deformed polar coordinates of y ($x \in (0, 1)$), and R, $b_{l,m}$ are the coordinates describing the motion of the surface. $b_{l,m}$ is responsible for an arbitrary deformation at a fixed volume, while a dilation can be described by R.

The Hamiltonian and the constraints have the form

$$H = \int \mathrm{d}^3x \left(\Pi^* \cdot \Pi M + M_{ij} \frac{\partial \phi^*}{\partial x_j} M_{ik} \frac{\partial \phi}{\partial x_k} M^{-1} + BM^{-1} \right) + c_\alpha \chi_\alpha^{(1)},$$

$$\chi_\alpha^{(1)} = P_\alpha - \int \mathrm{d}^3x \left(\frac{\delta y_i}{\delta b_\alpha} M_{ij} \frac{\partial \phi^*}{\partial x_j} \Pi + \text{c.c.} \right) = 0,$$

where b_α is a shorthand notation for all the boundary coordinates $R, b_{l,m}$; M_{ij} is the inverse of the matrix $\partial y_i / \partial x_j$ and $M = \det M_{ij}$. Π and p_α are the canonical momenta conjugate to ϕ and b_α respectively.

As we have learned from the previous example, the consistency conditions of $\chi_\alpha^{(1)}$ lead to new constraints $\chi_\alpha^{(2)}$ (equivalent to the non-linear boundary condition (5.12)) and $\chi_\alpha^{(1)}$, $\chi_\alpha^{(2)}$ form a second class system.

Let us expand the fields into the eigenstates of the spherical cavity,

$$\phi = \sum_{l,m,n} \mathrm{i} N_{ln} \frac{a_{lmn} - b_{lmn}^*}{\sqrt{2\omega_{ln}} R_0} J_l(\omega_{ln} x) Y_m^l(\vartheta, \varphi),$$

$$\Pi = \sum_{l,m,n} N_{ln}(a_{lmn} + b_{lmn}^*) R_0 \sqrt{\frac{\omega_{ln}}{2}} J_l(\omega_{ln} x) Y_m^l(\vartheta, \varphi),$$

where J_l is the lth spherical Bessel function, $J_l(\omega_{ln}) = 0$. N_{lm} is a normalization constant. The static cavity solution is characterized now by $a_{001} = A$, and, in the small oscillation approximation, all the other variables can be considered as small.

The next step is to expand H up to second order in these small variables. The variables with different l and m decouple. Consider the $l = 1$ case as an example,

$$H = \frac{16\pi B}{3} \left(\frac{Q}{4B} \right)^{3/4} + \frac{1}{R_0} \sum_{n=1}^{\infty} \sum_{m=1}^{3} [(\omega_{1n} - \pi) a_{1mn}^* a_{1mn} +$$

$$+ (\omega_{1n} + \pi) b_{1mn}^* b_{1mn}] + c_{1m} \chi_{1m}^{(1)} + (l \neq 1 \text{ terms}),$$

where Q is the total charge of the system,

$$Q = A^* A + \sum_{l,m,n \neq 0,0,1} (a_{lmn}^* a_{lmn} - b_{lmn}^* b_{lmn}).$$

In terms of the new variables the constraint $\chi_{1,m}^{(1)}$ becomes

$$\chi_{1,m}^{(1)} = p_{1,m} + \frac{b_{1m}}{R_0} \sum_{n=1}^{\infty} (-1)^n \sqrt{\frac{\omega_{1n}}{\pi}} \left(\frac{a_{1mn} A^* - a_{1mn}^* A}{(\omega_{1n} - \pi)} + \frac{b_{1mn}^* A^* - b_{1mn} A}{(\omega_{1n} + \pi)} \right) + (\text{higher order terms}).$$

By a canonical transformation, we take $\chi^{(1)}_{1,m}$ as the new momentum variable conjugate to b_{1m}:

$$p_{1m} \to P_{1m} = \chi^{(1)}_{1,m},$$

$$a_{1mn} \to \tilde{a}_{1mn} = a_{1mn} + \frac{b_{1m}}{R_0} A(-1)^n \sqrt{\frac{\omega_{1n}}{\pi}} \frac{1}{\omega_{1n} - \pi} + \text{(higher order terms)},$$

$$b_{1mn} \to \tilde{b}_{1mn} = b_{1mn} - \frac{b_{1m}}{R_0} A^*(-1)^n \sqrt{\frac{\omega_{1n}}{\pi}} \frac{1}{\omega_{1n} + \pi} + \text{(higher order terms)}.$$

It is straightforward to express H in terms of the transformed variables and to find the secondary constraints $\chi^{(2)}_{1m}$

$$\chi^{(2)}_{1m} = \{\chi^{(1)}_{1m}, H\}_{\mathrm{P}} = 0.$$

$\chi^{(1)}_{1m} = P_{1m}$ and $\chi^{(2)}_{1m}$ form the specified type of second class constraint pair which we were looking for. The variable b_{1m} can be eliminated using the constraint $\chi^{(2)}_{1m}$, and the Hamiltonian will be expressed entirely in terms of the field degrees of freedom. This Hamiltonian can be diagonalized and we get the eigenvalue equation:

$$\omega^2 \sum_n \left\{ \frac{\omega_{n1}}{\omega_{n1} - \pi} \frac{1}{\omega^2 - (\omega_{n1} - \pi)^2} + \frac{\omega_{n1}}{\omega_{n1} + \pi} \frac{1}{\omega^2 - (\omega_{n1} + \pi)^2} \right\} = 0.$$

The $\omega = 0$ solution corresponds to the rigid displacement of the bag as a whole, it is not a genuine excitation. Let us denote the positive solutions of the eigenvalue equation by ω_n. Then the P-wave small oscillations of the bag are described by the Hamiltonian

$$H = \left(\frac{Q}{4B}\right)^{-1/4} \left\{ \frac{4\pi}{3} Q + \sum_{n=1}^{\infty} \sum_{m=1}^{3} \omega_n c^*_{nm} c_{nm} \right\}, \tag{5.13}$$

where the c_{nm} amplitudes satisfy the commutation relation

$$[c_{nm}, c^*_{n'm'}] = \delta_{nn'} \delta_{mm'}.$$

It can be seen from eq. (5.13) that the small parameter of the small oscillation expansion is $1/Q$.

Consider a bag with total charge Q in the lowest S state. The excitation to the lowest P state would require some extra energy:

$$\Delta E = \omega_1 \left(\frac{Q}{4B}\right)^{-1/4} \approx 3.537 \left(\frac{Q}{4B}\right)^{-1/4}.$$

This excitation energy is much larger than that of required to replace an S-wave state with a P-wave state in the static cavity approximation

$$\Delta E_{\mathrm{cav}} = 1.351 (Q/4B)^{-1/4}.$$

Of course, a P-wave state in a spherical bag is not a solution – the non-linear boundary condition is violated. The striking difference between the numerical results above is a strong warning against degrading the bag model to the level of a potential picture of the old static quark model. We shall return to this question in the next section.

5.4. Surface tension. Point-like quarks coupled to gauge fields

Quite apart from physical considerations, the introduction of surface tension into the model offers a great advantage: there are no non-linear constraints in the theory.

Let us consider an Abelian gauge field confined by surface tension and coupled to point-like quarks. As we argued previously, a system of curvilinear coordinates x^μ has to be introduced where the surface of the bag is fixed. We identify it with the $x^1 = 1$ surface. We proceed similarly as in the case of Dirac's electron bag model. For reference, we introduce a rectilinear and orthogonal coordinate system y^Λ. The inside of the bag is fitted in with an arbitrary deformed system of polar coordinates where x^1 varies in the interval (0, 1):

$$\begin{aligned} y^0 &= x^0, \\ y^1 &= x^1 \rho \cos x^2, \\ y^2 &= x^1 \rho \sin x^2, \\ y^3 &= x^3. \end{aligned} \tag{5.14a}$$

The function $\rho = \rho(x^0, x^2, x^3)$ describes the shape and motion of the surface. We take now as general coordinates the $A_\mu(x)$ for an Abelian gauge field, ξ_n^i for the nth quark ($\xi_n^0 = x^0 = y^0$), and $\rho(x^2, x^3)$ for the surface.

Let us consider the case of a quark and antiquark inside the bag. The action W is written as

$$W = -\int_{x^1 \in (0,1)} \mathrm{d}^4x J\left(\tfrac{1}{4} g^{\mu\rho} g^{\nu\sigma} F_{\mu\nu} F_{\rho\sigma} + j^\mu A_\mu\right) - \sigma \int_{x^1 = 1} M \, \mathrm{d}x^0 \, \mathrm{d}x^2 \, \mathrm{d}x^3$$
$$- \sum_{n=1}^{2} m \int \mathrm{d}^4x \sqrt{\xi_{n,0}^\nu \xi_{n,0}^\mu g_{\mu\nu}}\, \delta^3(x^r - \xi_n^r), \tag{5.14b}$$

where $g_{\mu\nu} = y^\Lambda_{,\mu} y_{\Lambda,\nu}$ and $J = \sqrt{-\det g_{\mu\nu}}$ is the Jacobian of the invariant four-dimensional volume element. M^2 is the determinant of g_{ab} (a, b take on the values of 0, 2, 3), while the current four-vector of the quarks is given by

$$j^\mu(x) = \frac{1}{J} \sum_{n=1}^{2} g_n \xi_{n,0}^\mu \delta^3(x^r - \xi_n^r), \quad g_1 = -g_2 = g.$$

Here g sets the quark–gluon coupling.

This is also a constrained system due to the presence of vector gluon fields, but its handling does not require extra effort relative to the conventional case.

Without going into the calculational details we summarize the results. The Hamiltonian has the following form:

$$H = \int_{x^1 \in (0,1)} \mathrm{d}^3x \left(-\frac{1}{2K} g_{rs} B^r B^s + \tfrac{1}{4} K e^{rs} e^{tu} F_{rt} F_{su}\right) + \sum_{n=1}^{2} (m^2 - e^{rs} p_{nr}^* p_{ns}^*)^{1/2} +$$
$$+ \int_{x^1 = 1} \left[\left(\frac{\eta^* \rho}{K}\right)^2 + \sigma^2\right]^{1/2} (g_{22} g_{33} - g_{23}^2)^{1/2} \, \mathrm{d}x^2 \, \mathrm{d}x^3 + \int \mathrm{d}^3x (c_1 \chi_1 + c_2 \chi_2), \tag{5.15}$$

where B^μ is the canonical momentum conjugate to A_μ, χ_1 and χ_2 are first class constraints of the

vector gluon theory,

$$\chi_1 = B^0(x) = 0,$$

$$\chi_2 = B^r{}_{,r}(x) - \sum_{n=1}^{2} g_n \delta^3(\boldsymbol{x} - \boldsymbol{\xi}_n).$$

They are multiplied by the arbitrary coefficients c_i in the Hamiltonian (the gauge freedom is reflected in this arbitrariness). The indices r, s, t, u take on the values of $1, 2, 3$, e^{rs} is the inverse of g_{rs}, $K = \sqrt{-\det g_{rs}}$ and η^*, p^*_{nr} are defined by

$$\eta^*(x^2, x^3) = \eta(x^2, x^3) - \frac{1}{\rho}\int_0^1 \mathrm{d}x^1 x^1 F_{r1} B^r - \frac{1}{\rho}\sum_{n=1}^{2} \xi^1_n p^*_{n1} \delta(x^2 - \xi^2_n)\delta(x^3 - \xi^3_n),$$

$$p^*_{nr} = p_{nr} + g_n A_r(\boldsymbol{\xi}_n),$$

where $\eta(x^2, x^3)$ and $\rho(x^2, x^3)$ as well as p_{nr} and ξ^r_n are canonically conjugate pairs of variables with the Poisson brackets

$$\{\rho(x^2, x^3), \eta(x^{2'}, x^{3'})\}_{\mathrm{P}} = \delta(x^2 - x^{2'})\delta(x^3 - x^{3'}),$$

$$\{\xi^r_n, p_{n's}\} = \delta_{nn'}\delta_{rs}.$$

Further we get the following boundary conditions:

$$B^1|_{x^1=1} = 0,$$

and

$$\left(\delta_{r1}\frac{\dot\rho}{\rho}B^1 - \frac{\dot\rho}{\rho}B^r - Ke^{s1}e^{rt}F_{st}\right)\Big|_{x^1=1} = 0.$$

There are equivalent to $n_\mu F^{\mu\nu}|_{x^1=1} = 0$ in the Lagrangian formulation. The radial velocity $\dot\rho$ is defined here as $\dot\rho = \{\rho, H\}_{\mathrm{P}}$ in terms of the coordinates and momenta.

The first term in the Hamiltonian (5.15) is the contribution of the vector gluon field as expressed in curvilinear coordinates. The third term is the surface Hamiltonian. A fixed point in the rectilinear laboratory coordinate system performs a nonphysical motion in the curvilinear system according to the specified parametrization of (5.14). This contribution is included in the momentum $\eta(x^2, x^3)$, so it must be subtracted away. That is the reason that $\eta^*(x^2, x^3)$ occurs in the surface Hamiltonian.

The Hamiltonian in (5.15) is rather complex. It will be useful to consider an approximation in order to gain some insight into the surface dynamics and its connection with the gluon field. Let us assume that the quarks are heavy and approximate them by two external sources fixed on the x^3 axis at $x^3 = \pm a/2$.

If a is large (relative to $\sigma^{-1/3}$), there is an approximate static, classical solution: a vortex, which has been discussed in some detail in subsection 3.3. We shall consider the quantization of the small radial oscillations around this classical solution. The variables depend only on x^1 and x^0.

Instead of using first class constraints and subsidiary conditions, let us introduce two extra constraints into the theory,

$$\chi_3 = A_0(x) = 0,$$

$$\chi_4 = (Ke^{ir}A_r)_{,i} = 0.$$

χ_i, $i = 1, \ldots, 4$ form a second class constraint-system and they become operator equations in the quantized theory. If we restrict ourselves to radial excitations, it is easy to show that A_0, B^0, A_1, B^1 can be eliminated from the theory, A_2, B^2 form an unconstrained pair of variables, while A_3, B^3 are constrained by

$$\chi = \int_0^1 \mathrm{d}x^1 B^3 = g/2\pi,$$

$$\bar{\chi} = \int_0^1 \mathrm{d}x^1 x^1 A_3 = 0.$$

The form of the vortex solution in terms of these variables is given by

$$B^r = \delta_{r3} \frac{g}{\pi} x^1, \qquad A_r = 0,$$

$$\rho = \rho_0; \qquad \rho_0 = g^2/2\pi^2\sigma.$$

Let us introduce

$$B^r_{\mathrm{T}} = B^r - \delta_{r3} \frac{g}{\pi} x^1, \qquad \epsilon = \rho - \rho_0,$$

and expand the Hamiltonian up to second order in terms of the small variables. We find the following result

$$H = \int_0^1 \mathrm{d}x^1 \left[\left(\tfrac{1}{2} x^1 (\bar{B}^2_{\mathrm{T}})^2 + \frac{1}{2\rho_0^2 x^1} (\bar{B}^3_{\mathrm{T}})^2 \right) \frac{1}{2\pi a} + \left(\frac{1}{2\rho_0^2 x^1} F_{12}^2 + \tfrac{1}{2} x^1 F_{13}^2 \right) 2\pi a \right] +$$

$$+ \frac{3\pi a \sigma}{\rho_0} \epsilon^2 + \frac{1}{4\pi a \rho_0 \sigma} \bar{\eta}^{*2} + (c\text{-number}),$$

where

$$\bar{B}^i_{\mathrm{T}}(x^1) = \int_0^{2\pi} \mathrm{d}x^2 \int_{-a/2}^{a/2} \mathrm{d}x^3 B^i_{\mathrm{T}}(x),$$

$$\bar{\eta} = \int_0^{2\pi} \mathrm{d}x^2 \int_{-a/2}^{a/2} \mathrm{d}x^3 \eta,$$

$$\bar{\eta}^* = \bar{\eta} + \frac{2ag}{\rho_0} \int_0^1 \mathrm{d}x^1 (x^1)^2 F_{13},$$

$$F_{12} = A_{2,1}, \qquad F_{13} = A_{3,1},$$

and we have two second class constraints

$$\chi = \int_0^1 \mathrm{d}x^1 \bar{B}^3_{\mathrm{T}} = 0, \qquad \bar{\chi} = \int_0^1 \mathrm{d}x^1 x^1 A_3 = 0.$$

The corresponding Dirac brackets (valid in the interior points) are given by

$$\{A_2(x^1), B_T^2(x^{1'})\}_D = \delta(x^1 - x^{1'}),$$
$$\{A_3(x^1), B_T^3(x^{1'})\}_D = (\delta(x^1 - x^{1'}) - 2x^{1'}),$$
$$\{\epsilon, \bar{\eta}\}_D = 1.$$

All the other brackets are equal to zero.

It is then straightforward to derive the Hamilton equations which have to be solved together with the boundary conditions

$$F_{12}|_{x'=1} = 0,$$
$$\left(F_{13} + \frac{g}{2\pi^2 a\sigma\rho_0^2}\bar{\eta}^*\right)\Big|_{x^1=1} = 0.$$

We find the following general solution

$$A_2 = \mathrm{i}\sum_i \rho_0^2 x^1 \frac{1}{\lambda_i} J_1(\lambda_i x^1) \frac{1}{N_i}\left(a_i \exp\left\{-\mathrm{i}\frac{\lambda_i}{\rho_0} t\right\} - \text{h.c.}\right),$$
$$B_T^2 = \sum_i \rho_0 J_1(\lambda_i x^1) \frac{1}{N_i}\left(a_i \exp\left\{-\mathrm{i}\frac{\lambda_i}{\rho_0} t\right\} + \text{h.c.}\right),$$
$$A_3 = \mathrm{i}\rho_0 \sum_i \frac{1}{\gamma_i}\left(J_0(\gamma_i x^1) - \frac{2}{\gamma_i} J_1(\gamma_1)\right)\frac{1}{Z_i}\left(b_i \exp\left\{-\mathrm{i}\frac{\gamma_i}{\rho_0} t\right\} - \text{h.c.}\right),$$
$$B_T^3 = \rho_0^2 x^1 \sum_i \left(J_0(\gamma_i x^1) - \frac{2}{\gamma_i} J_1(\gamma_i)\right)\frac{1}{Z_i}\left(b_i \exp\left\{-\mathrm{i}\frac{\gamma_i}{\rho_0} t\right\} + \text{h.c.}\right),$$
$$\epsilon = -\frac{\pi\rho_0^3}{g}\sum_i \frac{1}{\gamma_i} J_1(\gamma_i)\frac{1}{Z_i}\left(b_i \exp\left\{-\mathrm{i}\frac{\gamma_i}{\rho_0} t\right\} + \text{h.c.}\right), \tag{5.16}$$

where λ_i and γ_i are defined by the equations

$$J_0(\lambda_i) = 0,$$
$$(\gamma_i^2 + 1)J_1(\gamma_i) = 2\gamma_i J_0(\gamma_i).$$

$J_k(x)$ is the kth spherical Bessel function. The normalization factors are

$$N_i = \sqrt{\frac{2\pi a}{\lambda_i}}\,\rho_0^{3/2} J_1(\lambda_i),$$
$$Z_i = \sqrt{\pi a \frac{\gamma_i^4 + 6\gamma_i^2 - 3}{2\gamma_i^3}}\,\rho_0^{3/2} J_1(\gamma_i).$$

One can see by inspection of eqs. (5.16) that there are two types of radial excitations of the vortex. A color magnetic field along the vortex together with an azimuthal electric field can be excited without forcing the surface to oscillate. The other case is a collective motion, where the surface motion is intimately connected with the gluon gauge fields.

It can be shown that all the prescribed commutators are satisfied in the internal points of the bag, if we assign for a and b the following Dirac brackets

$$[a_i, a_j^+] = \delta_{ij},$$
$$[b_i, b_j^+] = \delta_{ij},$$

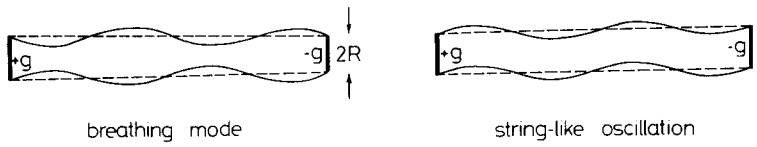

Fig. 5.1. Excitations of the elongated bag (vortex tube) with small amplitudes. The breathing mode of a massive gluon excitation and the string-like oscillation are shown.

and the Hamiltonian has the form

$$H = \sum_i \frac{\lambda_i}{\rho_0}\frac{1}{2}(a_i a_i^+ + a_i^+ a_i) + \sum_i \frac{\gamma_i}{\rho_0}\frac{1}{2}(b_i b_i^+ + b_i^+ b_i) + (c\text{-number}).$$

The general case can be treated along similar lines. The following physical picture emerges: there is an infinite mass spectrum of gluons generated by gauge field confinement. There are collective breathing and pure gluon excitations. We get also massless excitations propagating with the velocity of light along the vortex. These modes correspond to the oscillations of a string of finite width (electric vortex) without internal excitations (fig. 5.1).

5.5. The empty bag and the physical structure of the vacuum

For theoretical considerations and later spectroscopic applications it would be important to understand the possible relation between an empty bag and the structure of the physical vacuum.

One can demonstrate the existence of an "empty" bag in bagged quantum theory as follows. It is known from the first publication of the M.I.T. group [1.1] that there exists an exact solution in $1+1$ dimension for massless fermion fields confined by pure volume tension. Here we shall use their elegant results for demonstration.

Consider the spinor field $\psi(z, t)$ in $1+1$ dimension confined by pure volume tension. Inside the bag $\psi(z, t)$ satisfies the free Dirac equation and the linear boundary condition (4.1) together with the non-linear equation (4.3) are required on the boundary (end points) of the one-dimensional bag.

It can be shown that in light-cone variables $x^+ = \tau = (t+z)/\sqrt{2}$, $x^- = x = (t-z)/\sqrt{2}$ the general solution is of the form

$$\psi = \begin{pmatrix} ig(x) \\ f(\tau) \end{pmatrix}$$

for the two-component spinor field ψ. The lower component $f(\tau)$ may be expressed in terms of the dynamical variables

$$b_m(\tau) = b_m \exp\{-2\pi i m(B\tau/p)\}$$

as

$$f(\tau) = 2^{-1/4}\sqrt{\frac{B}{p}} \sum_{m=-\infty}^{+\infty}{}' b_m \exp\left\{-2\pi i m \frac{B\tau}{p}\right\},$$

where the prime on Σ indicates that m is summed over half-odd integers. A similar, though formally much more complicated expansion may be written for $g(x)$ through a non-linear transformation.

The dynamical variables $b_m(\tau)$ require the anti-commutation relations

$$\{b_m(\tau), b_n(\tau)\}_+ = 0,$$
$$\{b_m(\tau), b_n^+(\tau)\}_+ = \delta_{mn},$$

and the momentum operator $P = P^+$ in light-cone variables commutes with all b_m's. The momentum operator P and the average coordinate $\bar{x}(\tau)$ in the light-cone system are independent canonical variables with regard to the b_m's satisfying the quantum mechanical commutation relation

$$[\bar{x}(\tau), P] = \mathrm{i}.$$

The spectrum of P is continuous in the $(-\infty, \infty)$ interval.

The Hamiltonian operator $H \equiv P^-$ in the light-cone frame is given by

$$H = \frac{2\pi B}{P} \sum_{m=-\infty}^{+\infty}{}' m b_m^+ b_m. \tag{5.17}$$

To achieve a positive energy spectrum we must interpret the b_m's as follows ($m > 0$):

b_m	annihilates a fermion
$b_{-m} \equiv d_m^+$	creates an antifermion
b_m^+	creates a fermion
$b_{-m}^+ \equiv d_m$	annihilates an antifermion.

Then we can write the Hamiltonian (5.17) as

$$H = \frac{2\pi B}{P}\left[\sum_{m=1/2}^{\infty} m(b_m^+ b_m + d_m^+ d_m) + \frac{m_0^2}{4\pi B}\right],$$

where we have introduced m_0, the mass of the empty bag, which is undetermined due to the infinite zero-point fluctuations. The expression for the fermion charge is given by

$$Q = \sum_{m=1/2}^{\infty}{}' (b_m^+ b_m - d_m^+ d_m).$$

Briefly summarizing, there are positive energy fermions and antifermions with a (mass)^2 spectrum of half-odd integral multiples of $4\pi B$, and the possible states of the bag are represented by polynomials of b_m^+ and d_m^+ acting upon the empty bag state, $|\Omega_p\rangle$ which is defined by

$$d_m|\Omega_p\rangle = b_m|\Omega_p\rangle = 0,$$
$$P|\Omega_p\rangle = p|\Omega_p\rangle.$$

Unlike the vacuum in conventional field theory, the empty bag is a particle state in the quantum theory of a single bag. Since $[P, b_m^+] = [P, d_m^+] = 0$, the momentum of any state created by operating with b_m^+ or d_m^+ on the empty bag is the same as the momentum of the empty bag. In general, the empty bag can have a mass m_0 as well as momentum p.

One notes from the above discussion that there is an ambiguity in setting the absolute scale for the hadron spectrum when the bag is quantized in $1+1$ dimension. This is associated with the indeterminancy of m_0 due to the infinite zero-point fluctuations of the confined fields. Only the energy differences are determined by the value of the vacuum pressure B.

If we try to broaden our view beyond the quantization of a single bag, we have to recall from section 1 the two-phase picture of the physical vacuum. The normal phase of the physical vacuum does not allow for the propagation or fluctuation of hadron constituent fields. However, in the unobservable physical vacuum there always occur small fluctuations as closed hadron domains in the second phase inside which quark and gluon fields may fluctuate around a zero average value.

It is an unsolved problem yet whether the interpretation of the "empty" bag as a physical particle will be maintained when the structure of the physical vacuum and the theory of bags in interaction (fission and fusion) are better understood, or the empty bag perhaps disintegrates into the fluctuating hadron domains of the physical vacuum in a higher order approximation. We find the first possibility more likely.

6. Adiabatic bag dynamics

The bag as a dynamical system requires a rather complicated description in terms of several dynamical variables, even if only a few quark and gluon constituents are present and the collective variables of the bag shape are represented by a minimal number of necessary dynamical degrees of freedom.

A great simplification occurs, if inside the dynamical system of the bag we identify a slowly moving subsystem whose motion is instantaneously followed by the rest. This separation of the system into two parts is the working hypothesis of the adiabatic bag dynamics. The calculation of molecular spectra is a classical example for the hypothesis of adiabatic dynamics in quantum mechanical framework.

6.1. Born–Oppenheimer approximation

In order to understand the basic idea of the adiabatic approximation method, let us consider a molecule which consists of a given number of electrons with mass m and of atomic nuclei with mass M. The Hamiltonian can be written in the form

$$H = K_R + K_r + V(r, R),$$

where

$$K_r = -\frac{\hbar^2}{2m}\sum_i \frac{\partial^2}{\partial r_i^2}$$

is the operator for the kinetic energy of the electrons (light particles), and

$$K_R = -\frac{\hbar^2}{2M}\sum_i \frac{\partial^2}{\partial R_i^2}$$

is the kinetic energy of the nuclei (heavy particles). The electron coordinates with respect to the center of mass are designated by r, and R stands for the relative coordinates of the nuclei. $V(r, R)$ is the potential energy of the interaction.

In molecular physics due to the large ratio M/m of nuclear mass to electron mass the nuclear periods are much longer than the electronic periods. It is then a good approximation to regard the nuclei as fixed calculating the electronic motion. In the second step the nuclear motion can be

calculated under the assumption that the electrons have their steady motion for each instantaneous arrangement of the nuclei. This is the Born–Oppenheimer, or adiabatic approximation.

Mathematically it is based upon the hypothesis that the operator K_R for the kinetic energy of the heavy particles can be treated as a small perturbation. Thus, in the zeroth order approximation the Schrödinger equation

$$\left\{-\frac{\hbar^2}{2m}\sum_i \frac{\partial^2}{\partial r_i^2} + V(r, R)\right\}\varphi_n(R, r) = \epsilon_n(R)\varphi_n(R, r) \tag{6.1}$$

gives the stationary states $\varphi_n(R, r)$ for fixed values of the coordinates R of the heavy particles. The index n stands for the quantum numbers of the stationary states; the energies $\epsilon_n(R)$ and the wave functions $\varphi_n(R, r)$ depend upon R as upon a set of parameters.

Assuming that the solutions of (6.1) are known, the eigenfunctions of the complete Schrödinger equation

$$\left\{-\frac{\hbar^2}{2M}\sum_i \frac{\partial^2}{\partial R_i^2} - \frac{\hbar^2}{2m}\sum_i \frac{\partial^2}{\partial r_i^2} + V(r, R)\right\}\psi(R, r) = E\psi(R, r) \tag{6.2}$$

can be written as

$$\psi(R, r) = \sum_n \phi_n(R)\varphi_n(R, r), \tag{6.3}$$

since the functions $\varphi_n(R, r)$ form a complete set for given R.

Substituting (6.3) into (6.2), after multiplication by $\varphi_m^*(R, r)$ and integrating over the coordinates r, we find the following system of equations for $\phi_m(R)$:

$$(K_R + \epsilon_m(R) - E)\phi_m(R) = \sum_n \Lambda_{mn}\phi_n(R). \tag{6.4}$$

Here the operator Λ_{mn} is defined by

$$\Lambda_{mn} = \frac{\hbar^2}{M}\sum_i \int \mathrm{d}r\varphi_m^*(R, r)\frac{\partial}{\partial R_i}\varphi_n(R, r)\frac{\partial}{\partial R_i} - \int \mathrm{d}r\varphi_m^*(R, r)K_R\varphi_n(R, r).$$

The system of equations (6.4) is exact. In adiabatic approximation the right-hand side of (6.4) is set to zero and the system of equations for $\phi_m(R)$ decouples into independent equations,

$$[K_R + \epsilon_m(R)]\phi_{m\nu}^\circ(R) = E_{m\nu}^\circ\phi_{m\nu}^\circ \tag{6.5}$$

for each stationary state m of the light particles. One notes from (6.5) that the motion of the heavy particles is governed by the potential energy $\epsilon_m(R)$, which is the energy of the light particles for fixed position of the heavy particles.

Thus, in adiabatic approximation, the wave function $\psi(R, r)$ reduces to the simple product

$$\psi_{m\nu} = \phi_{m\nu}^\circ(R)\varphi_m(R, r)$$

so that for each stationary state m of the light particles, there are several states of motion of the heavy particles which are distinguished by the quantum numbers ν.

Using perturbation theory it can be shown that the condition for the applicability of the adiabatic approximation reduces to the inequality

$$|\langle\phi_{m\nu}^\circ|\Lambda_{mn}|\phi_{n\nu'}\rangle| \ll |E_{m\nu}^\circ - E_{n\nu'}^\circ| \tag{6.6}$$

for $m \neq n$ and for arbitrary quantum numbers ν and ν'.

A sufficient condition for the applicability of the adiabatic approximation is that the frequencies of vibration of the nuclei ω_σ should be small in comparison with the transition frequencies between electronic states:

$$\hbar\omega_\sigma \ll |\epsilon_m - \epsilon_n|. \tag{6.7}$$

The condition (6.7) is sufficient but not necessary. In some cases the adiabatic condition (6.6) is satisfied even when (6.7) is violated.

For a qualitative discussion of the above conditions in molecules, let us denote the linear dimension of a molecule by d. Then the energy of the electrons in the molecule is of the order

$$\epsilon \sim \hbar^2/md^2. \tag{6.8}$$

The vibrational energy of the nuclei is

$$E_{\text{vib}} = \hbar\sqrt{k/M}, \tag{6.9}$$

where k is the coefficient of elasticity which determines the potential energy of the vibrations of nuclei:

$$k = \left(\frac{\partial^2\epsilon}{\partial R^2}\right)_{R=R_0} \sim \frac{\epsilon}{d^2}. \tag{6.10}$$

Substituting (6.10) and (6.8) into (6.9) we find

$$E_{\text{vib}} \approx \eta^2\epsilon,$$

where $\eta = (m/M)^{1/4}$ is a small dimensionless parameter in molecular physics.

In the Born–Oppenheimer expansion of the molecular energies in powers of the small parameter η, the energy of the electrons is of the zeroth order with respect to η; the vibrational energy of the nuclei is proportional to η^2, and the rotational energy of the molecule is of the order of η^4.

6.2. Charmonium

The charmonium bound state may be treated in adiabatic approximation as a quark molecule whose charmed quarks correspond to the slowly moving heavy particles of the system. In close analogy with the hydrogen molecule we may conjecture the correspondences

protons – heavy charmed quarks
electrons – light quarks, massless gluons, collective bag variables
Coulomb potential – instantaneous $c\bar{c}$-interaction.

The adiabatic approximation is defined first in terms of the simplified problem where the dynamical degrees of freedom are the non-Abelian gauge field $A_{i\mu}$, the ordinary, light quark fields $q_{i\alpha}(x)$, the collective variables of the bag and a pair of static sources of the gauge field at positions $\boldsymbol{r}_1$ and $\boldsymbol{r}_2$. The static sources consist of a pair of color spins represented by the $\frac{1}{2}\lambda_i$ matrices of color SU(3) with the interaction

$$H_{\text{int}} = \tfrac{1}{2}gA_{i0}(\boldsymbol{r}_1)\lambda_i^{(1)} + \tfrac{1}{2}gA_{i0}(\boldsymbol{r}_2)\lambda_i^{(2)},$$

where $\frac{1}{2}\lambda_i^{(1,2)}$ are the color spin degrees of freedom of the two static sources.

We shall assume that the ground state eigenvectors and eigenvalues of the static source Hamil-

tonian are given by

$$H_{\text{stat}}|\chi(r_1, r_2)\rangle = E(r_1, r_2)|\chi(r_1, r_2)\rangle,$$

where r_1 and r_2 are parameters in the Hamiltonian, similarly to the variables R in the Schrödinger equation (6.1). In adiabatic approximation at any instant when the heavy quarks are located at r_1 and r_2, the other dynamical degrees of freedom are described by the state $|\chi(r_1, r_2)\rangle$, that is the light variables can instantaneously readjust themselves to the slowly moving sources and remain in ground state.

In this molecular approximation at every instant of time the energy stored in the gauge field and light quarks, together with the surface and volume energies of the bag, is

$$E(r_1, r_2) = V(r), \qquad r = |r_1 - r_2|,$$

so that the charmonium molecule is described by the Hamiltonian

$$H = 2m_c + \frac{p_1^2}{2m_c} + \frac{p_2^2}{2m_c} + V(r). \tag{6.11}$$

When the light quarks are ignored, the Hamiltonian in (6.11) determines the charmonium spectrum in first approximation (see subsection 7.3). The Yang–Mills color electric field between the charmed quark–antiquark pair becomes squeezed into a tube-like configuration when r is large.

Kogut and Susskind have considered the effects of the light quarks. As r and the field energy increase, it becomes energetically favorable at a certain point to lower the energy by creating ordinary $q\bar{q}$-pairs inside the stretched tube-like bag: the long range force can be screened by producing a color neutralizing light quark near each heavy quark. Therefore, as $r \to \infty$ the energy of a $c\bar{c}$-quark pair surrounded by a screening cloud becomes the sum of the masses of two charmed mesons. The bag splits and disintegrates into a pair of D and $\bar{D}$ mesons.

In molecular physics the ratio of masses is $m/M \sim 10^{-3}$, so that excellent quantitative calculations are possible. In the charmonium molecule, however, the excitation of the light dynamical degrees of freedom, a light $q\bar{q}$-pair, say, requires about 600 MeV energy. This is not a very large energy on the scale of charmonium physics where a typical level separation is also in the energy range of 5–600 MeV. The notion of an effective potential $V(r)$, and the adiabatic picture in general, has only a limited region of validity in charmonium physics.

6.3. Nucleon model in adiabatic approximation

We shall motivate here, on the basis of dynamical considerations, the bag model's version of what has become the classical quark model: the description of the SU(6) baryon multiplet 56 and meson multiplet 35. The underlying adiabatic bag dynamics will be stressed here, and spectroscopic considerations are left for subsection 7.1.

The lowest allowed color singlet state for the baryon has three quarks, whereas the lowest meson carries a quark and an antiquark. The quarks satisfy the massless free Dirac equation inside the bag, under the assumption that the presence of the color gauge fields may be neglected in zeroth approximation. An additional quark mass term can always be included in the Dirac equation.

In contrast with the charmonium molecule, we shall apply here a different adiabatic approximation scheme for the description of light quarks inside the bag. The collective variables of the bag are regarded as the slowly moving part of the system in comparison with the massless quarks, and gluons

in later considerations. We shall conjecture the following correspondence with molecular physics:

nuclei – collective bag variables
electrons – light quarks and massless gluons.

As a first step, the bag equations are solved for a fixed static surface, so that the energy levels of the confined quarks or gluons are in analogy with the energy levels $\epsilon_n(R)$ from the Schrödinger equation (6.1) for fixed position of the nuclei. The quark energy levels will depend on the shape of the bag generating potential energy for the collective surface variables. In the next step we have to solve a generalized Schrödinger equation with the Hamiltonian of the surface variables in the presence of the potential energy generated by the confined quarks.

The lowest mass states are expected to have minimum kinetic energy for the light quarks and thus the quarks should move in the most symmetrical way in space. We may conjecture, therefore, that the wave functions of the quark orbits dominantly exert a spherically symmetric pressure on the bag surface. Accordingly, the surface which results from balancing this pressure against the homogeneous and isotropic bag pressure B and surface tension σ, should be dominantly spherical, and classically at rest. This is called the static bag approximation.

As we shall see, the surface is fuzzy quantum mechanically and the static bag approximation is valid only in an average sense. We note here that the quark wave functions effectively satisfy the linear M.I.T. boundary condition (4.1) on a static bag surface in the absence of gluon fields (see subsection 4.1 for the $\alpha_c \to 0$ limit).

In adiabatic approximation, the wave function may be written as a product

$$\psi^{(n)}_{\{k_1,k_2,k_3\}}(\rho, \boldsymbol{r}_1, \boldsymbol{r}_2, \boldsymbol{r}_3) = \phi^{(n)}_{\{k_1,k_2,k_3\}}(\rho)\chi^{(k_1)}_\rho(\boldsymbol{r}_1)\chi^{(k_2)}_\rho(\boldsymbol{r}_2)\chi^{(k_3)}_\rho(\boldsymbol{r}_3),$$

where the spinor wave function $\chi^{(k_i)}_\rho(\boldsymbol{r}_i)$ is an eigenfunction of the free Dirac equation inside a spherical surface of radius ρ,

$$(-\mathrm{i}\boldsymbol{\alpha}\nabla_{r_i} + \beta m_i)\chi^{(k_i)}_\rho(\boldsymbol{r}_i) = \epsilon^{(k_i)}(\rho)\chi^{(k_i)}_\rho(\boldsymbol{r}_i) \tag{6.12}$$

under the constraint of the linear boundary condition

$$\mathrm{i}\frac{\boldsymbol{r}_i}{r_i}\boldsymbol{\alpha}\chi^{(k_i)}_\rho(\boldsymbol{r}_i) = \beta\chi^{(k_i)}_\rho(\boldsymbol{r}_i) \tag{6.13}$$

on the static surface. The suffix i refers to the ith quark, and k_i stands for the k_ith eigenvalue. The equations are similar for the other two quarks.

For given quantum numbers k_1, k_2, k_3, the wave function of the surface satisfies the eigenvalue equation

$$\int_0^\infty \mathrm{d}\rho' K(\rho,\rho')\phi^{(n)}_{\{k_1,k_2,k_3\}}(\rho') + \left[B\frac{4\pi}{3}\rho^3 + \sum_{i=1}^{3}\epsilon^{(k_i)}(\rho)\right]\phi^{(n)}_{\{k_1,k_2,k_3\}}(\rho) = E^{(n)}_{(k_i)}\phi^{(n)}_{\{k_1,k_2,k_3\}}(\rho) \tag{6.14}$$

in adiabatic approximation. One notes the close analogy with eq. (6.4) in molecular approximation.

First, we shall solve the quark problem for a fixed bag radius ρ. Since the equations are identical for the three quarks, we shall drop the quark index in what follows below. Further, the quark masses and B are set to zero here, though they may be included in a more general treatment, in a trivial manner.

The requirement of spherical quark pressure on the surface allows only $J = \frac{1}{2}$ solutions to Dirac's equation, with two values $\kappa = \pm(J + \frac{1}{2})$ for the Dirac quantum number. The values of κ label the

two states of opposite parity for each value of J. For $J = \frac{1}{2}$ either $\kappa = -1$,

$$\psi^{(n)}_{-1,\,1/2,\,m}(\boldsymbol{r}) = \frac{N(\omega_{n\kappa})}{\sqrt{4\pi}} \begin{pmatrix} \mathrm{i} j_0\left(\omega_{n,-1}\frac{r}{\rho}\right) U_m \\ -j_1\left(\omega_{n,-1}\frac{r}{\rho}\right) \boldsymbol{\sigma}\frac{\boldsymbol{r}}{r} U_m \end{pmatrix},$$

or $\kappa = 1$,

$$\psi^{(n)}_{1,\,1/2,\,m}(\boldsymbol{r}) = \frac{N(\omega_{n\kappa})}{\sqrt{4\pi}} \begin{pmatrix} \mathrm{i} j_1\left(\omega_{n,1}\frac{r}{\rho}\right) \boldsymbol{\sigma}\frac{\boldsymbol{r}}{r} U_m \\ j_0\left(\omega_{n,1}\frac{r}{\rho}\right) U_m \end{pmatrix} \tag{6.16}$$

for the solutions of the massless Dirac equation. U_m is a two-component Pauli spinor and $j_l(z)$ are conventional spherical Bessel functions. The index n labels the eigenfrequencies which are determined from the boundary condition (6.13). The corresponding eigenvalue condition for the frequencies $\omega_{n,\kappa}$ is

$$j_0(\omega_{n\kappa}) = -\kappa j_1(\omega_{n\kappa}),$$

or

$$\tan \omega_{n\kappa} = \frac{\omega_{n\kappa}}{\omega_{n\kappa} + \kappa}\,\kappa. \tag{6.17}$$

We choose positive (negative) n sequentially to label the positive (negative) roots of eq. (6.17). The first few eigenfrequencies from (6.17) are

$$\kappa = -1: \quad \omega_{1-1} = 2.04; \quad \omega_{2-1} = 5.40,$$
$$\kappa = +1: \quad \omega_{11} = 3.81; \quad \omega_{21} = 7.00.$$

There appears a normalization constant in (6.15) and (6.16) which is defined by

$$N(\omega_{n\kappa}) = \left(\frac{\omega^3_{n\kappa}}{2\rho^3(\omega_{n\kappa} + \kappa)\sin^2 \omega_{n\kappa}}\right)^{1/2}.$$

Now we have all the necessary ingredients to construct the nucleon wave function in adiabatic approximation. The two up quarks and the down quark of the nucleon form a color singlet state, so that the spin–isospin-spatial state must be totally symmetric. We shall not give here the rather trivial procedure of distributing the up and down quarks with $J = \frac{1}{2}$ among the available quark orbitals of the static bag with fixed radius ρ.

The nucleon wave function in ground state is

$$\psi = \phi^{(0)}(\rho)\chi^{(1)}_\rho(\boldsymbol{r}_1)\chi^{(1)}_\rho(\boldsymbol{r}_2)\chi^{(1)}_\rho(\boldsymbol{r}_3), \tag{6.18}$$

where the above mentioned symmetrization of ψ is understood. The up and down quarks occupy in (6.18) the same quark orbital with the lowest positive frequency $\omega_{1-1} = 2.04$.

Given the wave function ψ in eq. (6.18), the radial shape of the bag is determined from the eigenvalue equation (6.14) which is now

$$\int_0^\infty \mathrm{d}\rho' K(\rho, \rho')\phi^{(n)}(\rho') + \frac{3\omega_{1-1}}{\rho}\phi^{(n)}(\rho) = E^{(n)}\phi^{(n)}(\rho), \tag{6.19}$$

since B was set to zero. One notes the similarity of (6.19) with eq. (2.25) for the radial excitations of Dirac's bubble. If $\alpha/2$ in (2.25) is replaced by $3\omega_{1-1}$ we get the same integral equation which was solved in subsection 2.2. Only the potential energy for the bag surface is different in its strength.

The first few eigenvalues of eq. (6.19) are given by

$$(4\pi\sigma)^{-1/3}\begin{cases} E_0 = 7.12 \\ E_1 = 8.40 \\ E_2 = 9.49, \end{cases} \tag{6.20}$$

and the corresponding wave functions are shown in fig. 6.1. They describe the radial excitations of the surface when the three quarks occupy the lowest orbital in adiabatic approximation. Figure 6.2 shows the probability distribution for finding the bag in its ground state with a radius between ρ and $\rho + d\rho$. The arrow indicates the classical radius of the static bag which is given by setting the kinetic energy η^2 of the surface to zero and minimizing the static classical energy

$$E_{st} = \sigma 4\pi\rho^2 + (3\omega_{1-1}/\rho)$$

with respect to the bag radius ρ.

As we can see from fig. 6.2 the surface of the bag is blurred quantum mechanically, though the probability distribution is sharply peaked around the classical radius of the static bag. This observation serves as the basis of the static bag approximation where the kinetic energy of the surface from the quantum mechanical uncertainty relation is neglected and a sharp boundary is assumed, approximately. The energy of zero-point oscillations of the surface gives some correction to the classical energy, though the ground state energy at the bottom of the excitation spectrum can always be adjusted by a suitable choice of the strength σ of surface tension.

It is interesting to observe that the excitation spectrum of the surface in (6.20) is well approximated by the WKB method, or even the small oscillation approximation about the static equilibrium yields reasonable results. Both methods were discussed in subsection 2.2, and we give here the results, for the sake of comparison:

	E^n	E^n_{WKB}	$E^n_{osc} = E_{st} + (n+\frac{1}{2})h\nu$
$n=0$	7.12	7.10	7.16
$n=1$	8.40	8.39	8.84
$n=2$	9.49	9.49	10.52

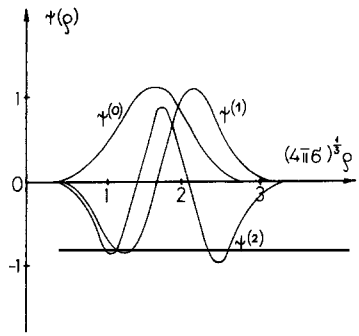

Fig. 6.1. The quantum mechanical wave functions of the surface are shown for the ground state and the first and second excited states of the nucleon.

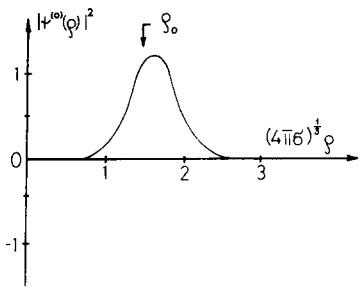

Fig. 6.2. The probability density for finding the nucleon with radius ρ in its ground state. ρ_0 stands for the classical radius of the static bag.

The energy spectrum E^n_{WKB} is calculated from the Bohr–Sommerfeld quantization conditions (2.18) and (2.19). The frequency ν of the harmonic oscillations about the static equilibrium of the bag, and the corresponding quantum energy $h\nu$ is taken from (2.15) where $\alpha/2$ is replaced by $3\omega_{1-1}$.

In the derivation of the energy spectrum (6.20) we have assumed that the three colored quarks occupy the lowest orbital in a bag whose radius adiabatically varies in time. Even when the quarks are in their ground states, on the lowest orbital, there are surface excitations as a manifestation of the independent dynamical variables of the boundary between the hadron phase and the vacuum phase. This spectrum is analogous to the vibrational energies of the heavy nuclei in molecules.

When the surface is in its ground state, there are several quark orbitals available for quark excitations inside the bag. In order of increasing energy we find

$1S_{1/2}$ with $= 2.04$,
$1P_{1/2}$ with $= 3.84$,
$2S_{1/2}$ with $= 5.4$,
etc.

These excitations are analogous to electron excitations inside molecules when the heavy nuclei are in their ground state. Since the excited quark states generate a different potential energy ("van der Waals force") for the surface, the wave function of the bag's shape varies with quark excitations.

There are then a third type of excitations when both the surface and the quarks are excited.

As we have discussed in subsection 5.5, it is rather problematic how to relate the eigenvalue series of eq. (6.20) to the measurable hadron spectrum. The lowest eigenvalue E_0 differs from the static energy E_{st} by the contribution of the radial zero-point fluctuation. By introducing new surface coordinates describing deformed bags, E_0 will always be shifted to higher values due to the vacuum fluctuations of the new variables. The energy differences, however, will stay approximately fixed.

As in the case of the exactly soluable $1+1$ dimensional model, we have to renormalize the energy levels, and a new dimensional parameter m_0 which is undetermined will appear. This may be chosen to be the mass of the empty bag if it is a physical particle, or zero if it somehow turns out to be part of the physical vacuum. Or equivalently, the two dimensional parameters m_0 and σ can be used to fit the mass of the nucleon and the first radial excitation. Then the mass of the empty bag is fixed and calculable.

The strategy of the M.I.T. group who have initiated the spectroscopic calculations for hadrons is different. In the case of pure volume energy, when σ is set to zero already in the Lagrangian, only the static bag approximation is available so far. There is a hope that the quantum mechanical fluctuations of the bag surface may be calculated in the future following the method of subsection 5.1.

In the static bag approximation with pure vacuum pressure the static energy

$$E_{\mathrm{st}} = B\frac{4\pi}{3}\rho^3 + \frac{3\omega_{1-1}}{\rho}$$

is minimized with respect to the bag radius – an equivalent procedure to that solving the non-linear boundary condition for a static, spherical surface. The minimized energy is accepted as the average mass of the $N-\Delta$ system and B is fixed by this requirement. The zero-point energy of the collective motions is not considered at this level. The zero-point energy of the gluon and fermion fields is taken into account by considering a fixed surface in adiabatic approximation, a procedure to be discussed in the next subsection.

If we consider a static and classical surface the results are practically independent of whether we use surface or volume tension. We shall present here the original M.I.T. version with pure volume tension.

The value of B from the average mass of the N – Δ system is $B^{1/4} = 120$ MeV. The quark excitation spectrum is shown in fig. 6.3. Only those states are depicted where the quark pressure is spherically symmetric on the boundary.

As an application of the nucleon model in static bag approximation we calculate the magnetic moment and charge radius of the proton and neutron, and the axial-vector charge of the proton. We shall present here the original M.I.T. version with pure volume tension.

The magnetic moment of a confined quark in the spherical bag is defined by

$$\boldsymbol{\mu} = Q \int_{\text{bag}} \mathrm{d}^3 r \tfrac{1}{2} \mathbf{r} \times \psi^+ \boldsymbol{\alpha} \psi,$$

where the charge Q is $\frac{2}{3}$ for an up quark and $-\frac{1}{3}$ for a down quark. The wave function is given by (6.15). After elementary calculation we find

$$\mu = \frac{\rho_0}{12} \frac{4\omega_{1-1} - 3}{\omega_{1-1}(\omega_{1-1} - 1)}, \tag{6.21}$$

where ρ_0 is the static radius of the bag:

$$\rho_0 = \left(\frac{3\omega_{1-1}}{4\pi B}\right)^{1/4}.$$

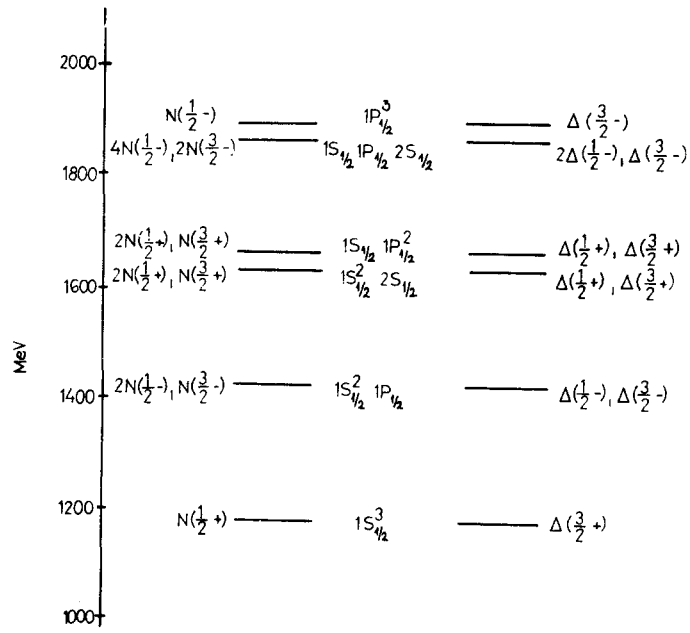

Fig. 6.3. Low-lying three-quark nonstrange baryon states with $J \leq \frac{3}{2}$ in the quark bag model.

Using the complete wave function of the proton we find the gyromagnetic ratio of

$$g_p = 2M\mu = 2.6$$

from (6.21), if the value $B^{1/4} = 120$ MeV is taken from a fit to the average N – Δ mass.

The neutron's magnetic moment is calculated analogously and $g_n = -\frac{2}{3}g_p$ is obtained. One notes that the origin of the magnetic moment in the quark bag model is quite different from that of the non-relativistic quark model. Confinement sets a scale for the wave function of massless quarks and the magnetic moment comes from a cross term between the upper and lower components of the wave function.

The contribution of a quark orbital to the charge radius is defined by

$$\langle r^2 \rangle = Q \int_{\text{bag}} \mathrm{d}^3 r \psi^+(r) r^2 \psi(r),$$

which may be evaluated for the wave function (6.15) or (6.16):

$$\langle r^2 \rangle = Q \frac{\rho_0^2}{\sigma} \frac{2\omega_{n\kappa}^3 + 2\kappa\omega_{n\kappa}^2 + 4\omega_{n\kappa} + 3\kappa}{\omega_{n\kappa}^2(\omega_{n\kappa} + \kappa)}.$$

For the proton we obtain

$$\langle r^2 \rangle_p^{1/2} = 1.04 \text{ fermi}$$

for the neutron $\langle r^2 \rangle_n^{1/2} = 0$.

The axial-vector coupling constant of β-decay is defined for the proton as

$$g_A = \left\langle pS_z = \tfrac{1}{2} \middle| \int_{\text{bag}} \mathrm{d}^3 r \psi^+(r) \tau_3 \sigma_z \psi(r) \middle| pS_z = \tfrac{1}{2} \right\rangle, \tag{6.22}$$

where τ_3 is the third component of the isospin in (u, d) space. From an explicit calculation of (6.22) one obtains for the proton

$$g_A = \frac{5}{3}\left(1 - \frac{2\omega_{1-1} - 3}{3(\omega_{1-1} - 1)}\right) = 1.09.$$

In the non-relativistic quark model $g_A = \frac{5}{3}$. The result of the quark bag model differs, since the lower components of the quark wave function in (6.15) are important and have opposite spin orientation from the upper components.

Needless to say that a very similar calculation can be repeated with surface tension instead of vacuum pressure. What makes the latter calculation interesting is that it is comparable with the results from the adiabatic approximation where the surface is smeared out quantum mechanically. The static formulae, say (6.21) for μ, will be weighted then by the probability distribution of finding the surface between the radius ρ and $\rho + \mathrm{d}\rho$:

$$\mu = \frac{4\omega_{1-1} - 3}{12\omega_{1-1}(\omega_{1-1} - 1)} \int_0^\infty \mathrm{d}\rho \phi^{(0)*}(\rho) \rho \phi^{(0)}(\rho). \tag{6.23}$$

Equation (6.23) implies that the static radius ρ_0 in the formula (6.21) will be replaced by the average value of ρ in the quantum mechanical ground state of the surface. Since $\phi^{(0)*}(\rho)\phi^{(0)}(\rho)$ is strongly

peaked near the static radius, fig. 6.2, the static nucleon parameters μ, and $\langle r^2 \rangle$ do not change significantly in adiabatic approximation with a blurred bag surface.

The effects of the quark–gluon interaction will be discussed in subsection 7.1. Incidentally, this will bring up the interesting phenomenon of the zero-point fluctuations of confined fields.

6.4. *The Casimir effect*

When a quantum field, say the electromagnetic field, is confined to a finite region of space, a measurable long-range force exerted on the confining walls is generated by the zero-point fluctuations of the field.

This effect may be understood by recalling that the quanta of the confined field occupy the eigenmodes of the confining geometry. Now, the zero-point energy of the radiation field is given by $\frac{1}{2}\hbar\omega$ per normal mode. But the frequencies ω depend upon the geometrical configuration of the walls. Thus, changing the position of the walls changes the frequencies ω of the normal modes, and hence changes the zero-point energy of the radiation field. This change of energy which depends on the position of the confining walls is the potential function of the above mentioned long-range force.

The first zero-point energy calculation was performed by Casimir in 1948, for the electromagnetic field confined by two perfectly conducting plates of cross section A separated by a distance L (see fig. 6.4). Casimir has found the zero-point energy

$$E_0 = 3\pi^2 \hbar c A L \frac{1}{\lambda^4} - \frac{\pi^2}{2} \hbar c A \frac{1}{\lambda^3} - \frac{\pi^2}{720} \frac{\hbar c A}{L^3} \tag{6.24}$$

between the two plates, where λ is a cut-off parameter at very short wave lengths. The physical problem suggests the use of the wavelength as a cut-off quantity, since the plates are good conductors at long wave lengths, but their conductivity becomes poor at sufficiently short wave lengths. Anyway, $\lambda \to 0$ is taken in the ideal limit.

The first term in (6.24) is proportional to the volume of the confining geometry and divergent in the $\lambda \to 0$ limit. The second term is also divergent being proportional to the surface of the confining geometry. These two terms are not physically measurable, since the quantum fluctuations of the outside field when added to (6.24) cancel the geometry-dependent divergent parts.

Nevertheless, the third term in (6.24) is finite (independent of the cut-off) and measurable! Thus the net force between the two plates is attractive and given by

$$F = -\frac{\pi^2}{240} \hbar c \frac{A}{L^4} \tag{6.25}$$

to be expected on any parallel plates which are conducting for wave lengths significantly shorter then the separation of the plates.

The force (6.25) was measured in 1958 using chromium steel plates of area 1 cm^2. At a separation of about 0.5 μ, the force of attraction was 0.2 dyne/cm^2, in agreement with (6.25). It almost makes one

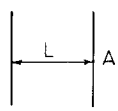

Fig. 6.4. Casimir effect for a slab of two conducting plates at a distance L with a cross-sectional area A.

believe in the ether! Although, the attractive force may be explained eventually in terms of the long range van der Waals forces between the molecules of the two plates.

The presence of a spherical conducting shell in space will also change the zero-point energy of the electromagnetic field in the universe. The finite and measurable part of this energy for a sphere with radius a is

$$E_0 = -\tilde{c}(\hbar c/2a), \tag{6.26}$$

where $\tilde{c}$ is a number. Casimir conjectured that the inward force from (6.26) balances the outward Coulomb force in the semi-classical Abraham–Lorentz model of the electron as charge distributed over a spherical shell.

Specifically, the electrostatic energy of the charge is associated with the stresses

$$F_{\text{est}} = \frac{e^2}{8\pi a^4},$$

whereas the Poincaré stresses are provided by the quantum zero-point forces arising from the presence of the conducting boundary:

$$F_{\text{zp}} = -\tilde{c}\frac{\hbar c}{8\pi a^4}.$$

Thus, the condition for balancing the stresses is

$$\frac{e^2}{8\pi a^4} \approx \tilde{c}\frac{\hbar c}{8\pi a^4},$$

or

$$e^2/\hbar c = \tilde{c}. \tag{6.27}$$

Therefore, at a particular value of the charge e, the extended electron should be stable independent of the radius a. Casimir conjectured that the zero-point energy might be the basis for charge quantization according to (6.27).

Unfortunately, the idea fails, since the number $\tilde{c}$ as calculated in 1968 by Boyer is negative,

$$\tilde{c} = -0.093,$$

so that the force generated by the zero-point energy on the surface of the sphere is outward.

Let us turn now to the bag. In adiabatic approximation, for a fixed bag shape, there is always a geometrical zero-point energy from the quantum fluctuations of the confined fields. Since there are no dynamical degrees of freedom outside the bag, the divergent part of the zero-point energy which is analogous to the first two terms of (6.24) is not "cancelled" by the outside fluctuations, not converting it into a geometry-independent and thereby ignorable infinity.

Indeed, Balian and Bloch have shown the following theorem. Let us consider the Helmholtz equation

$$\Delta\varphi + k^2\varphi = 0$$

for a volume V of arbitrary shape, and for the general boundary condition

$$(\partial\varphi/\partial n) = \kappa\varphi \tag{6.28}$$

on the surface S, assumed to be smooth. Then, in the limit of wave-lengths small compared to any characteristic dimension of the system, the eigenvalue density, smoothed to eliminate its fluctuating part, is given by the asymptotic expansion:

$$\rho(k) = \frac{1}{4\pi^2}\left\{ Vk^2 + S\left(\frac{\pi}{4} - \delta\right)k + (\tfrac{1}{3} + \cos^2\delta - \delta\cot\delta)\int \mathrm{d}\sigma \tfrac{1}{2}\left(\frac{1}{R_1} + \frac{1}{R_2}\right) + \cdots \right\}, \tag{6.29}$$

where R_1 and R_2 are the main curvature radii of S, with

$$\delta = \frac{1}{\kappa}\tan^{-1}\kappa.$$

Both the surface and curvature terms depend on the boundary condition (6.28). Neumann and Dirichlet boundary conditions are recovered for $\kappa = 0$ and $\kappa \to \infty$. A similar theorem can be derived for vector and spinor fields in which case the surface term of the asymptotic expansion may be missing.

From the eigenvalue density $\rho(k)$ of (6.29) we can isolate the divergent parts of the zero-point energy E_{zp} for the scalar field φ as being proportional to the integral

$$E_{zp} \sim \int^{\Lambda} k\rho(k)\,\mathrm{d}k. \tag{6.30}$$

There is a quartic divergence proportional to the volume V, a cubic term proportional to the surface area S, and a quadratic divergence related to the integrated mean curvature of the surface.

Bender and Hays have evaluated the zero-point energies for a static and spherical bag of radius ρ, in the case of scalar, vector, and fermion fields with the corresponding linear boundary conditions for a bag surface. Their results yield a similar picture as expected from the above theorem of Balian and Bloch. The new element in their calculation is the explicit proof that for spinor and vector fields with linear bag boundary conditions the second term in (6.29) vanishes.

The leading quartic divergence of (6.30) may be absorbed into the volume part of the bag Hamiltonian by the renormalization of the vacuum pressure B. Similarly, the cubic divergence for a scalar field may be absorbed into the surface part of the bag Hamiltonian by the renormalization of σ. However, the quadratic divergence in (6.30) is a new term which requires a new counter term

$$W_\gamma = -\gamma \int_{x^1=1} R\sqrt{\det g_{ab}}\,\mathrm{d}x^0\,\mathrm{d}x^2\,\mathrm{d}x^3 \tag{6.31}$$

in the action integral. W_γ is written in curvilinear coordinates in eq. (6.31) where R is the mean curvature in Minkowski space of the intrinsic geometry on the three-dimensional surface of the tube swept out by the bag boundary.

The remaining finite part of the zero-point energy is determined by the long wavelength part of the eigenvalue spectrum which may generate a geometry-dependent finite potential term in the wave equation of the collective bag variables in adiabatic approximation.

However, it remains an open question what happens with the problem of the zero-point fluctuations of the confined fields in a more refined quantum theoretic calculation beyond the adiabatic approximation.

7. Hadron spectroscopy, I (non-exotic states)

In this section we shall describe the spectrum of hadrons which are built from the minimum allowed number of quark and gluon constituents. These are frequently called non-exotic states. Accordingly, the gluonium with two or three valence gluons as the only constituents is also a non-exotic hadron state.

7.1. Static bag approximation with quark–gluon interaction (non-exotic light baryons and mesons)

The quark bag model will be treated here in the spirit of the adiabatic approximation (see subsection 6.3) but in addition to quarks, the quark–gluon interaction will also be included in the calculations.

Let us consider a bag with static, spherical boundary whose interior is populated with quark orbitals (or gluon constituents in gluonium) where the quark–gluon-interaction is taken into account in lowest order of α_c. The static equilibrium of the bag is calculated from the total energy which is minimized with respect to the bag radius ρ. The spectrum of hadrons derived from this calculational scheme is associated with the so-called M.I.T. cavity approximation.

Since the boundary of the bag is treated here classically, as a static surface, confinement of the quark and gluon fields by surface tension or vacuum pressure yields practically the same results. Therefore we shall follow the original calculation of the M.I.T. group with pure vacuum pressure.

Quark–gluon interaction

In lowest order of α_c the gluon exchange graphs are shown in fig. 7.1. Since the quarks remain in the lowest cavity mode in fig. 7.1(a), the current at the vertices is time-independent. Consequently, only the static part of the gluon propagator contributes in fig. 7.1(a).

To lowest order in α_c the non-Abelian gluon self-coupling does not contribute and the gluons act as eight independent Abelian fields without self-interaction. The problem of finding the confined gluon propagator reduces to color electrodynamics inside a cavity of radius ρ, with the boundary conditions

$$\hat{r} \cdot \boldsymbol{E}_i = 0, \tag{7.1}$$

$$\hat{r} \times \boldsymbol{B}_i = 0, \qquad i = 1, 2 \ldots, 8 \tag{7.2}$$

on the surface. From the solution of the Maxwell equations in polar coordinates for a pure radiation field inside the cavity we can determine the TE and TM eigenmodes of the colored gluons, if the boundary conditions (7.1) and (7.2) are taken into account. The confined gluon propagator can be constructed from these eigenmodes in the usual manner.

In the self-energy diagrams of fig. 7.1(b) the intermediate quark may be in any cavity mode. A large (divergent) part of its contribution must be absorbed into the renormalization of the quark mass. In the cavity approximation a conventional procedure to treat this diagram would be as follows.

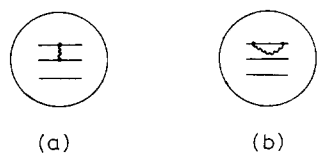

Fig. 7.1. Lowest order gluon interaction diagrams for a baryon. (a) Gluon exchange; (b) gluon self-energy.

In QED the contribution of the self-energy graph is fixed to be zero for the free electron by mass renormalization. Then the relative energy shift for a bound electron is finite and calculable. In the bag model, where the "bare" quark mass is defined as the mass parameter of the free Dirac equation for the quark orbitals of subsection 6.3, we may fix the contribution of the self-energy graph for a quark orbital in the nucleon's ground state in an arbitrary manner. Then, in the different hadron states, the relative energy shifts are calculable.

The source of this relative contribution is twofold. In general, the quark wave function will change from hadron to hadron for a fixed radius ρ (Lamb shift type correction), on the other hand the confined gluon propagator will also change with a different cavity radius ρ.

The M.I.T. group suggested a different procedure. In their approximation the sum over the intermediate quark states is truncated and only the term in which the quark remains in the lowest mode is considered. The gluon propagator in fig. 7.1(b) will be again the static propagator in this case.

We do not see any reasonable argument for the truncation of the intermediate sum in fig. 7.1(b), except perhaps the insistence on analytic calculations. Since the electrostatic parts of diagrams 7.1(a) and 7.1(b) cancel, we would get the inconceivable result that there is no electrostatic contribution to the ground state energy of a positronium confined to a cavity, if the M.I.T. procedure is applied.

This is probably wrong for massive quarks, though the situation is less clear when the quark mass vanishes. Chodos and Thorn have shown that the electromagnetic self-energy diagram is finite for massless quarks confined to a slab (zero mass parameter in the free Dirac equation), and the static part of the diagram dominates the energy shift. If this feature of their calculation remains valid for a confined gluon propagator and spherical cavity instead of a free photon propagator and a slab, then the M.I.T. approximation becomes better motivated for massless quarks. Since a non-vanishing mass parameter in the free Dirac equation is a new and arbitrary dimensional parameter, the results of Chodos and Thorn are not applicable in this case.

Though the approximations seem to be crude, and not well motivated, the calculation of the M.I.T. group is rather instructive for two reasons. First, it gives a zeroth order insight into the mechanism of spin-dependent quark–gluon interaction with spectroscopic applications and further, a definite program is provoked for later refinements.

Let us calculate now the field energy of the quark–gluon interaction. The color electrostatic interaction energy of a static color charge distribution is

$$\Delta E_{\mathrm{E}} = \tfrac{1}{2}g^2 \sum_{i=1}^{8} \int_{\mathrm{bag}} \mathrm{d}^3 r \boldsymbol{E}_i(\boldsymbol{r}) \boldsymbol{E}_i(\boldsymbol{r}),$$

whereas the color magnetostatic interaction energy may be written as

$$\Delta E_{\mathrm{M}} = -\tfrac{1}{2}g^2 \sum_{i=1}^{8} \int_{\mathrm{bag}} \mathrm{d}^3 r \boldsymbol{B}_i(\boldsymbol{r}) \boldsymbol{B}_i(\boldsymbol{r}),$$

where $\boldsymbol{E}_i$ and $\boldsymbol{B}_i$ are determined from the quark charge and current distributions by Maxwell's equation and the boundary conditions (7.1) and (7.2).

The color magnetic field satisfies

$$\nabla \times \boldsymbol{B}_i^{(k)} = \boldsymbol{j}_i^{(k)}, \qquad r < \rho$$

$$\nabla \cdot \boldsymbol{B}_i^{(k)} = 0, \qquad r < \rho$$

$$\hat{\boldsymbol{r}} \times \sum_k \boldsymbol{B}_i^{(k)} = 0, \qquad r = \rho$$

where $j_i^{(k)}$ is the color current of the kth quark on a given orbit:

$$j_i^{(k)} = q^{+(k)} \alpha \tfrac{1}{2} \lambda_i^{(k)} q^{(k)} = -\frac{3}{4\pi} \hat{r} \times \sigma^{(k)} \tfrac{1}{2} \lambda_i^{(k)} \frac{\tilde{\mu}_k(r)}{r^3}.$$

Here $\tilde{\mu}_k(r)$ is the scalar magnetization density of a quark of mass m_k in the lowest cavity eigenstate. The integral

$$\mu(m_k, \rho) = \int_0^\rho \mathrm{d}r \tilde{\mu}_k(r)$$

yields the color magnetic moment generated by the quark wave function in the cavity eigenmode.

It is easy to show that the static $\boldsymbol{B}_i$ field of fig. 7.1(a) satisfies the boundary condition (7.2) by itself. With this observation, the M.I.T. group leaves out the static contribution of fig. 7.1(b) to $\boldsymbol{B}_i$ so that the magnetic interaction energy of a hadron is written as

$$\Delta E_{\mathrm{M}} = -g^2 \sum_i \sum_{k>l} \int_{\mathrm{bag}} \mathrm{d}^3 r \boldsymbol{B}_i^{(k)}(\boldsymbol{r}) \boldsymbol{B}_i^{(l)}(\boldsymbol{r}),$$

where $\boldsymbol{B}_i^{(k)}$ is the color magnetic field generated by the kth quark of the hadron.

The final expression for the magnetic interaction energy is

$$\Delta E_{\mathrm{M}} = 2\alpha_{\mathrm{c}} \lambda \sum_{k>l} (\boldsymbol{\sigma}^{(k)} \cdot \boldsymbol{\sigma}^{(l)}) \frac{\mu(m_k, \rho)\mu(m_l, \rho)}{\rho^3} I(m_k\rho, m_l\rho), \tag{7.3}$$

where

$$I(m_k\rho, m_l\rho) = 1 + 2 \int_0^\rho \frac{\mathrm{d}r}{r^4} \mu(m_k, \rho)\mu(m_l, \rho).$$

In eq. (7.3) $\lambda = 1$ for a baryon, 2 for a meson.

We turn now to the gluon electrostatic energy. Here the static term from fig. 7.1(b) is included in the calculation of the color electric field $\boldsymbol{E}_i$:

$$\Delta E_{\mathrm{E}} = \tfrac{1}{2} g^2 \sum_i \sum_{k,l} \int_{\mathrm{bag}} \mathrm{d}^3 r \boldsymbol{E}_i^{(k)}(\boldsymbol{r}) \boldsymbol{E}_i^{(l)}(\boldsymbol{r}). \tag{7.4}$$

The color electric field of a single quark satisfies in lowest order of α_{c}

$$\nabla \boldsymbol{E}_i^{(k)} = j_i^{0(k)}, \qquad r < \rho$$
$$\nabla \times \boldsymbol{E}_i^{(k)} = 0, \qquad r < \rho$$

with the boundary condition

$$\sum_k \hat{r} \cdot \boldsymbol{E}_i^{(k)} = 0, \qquad r = \rho.$$

$j_i^{0(k)}(\boldsymbol{r})$ is the color charge density of a single quark in a given orbital:

$$j_i^{0(k)} = q^{+(k)} \tfrac{1}{2} \lambda_i^{(k)} q^{(k)} = \frac{\frac{1}{2}\lambda_i^{(k)}}{4\pi r^2} \tilde{\rho}^{(k)}(r).$$

The color electric field is determined from Gauss's law:

$$\boldsymbol{E}_i^{(k)} = \frac{\frac{1}{2}\lambda_i^{(k)}}{4\pi r^2}\hat{r}\rho^{(k)}(r),$$

where $\rho^{(k)}(r)$ is the integral

$$\rho^{(k)}(r) = \int_0^r \mathrm{d}r'\tilde{\rho}^{(k)}(r').$$

Now if all the quarks are massless in a hadron or more generally, they have the same mass, then $\rho^{(k)}(r)$ is independent of the index k and the total color electric field is given by

$$\boldsymbol{E}_i = \frac{\hat{r}}{4\pi r^2}\rho(r)\sum_k \tfrac{1}{2}\lambda_i^{(k)}.$$

For a color-singlet hadron $\Sigma_k \frac{1}{2}\lambda_i^{(k)}|H\rangle = 0$ so that $\boldsymbol{E}_i$ vanishes. Therefore, there is no color electrostatic energy shift in this case. For different quark masses the term (7.4) is non-zero and included in the spectroscopic calculation.

Zero-point energy

We have seen in subsection 6.4 that the zero-point fluctuations of the quark and gluon fields may generate a finite zero-point energy which should be of the form of

$$E_{\mathrm{zp}} = -Z_0/\rho \tag{7.5}$$

for massless quarks, on the basis of dimensional reasons. The term (7.5) is not firmly grounded theoretically, rather it seems to be a phenomenological term for ill-understood effects in fitting the data.

Hadron masses and other parameters

We have now all the necessary ingredients for calculating the mass of each hadron. For a given radius ρ of the spherical bag, the total energy is given by

$$E_{\mathrm{h}}(\rho) = E_B + E_{\mathrm{q}} + E_{\mathrm{q-g}} - E_{\mathrm{zp}}, \tag{7.6}$$

where the interaction energy $E_{\mathrm{q-g}}$ and the zero-point energy E_{zp} were discussed above. The energy E_{q} of the quark eigenmodes was calculated in subsection 6.3 for massless quarks. A similar procedure applies for massive quarks as well. The volume energy E_B is well-known by now.

The minimization of E_{h} in (7.6) with respect to the bag radius ρ yields the rest mass of the corresponding hadron in the static bag approximation.

There are four parameters available to fit the low-lying meson and baryon spectrum: the vacuum pressure B, the quark–gluon coupling constant α_{c}, the coefficient Z_0 in the zero-point energy of (7.5), and the strange quark mass m_{s}. The up and down quarks are kept massless in the fit, though relaxing this condition does not alter the results noticeably.

The spectrum from the best M.I.T. fit is shown in fig. 7.2. We hope to attribute the abnormally large value of α_{c} to the above discussed rough approximations. The qualitative picture is quite encouraging,

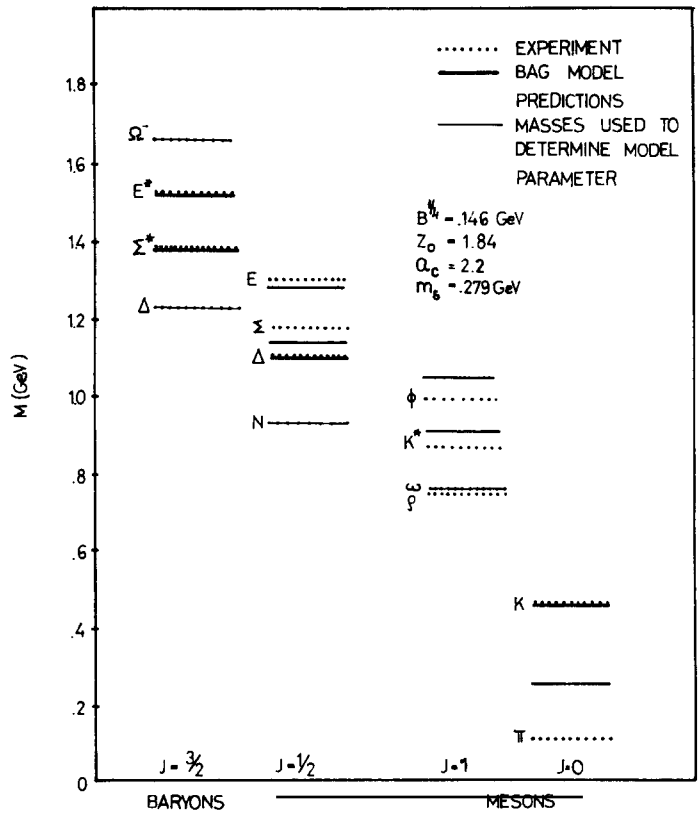

Fig. 7.2. The M.I.T. fit to the hadron masses where the non-strange quarks are assumed to be massless. The experimental values are given by dotted lines for comparison. There are four parameters B, α_c, Z_0 and m_s (strange quark mass) to fit. The masses of the N, Δ, ω, and Ω were used to determine the parameters.

and there is enough motivation, we believe, for further and more elaborate work in this approach to the spectrum of light hadrons.

The relative magnetic moments of baryons as determined from the best fit of fig. 7.2 is given in the following table:

Hadron	Magnetic moment μ/μ_p	
	Experimental	Bag model
n	-0.69	$-\frac{2}{3}$
Λ	-0.24 ± 0.02	-0.255
Σ^+	0.93 ± 0.16	0.97
Σ^0	-	0.31
Σ^-	-0.53 ± 0.13	-0.36
Ξ^0	-	-0.56
Ξ^-	-0.69 ± 0.27	-0.23

The bag model is less accurate in the static approximation on the over-all normalization of the octet magnetic moments. In subsection 6.3 we found $2M_p\mu_p = 2.6$ for the gyromagnetic ratio of the

proton (experiment is 2.79). The inclusion of the quark–gluon interaction in this section leads to a larger value for B than in subsection 6.3, and a consequently smaller proton radius. This results in a somewhat too small gyromagnetic ratio for the proton: $2M_p\mu_p = 1.9$ from the fit of fig. 7.2.

The three best-known charge radii of the four-parameter fit to the spectrum are given in the next table in comparison with the experimental data:

	Charge radii $\langle r^2\rangle^{1/2}$	
Hadron	Experimental	Bag model
p	0.88 ± 0.03 fm	0.73 fm
n	-0.12 ± 0.01 fm	0
π	0.78 ± 0.10 fm	0.5 fm

Given the rather rough assumptions in certain stages of the above calculations, we feel restrained to comment upon the details of the fit in fig. 7.2, and upon the "goodness" of the various static parameters of mesons and baryons in the static bag approximation. Only further hard work can decide whether we are on the right track in hadron phenomenology.

7.2. Charmonium

We shall study here a simple approach to bound states of heavy charmed quarks in adiabatic approximation. The charmed quarks are treated non-relativistically in their motion, whereas gluons and light quarks, together with the bag surface, may be handled in the future in the spirit of the Born–Oppenheimer approximation. With further simplification, the interaction between a charmed quark and antiquark will be described by a non-relativistic potential $V(r)$ in the Schrödinger equation of the reduced problem.

The charmonium bound state in Born–Oppenheimer approximation is roughly like a quark molecule whose heavy charmed quarks are associated with the heavy nuclei in molecules. The surface variables, transverse gluons, and light quarks are treated as the light electrons in molecules as it was discussed in subsection 6.2.

The level separation for quark excitations in the charmonium is approximately

$$\Delta E_q = 5\text{–}600\ \text{MeV}.$$

We can estimate the level separation of gluon and surface excitations from the quantization of the color-electric vortex of subsection 5.3. The effective mass of the confined gluons (gluon excitations) is about

$$\Delta E_{\text{gluon}} \approx \pi/R \approx 1\ \text{GeV}$$

with a classical radius $R = 0.5$ fermi for the vortex. The energy of string-like excitations is

$$\Delta_{\text{string}} \approx \pi/\langle r\rangle \approx 1\ \text{GeV},$$

where $\langle r\rangle$ is the average length of the elongated charmonium molecule.

This qualitative estimate shows that the periods of gluonic or surface excitations are not much shorter than heavy quark periods, so that the adiabatic approximation is a rather rough one here. Nevertheless, it gives a qualitative insight into the physical problem.

We imagine a pair of static sources which are coupled to the bagged non-Abelian gauge field $A_{i\mu}$. The position vectors $\boldsymbol{r}_1$ and $\boldsymbol{r}_2$ of the static sources are parameters in the static Hamiltonian $H_{st}(\boldsymbol{r}_1, \boldsymbol{r}_2)$ whose dynamical variables include the gauge field, the ordinary light quarks, and the "collective variables" of the bag.

Now, we assume that for slowly moving charmed quarks when the c-quark is at $\boldsymbol{r}_1$ and the $\bar{c}$-quark is at $\boldsymbol{r}_2$ the static Hamiltonian is still applicable, if the non-relativistic kinetic energy of the $c\bar{c}$-pair is added. Physically we assume that the bag can instantaneously readjust itself to the slowly moving, point-like $c\bar{c}$-pair.

In a further approximation we shall ignore the gluon and light quark degrees of freedom, together with the quantum energy of the surface which is treated classically. The Hamiltonian H_{st} becomes the potential energy $V(r)$ of the static sources which was calculated in subsection 3.3:

$$H_{st}(\boldsymbol{r}_1, \boldsymbol{r}_2) = V(r), \qquad r = |\boldsymbol{r}_1 - \boldsymbol{r}_2|.$$

After this drastic reduction of the problem we have to solve the Schrödinger equation

$$-\frac{\hbar^2}{2m}\nabla^2\psi(\boldsymbol{r}) + V(r)\psi(\boldsymbol{r}) = E\psi(\boldsymbol{r}),$$

where $\boldsymbol{r}$ stands for the relative three-vector of the $c\bar{c}$-pair, and m is the reduced mass. The potential energy $V(r)$, as shown in fig. 3.2, is well approximated by

$$V(r) \approx -\tfrac{4}{3}\alpha_c/r + \lambda r, \tag{7.7}$$

where $\lambda = 1\,\text{GeV/fermi}$, and $\alpha_c = 0.15$. The factor $\frac{4}{3}$ in (7.7) takes into account the fact that a color singlet charmonium state is an equal superposition of red–green, yellow–violet, and blue–orange $c\bar{c}$-pairs as it was shown in subsection 3.3.

Some authors have used a similar potential to $V(r)$ of eq. (7.7). We are close to their results in our calculation of the charmonium spectrum as shown in fig. 7.3, if $m = \frac{1}{2}m_c = 0.8\,\text{GeV}$ is put in the Schrödinger equation.

The spin-dependence of the $c\bar{c}$ interaction energy is a very interesting problem in the bag model. The force between a color charge and the bag surface is always repulsive, classically. A color magnetic moment, however, exerts an attractive force on the surface as dictated by the boundary condition $\boldsymbol{n} \times \boldsymbol{B} = 0$.

The attractive force is understandable, if we note that the outside vacuum phase acts as a perfectly

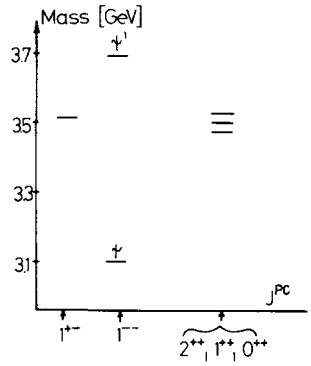

Fig. 7.3. The charmonium spectrum in the quark bag model.

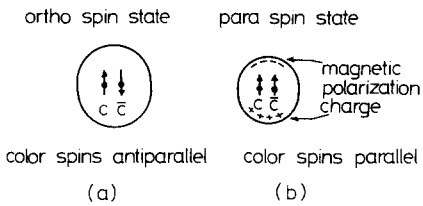

Fig. 7.4. The fairly strong spin-splitting of the ortho and para charmonium states might be associated with the interaction of color spin with the magnetic surface charge polarization.

permeable color-magnetic material with "polarization charge" on the boundary of the two phases when a color induction field $\boldsymbol{B}$ is present (fig. 7.4).

The net color-magnetic moment of a spin singlet state pulls in the surface of the bag reducing the energy of the system, as shown in fig. 7.4. This mechanism may explain the rather strong spin-splitting of the ψ and η_c in the charmonium spectrum.

String limit

We have seen in subsection 3.3 that for a quark–antiquark pair fixed at large separation an approximate, cylindrical vortex solution appears. The energy per unit length in the vortex is

$$\lambda = \tfrac{3}{2}(4\pi\sigma^2 g^2)^{1/3}, \tag{7.8}$$

with the radius

$$R = \lambda/3\pi\sigma.$$

The volume energy is set to zero here, with $B = 0$.

When the internal structure of the vortex is excited (subsection 5.4), the mass scale of confined gluons is set by π/R. In the weak coupling limit, where λ is kept fixed and $g \to 0$, the vortex shrinks and becomes very thin, $R \to 0$ ultimately. The excitation spectrum of massive gluons goes to infinity then, and only string-like oscillations are possible at finite energies.

The picture is similar when the point quarks are not held fixed at the end points of the vortex. The massive excitations become frozen in, if the weak coupling limit is taken, and the elongated bag is described by the dynamical variables of a string whose two ends are loaded with massive quarks.

In curvilinear coordinates x^μ, the quark and antiquark are connected inside the bag by the coordinate line x^3 as shown in fig. 7.5. This is the string. The two-dimensional surface swept out by the

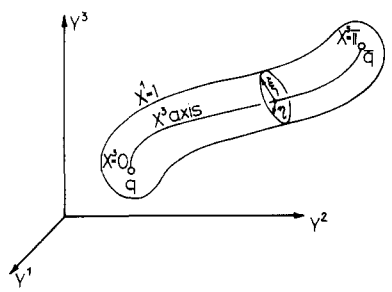

Fig. 7.5. The parametrization of the string-like bag.

string is described by

$$y^\Lambda = f^\Lambda(x^0, x^3),$$

where $x^3 \in [0, \pi]$ between the $q\bar{q}$-pair. The world lines of the quark and antiquark are represented by $f^\Lambda(x^0, 0)$, and $f^\Lambda(x^0, \pi)$ respectively.

The interior of the elongated bag is parametrized by general cylindrical coordinates

$$y^\Lambda(x) = f^\Lambda(x^0, x^3) + (\cos x^2 \xi^\Lambda + \sin x^2 \eta^\Lambda) x^1 \rho(x^0, x^2, x^3), \tag{7.9}$$

where $\xi^\Lambda(x^0, x^3)$ and $\eta^\Lambda(x^0, x^3)$ are space-like and orthogonal unit vectors at each point along the string. They are orthogonal to the surface swept out by the string in Minkowski space. $x^1 = 1$ describes the surface of the bag in (7.9).

It can be shown that the string-like motions of the thin, elongated bag may be characterized by $f^\Lambda(x^0, x^3)$ alone. We take $\rho(x^0, x^2, x^3) \sim R$, approximately, and the gauge field inside the bag is approximated by

$$F^{\Lambda\Lambda'}(y) = -\frac{g^2}{\pi R^2} \Delta^{-1} (f^\Lambda_{,0} f^{\Lambda'}_{,3} - f^\Lambda_{,3} f^{\Lambda'}_{,0}) \tag{7.10}$$

in the weak coupling limit. Δ is defined by

$$\Delta = \{(f^\Lambda_{,0} f_{\Lambda,3})^2 - f^\Lambda_{,0} f_{\Lambda,0} f^\Lambda_{,3} f_{\Lambda,3}\}^{1/2}.$$

For simplicity, an Abelian gluon field is taken in (7.10). The Ansatz (7.10) satisfies the Maxwell equations in the interior for arbitrary $f^\Lambda(x^0, x^3)$. The linear boundary condition $n_\mu F^{\mu\nu} = 0$ is also satisfied. When $F^{\mu\nu}$ and the associated four-potential A_μ are substituted into the action W of eq. (5.14b) for arbitrary $f^\Lambda(x^0, x^3)$, we find

$$W_{\text{gauge}} = -\tfrac{1}{4} \int_{\text{bag}} d^4x J F_{\mu\nu} F^{\mu\nu} = \frac{g^2}{2\pi R^2} \int dx^0\, dx^3 \Delta$$

$$W_{\text{surf}} = -\sigma \int_{x^1=1} M\, dx^0\, dx^2\, dx^3 = -\frac{g^2}{\pi R^2} \int dx^0\, dx^3 \Delta,$$

$$W_{\text{g-q}\bar{\text{q}}} = -\int_{\text{bag}} d^4x J j^\mu A_\mu = -\frac{g^2}{\pi R^2} \int dx^0\, dx^3 \Delta.$$

Thus the action W of eq. (5.14b) becomes

$$W = -\lambda \int dx^0\, dx^3 \Delta - m \int \sqrt{f^\Lambda_{,0}(x^0, 0) f_{\Lambda,0}(x^0, 0)}\, dx^0 - m \int \sqrt{f^\Lambda_{,0}(x^0, \pi) f_{\Lambda,0}(x^0, \pi)}\, dx^0. \tag{7.11}$$

The first integral in (7.11) is proportional to the surface area swept out by the string in Minkowski space, with the proportionality factor $-\lambda$. Therefore, the action in (7.11) describes a string loaded with two point particles of mass m at the end points. The vortex energy λ per unit length is identified as

$$\lambda = (2\pi\alpha'(0))^{-1} \tag{7.12}$$

in the string model. It is remarkable that $\lambda = 1\,\text{GeV/fermi}$ from the charmonium fit is close to the universal Regge slope $\alpha'(0) = 0.9\,\text{GeV}^{-2}$ in the string model.

The above considerations may be extended to the non-Abelian model.

7.3. Hadronic deformation energy with massless quarks

We have seen in the previous subsection that the charmonium molecule with heavy charmed quarks has a deformed cigar-like shape in the bag model as dictated by the bag equations and the non-spherical pressure of the color-electric field exerted on the bag's surface.

Now we are interested in the other extreme of hadronic deformations where massless quarks are put on bag orbitals in the spirit of subsection 7.1. We have seen in subsection 1.4 that a heavy nucleus may become deformed due to the non-spherical pressure exerted on the surface of the nucleus by valence nucleons (light particles compared with the nucleus bag) in non-zero angular momentum states. Similarly, the hadron bag becomes distorted from a spherical shape, if the pressure of the light constituents is non-spherical in ground state, or a centrifugal force is present in large orbital angular momentum states.

Recently DeTar made an interesting attempt to calculate the hadronic deformation energy in the bag model with massless quarks. His calculation is a useful introduction to the string-like excitations of light hadrons in the next subsection.

Following DeTar we shall describe here his constrained variational method which permits the calculation of the energy as a function of a collective variable δ. The bag cavity is permitted now to assume whatever shape is necessary in order to minimize the energy for a given expectation value of the collective variable. Pure volume tension will be applied for quark confinement and the surface remains classical throughout the calculations. The method is applied to a bag containing one $q\bar{q}$ pair and the energy as a function of the separation of the quarks is evaluated.

Consider a three-parameter azimuthally symmetric surface, defined in cylindrical coordinates z, ρ, φ by the expression for ρ as a function of z,

$$\rho^2 = n^2(1-(z^2/d^2))(1+a(z^2/d^2)) = q^2(z), \tag{7.13}$$

where n is the cylindrical radius at $z = 0$, d is the length of extension in z and

$a = 0$	ellipse
$-1 < a < 0$	distorted ellipse-bulge in middle
$0 < a < 1$	distorted ellipse-flattened in middle
$1 < a$	peanut shape
$a \to \infty, n \to 0$	fission
$-\infty < a < -1$	two bags.

A considerable large class of shapes can be studied with such a parametrization.

The quark orbitals for the bag geometry of (7.13) are described by the trial function

$$q = \begin{bmatrix} \varphi U \\ i\boldsymbol{\sigma}\mathbf{s}\varphi U \end{bmatrix}, \tag{7.14}$$

where U is a two-component Pauli spinor and

$$\varphi = \beta(z) + \alpha(z)R^2,$$

$$s = \frac{1}{\lambda}\nabla R; \qquad \lambda = |\nabla R|_{\rho=q(z)},$$

$$R^2 = R_0^2 + \rho^2 - q^2(z),$$

$$R_0^2 = \max_z q^2(z).$$

The vector s is constructed so that it is the unit normal to the surface when evaluated there ($\rho = q(z)$). The trial state (7.14) satisfies the linear boundary condition (4.1) explicitly.

The function φ depends on two functions of z, which are parametrized by

$$\beta_S = 1, \qquad \alpha_S = c, \tag{7.15}$$

and

$$\beta_A = \tanh(\eta z/d), \qquad \alpha_A = c\tanh(\eta z/d) \tag{7.16}$$

for symmetric and antisymmetric states, respectively. The separation of the quarks is achieved in the calculation by constraining the orbitals to separate into a left orbital and right orbital while preserving the spatial symmetry of the total wave function:

$$\psi(1,2) = \psi_L(1)\psi_R(2) + \psi_R(1)\psi_L(2).$$

Expressing the left and right orbitals in terms of orthogonal symmetric and antisymmetric orbitals, we have

$$\psi_L = \psi_S - \mu\psi_A; \qquad \psi_R = \psi_S + \mu\psi_A,$$

$$\psi(1,2) = \psi_S(1)\psi_S(2) - \mu^2\psi_A(1)\psi_A(2),$$

with the mixing parameter μ^2 ranging from 0 to 1 for maximal to minimal overlap between SS and AA orbitals. The mixing parameter μ^2 is determined variationally by minimizing the Hamiltonian for spontaneous deformations of the bag. ψ_S and ψ_A are constructed from the trial function (7.14) with the help of (7.15) and (7.16) respectively.

The quark–gluon interaction energy was calculated to second order in the coupling constant g by evaluating the diagrams of fig. 7.1(a) and fig. 7.1(b) for the bag geometry of (7.13) where a variational expression was introduced for the color-electric and color-magnetic fields. For the self-energy graph the truncation discussed in 7.1 has been applied. DeTar has also investigated the response of the system to the forced separation of the quark orbitals. The constraint of quark separation is imposed directly on the quark wave function. It can be shown that the parameter δ,

$$\delta = \frac{2\mu(1+\mu^2)}{1+\mu^4}\int \psi_S(r)\psi_A(r)z\,\mathrm{d}^2r \tag{7.17}$$

measures the average separation of left and right orbitals. The constraint is implemented by adding to the variational Hamiltonian the term δ with a Lagrange multiplicator.

The zero-point energies of the fields are ignored.

Preliminary results

For a spherical cavity without constraint the variational calculation reasonably reproduces the results of subsection 7.1, if the same assumptions are incorporated.

When the shape of the ρ meson is permitted to deviate from a spherical shape, the energy is reduced. A slightly deformed ρ meson is expected, since the color-magnetic dipole field exerts a non-uniform pressure on the bag surface. The deviation from sphericity is prolate for the state with spin projection $|m_s| = 1$ onto the axis of deformation and oblate for the state with spin projection $m_s = 0$. With the zero-point energy omitted and gluon coupling $\alpha_c = 2$, the ratio of the polar radius to equatorial radius is 1.11 for the ρ meson with $|m_s| = 1$. The reduction in energy is less than 1%.

For the calculation of deformed states with constraint the deformation energy is shown in fig. 7.6 as a function of the expectation value of the separation parameter δ of (7.15) for two values of the quark–gluon coupling constant, $\alpha = 2$ and $\alpha = 0$. The energy is given in units of $B^{1/4}$ and the separation δ is shown in units of $B^{-1/4}$. The fit of fig. 7.2 to the light hadrons gives $B^{1/4} \approx 145$ MeV or $B^{-1/4} \approx 1.3$ fermi.

In the presence of color-electric field the energy is approximately linear at large separations. The slope at large separation agrees with the result for a cylindrical tube. The slope in the cylindrical approximation is

$$dE/d\delta = \sqrt{4\pi \cdot \tfrac{4}{3}\alpha_c} = 5.8, \tag{7.18}$$

where the factor $\frac{4}{3}$ is included for color. The value from the variational calculation is 6. The radius of the cylindrical vortex with color

$$R = \sqrt[4]{\tfrac{4}{3}\alpha_c/\pi} = 0.81.$$

The value obtained in DeTar's calculation is between 0.8 and 0.83. Figure 7.7 shows the shapes of the deformed hadron corresponding to the various points indicated in fig. 7.6.

The color-electric and magnetic energies are shown in fig. 7.8. The color-electric field energy dominates over the color-magnetic energy at large separation. The slope of the color-electric field

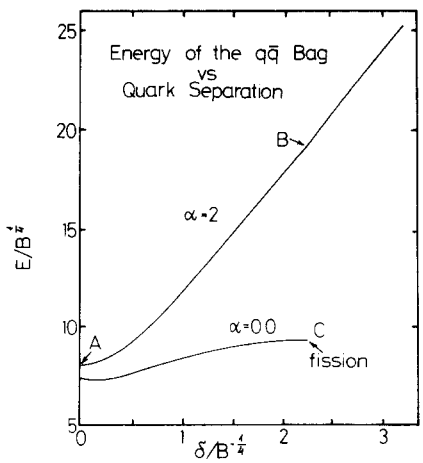

Fig. 7.6. Total energy of the bag in units of $B^{1/4} \approx 146$ MeV as a function of the average separation of the quark orbitals δ in units of $B^{-1/4}$ for two values of the quark–gluon coupling constant. The shape of the bag at points A, B and C is shown in fig. 7.7.

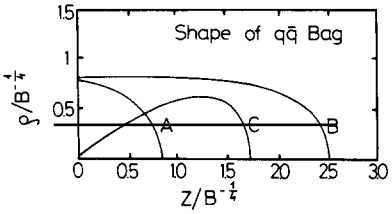

Fig. 7.7. Shape of one quadrant of the bag in longitudinal section at the three points *A*, *B* and *C* of fig. 7.6. The *z*-axis is the symmetry axis.

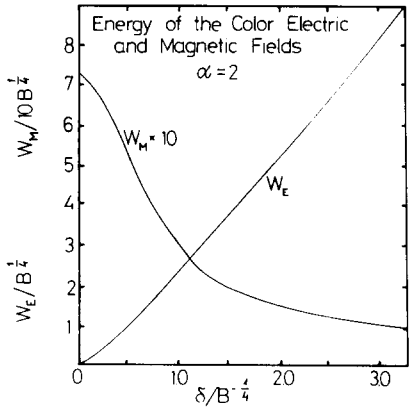

Fig. 7.8. Contribution to the total bag energy from the color electric and color magnetic field in units of $B^{1/4}$ as a function of the average separation δ of the quark orbitals.

energy W_E asymptotically is about one-half of the slope (7.18), in accordance with the expectation that the ratio of field energy to volume energy is 1:1 in a cylindrical vortex with pure volume tension.

In DeTar's calculation the bag is kept stretched by the constraint for the orbital separation δ. For a spinning bag the centrifugal force separates the quark orbitals without further constraint put in by hand. The elongated and spinning bag behaves then as a "fat" string (see subsection 7.4).

When the quark–gluon interaction is switched off and $\alpha_c = 0$, it is expected that the quark–antiquark bag could be pulled apart into two bags of a single quark (or antiquark) each, because the gluons which are essential to ensure that the bag has zero triality are absent. Indeed, the variational calculation shows the expected result.

The corresponding energy as shown in fig. 7.6 rises a little and becomes constant about 10% higher than the actual energy of two bags with one quark (or antiquark) each. The shape of the bag with $\alpha_c = 0$ is shown in fig. 7.7 as the neck radius shrinks to zero indicating that it undergoes fission. DeTar interprets the 10% energy access as the inadequacy of the variational calculation due to the tear-drop shape of the two bags at the point of fission.

The variational method is well-suited for the calculation of the nuclear potential and the structure of the deuteron as a six-quark bag.

7.4. String-like excitations of hadrons

Johnson and Thorn have suggested that string-like hadrons may be pictured as vortices of color flux lines which terminate on concentration of color at the end points. A meson with one quark and one antiquark would have the q at one end and $\bar{q}$ at the other. A baryon with three valence quarks would be arranged as a linear chain molecule where the largest angular momentum for a state of given mass is expected when two quarks are at one end and the third is at the other (fig. 7.9).

The color flux connecting opposite ends is the same for mesons and baryons giving an explanation for the same slope of meson and baryon trajectories.

We shall construct now the solution which yields maximal angular momentum for fixed mass. Accordingly, let us consider a bag with elongated shape rotating about the center of mass with an angular frequency ω (see fig. 7.9). It is assumed that the end points move with light velocity.

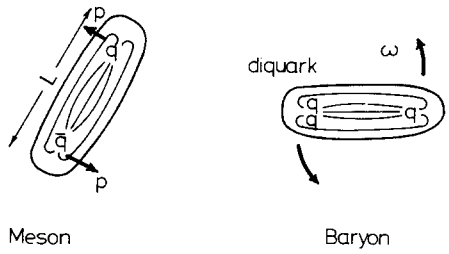

Fig. 7.9. String-like excitations of light mesons and baryons with large orbital angular momentum.

A given point inside the bag, at a distance x from the axis of rotation, moves with a velocity

$$v = \omega \cdot x = 2x/L,$$

where L is the length of the cigar-like bag.

In the present calculation the bag surface will be fixed by balancing the gluon field pressure against B, the confining vacuum pressure:

$$\tfrac{1}{2}\sum_{i=1}^{8} (\boldsymbol{E}_i^2 - \boldsymbol{B}_i^2) = B. \tag{7.19}$$

The color-electric field $\boldsymbol{E}_i$ is determined by Gauss's law,

$$E_i \cdot A = g\tfrac{1}{2}\lambda_i, \tag{7.20}$$

where A is the cross section of the bag at a point where the mean field strength associated with the color charge $g\frac{1}{2}\lambda_i$ is $\boldsymbol{E}_i$.

The color magnetic field $\boldsymbol{B}_i$ associated with the rotation of the color electric field is given by

$$\boldsymbol{B}_i = \boldsymbol{v} \times \boldsymbol{E}_i \tag{7.21}$$

at a point moving with velocity $\boldsymbol{v}$. This field is consistent with the linear boundary conditions in eq. (3.9).

If $\boldsymbol{E}_i$ from (7.20) and $\boldsymbol{B}_i$ from (7.21) are put in eq. (7.19), the cross section A can be expressed as a function of the orbital velocity v:

$$A = \sqrt{\tfrac{2}{3}}\, g \frac{1}{\sqrt{B}} \sqrt{1 - v^2}, \tag{7.22}$$

where we have used that $\langle \Sigma_{i=1}^{8} (\frac{1}{2}\lambda_i)^2 \rangle = \frac{4}{3}$ for a color triplet state. The cross section A in (7.22) shows the expected Lorentz contraction.

The total mass M of the rotating bag consists of three terms,

$$M = E_q + E_f + BV, \tag{7.23}$$

where E_q is the quark energy, E_f the gluon field energy, and BV is the volume energy.

The length L of the stretched bag is determined, for a given value of the total angular momentum J, by the condition

$$\partial M/\partial L = 0. \tag{7.24}$$

This is the condition that the angular momentum be a maximum for fixed M.

The different pieces of the total mass M in (7.23) are the following. The volume energy is

$$BV = BL\int_0^1 \mathrm{d}v A(v) = B\cdot L\sqrt{\tfrac{2}{3}}\frac{1}{\sqrt{B}}\int_0^1 \mathrm{d}v\sqrt{1-v^2},$$

and the energy of the colored flux lines is

$$E_\mathrm{f} = \tfrac{1}{2}\int_{\mathrm{bag}} \mathrm{d}^3 r\sum_{i=1}^{8}(\boldsymbol{E}_i^2+\boldsymbol{B}_i^2) = \sqrt{\tfrac{2}{3}}g\sqrt{B}L\int_0^1 \mathrm{d}v\,\frac{1+v^2}{\sqrt{1-v^2}}.$$

Since we assume that the valence quark wave functions are localized near the ends, the total quark energy E_q is

$$E_\mathrm{q} = 2p \tag{7.25}$$

for a convective quark momentum p at the ends. The total angular momentum

$$J = J_\mathrm{q} + J_\mathrm{f}$$

is the sum of the quark and gluon field angular momenta. The angular momentum of the color fields is

$$J_\mathrm{f} = \left|\int_{\mathrm{bag}} \mathrm{d}^3 r\sum_{i=1}^{8}\boldsymbol{r}\times(\boldsymbol{E}_i\times\boldsymbol{B}_i)\right| = \sqrt{\tfrac{2}{3}}L^2 g\sqrt{B}\int_0^1 \mathrm{d}v\,\frac{v^2}{\sqrt{1-v^2}},$$

whereas the total quark angular momentum is given by

$$J_\mathrm{q} = pL.$$

With the calculated ingredients we may express the total mass M as a function of L,

$$M = \frac{2J}{L} + \sqrt{\tfrac{2}{3}}Lg\sqrt{B}\frac{\pi}{2}, \tag{7.26}$$

for fixed total angular momentum J. From eqs. (7.24) and (7.26) we find an asymptotically linear trajectory:

$$J = \alpha'(0)M^2,$$

with the slope

$$\alpha'(0) = \frac{1}{8\pi^{3/2}}\sqrt{\frac{3}{2}}\frac{1}{\sqrt{\alpha_\mathrm{c}}}\frac{1}{\sqrt{B}}. \tag{7.27}$$

The parameters B and α_c have been determined in subsection 7.1 as $B = 55\,\mathrm{MeV/fermi}^3$ and $\alpha_\mathrm{c} = 2.2$. With these values in (7.27) we find

$$\alpha'(0) = 0.88(\mathrm{GeV})^{-2}$$

in very good agreement with the experimentally determined slope which is about $0.9\,\mathrm{GeV}^{-2}$. The analogous relation to (7.27) for confinement with surface tension has been given in eq. (7.12) if λ is taken from (7.8).

The slope $\alpha'(0)$ in (7.27) has been calculated for a state in which the colored objects at the two ends

belong to the 3 or $\bar{3}$ representation of color SU(3). If the expectation value of the Casimir operator $\Sigma_{i=1}^{8}(\frac{1}{2}\lambda_i)^2$ is C in a given color representation, the formula for the slope may be written as

$$\alpha'(0) = \frac{1}{\sqrt{C}}(32\pi^3\alpha_c B)^{-1/2}, \tag{7.27a}$$

where $\alpha'(0)$ reduces to (7.27) with $C = \frac{4}{3}$ in color triplet representation.

We shall argue now that (7.27) is equivalent to the dual string model formula for the slope if the "proper tension" along the string is associated with the proper energy per unit length of the color flux and spatial extension. The proper energy per unit length is defined as the energy T_0 per unit length at a point in the bag evaluated in the instantaneous rest system of that point;

$$T_0 = \tfrac{1}{2}\sum_{i=1}^{8} E_i^2 A_0 + BA_0 = 2BA_0,$$

where A_0 is the cross sectional area of the bag. If we use (7.22) for A with $v = 0$, we find

$$T_0 = 4\sqrt{\tfrac{2}{3}}\sqrt{\alpha_c}\sqrt{B}\sqrt{\pi}$$

for the proper tension. In the dual string model the slope and proper tension T_0 are related by the formula

$$T_0 = \frac{1}{2\pi\alpha'(0)},$$

so the slope is

$$\alpha'(0) = \frac{1}{8}\sqrt{\frac{3}{2}}\frac{1}{\pi^{3/2}}\frac{1}{\sqrt{\alpha_c}}\frac{1}{\sqrt{B}},$$

in agreement with (7.27).

We shall discuss now some approximations of the above calculations. The formula (7.25) for the total quark energy assumes that the energy $\sim(1/\sqrt{A})$ associated with the confinement of quarks may be ignored in comparison to the total energy of the system.

In this approximation the quark energy $E_q = 2p$ is zero for the following reason. For a given angular momentum J the quark energy E_q can be expressed, with the help of the relation $J = pL + J_f$, as

$$E_q = 2p = 2\left(\frac{J}{L} - \sqrt{\frac{2}{3}}\, Lg\sqrt{B}\int_0^1 dv \frac{v^2}{\sqrt{1-v^2}}\right), \tag{7.28}$$

where L is given by

$$\frac{\partial M}{\partial L} = 0 = -\frac{2J}{L^2} + \sqrt{\frac{2}{3}}\, g\sqrt{B}\,\frac{\pi}{2}. \tag{7.29}$$

The quark energy E_q in (7.28) is zero for the value of L from (7.29). Therefore, ignoring corrections of the order of $1/\sqrt{A}$, the total energy and angular momentum of the elongated bag is associated with the color flux lines. The quarks at the ends serve to terminate the color flux, otherwise they do not govern the dynamics.

This picture of the leading Regge trajectory is similar to the dual string model. However, the bag dynamics is associated with the color flux lines and the geometrical variables of the string merely serve to parametrize the motion of these fields. Further, since the cross section A in (7.22) is independent of J, the elongated bag as a string is "fat", with the transverse dimension of ordinary hadron ground states.

The calculation presented here is expected to be valid for an "asymptotic trajectory" with large angular momenta. The value of J should be of the order of five, or so. In that case

$$E_{\text{glue}} \gg 1/\sqrt{A},$$

and the string energy dominates over quark energies at the ends. The hope is that the asymptotic calculation remains sensible even at lower values of the angular momentum.

7.5. Gluonium

One of the most spectacular predictions of the quark bag model is the existence of quarkless gluonic hadrons. They are constructed in close analogy with the quark orbitals of subsection 6.3 in the spirit of the adiabatic approximation. Gluons populate then the eigenmodes of a spherical bag of radius ρ, where the wave functions of the valence gluon orbitals are subject to the linear boundary conditions

$$\boldsymbol{n} \cdot \boldsymbol{E}_i = 0, \tag{7.30}$$

$$\boldsymbol{n} \times \boldsymbol{B}_i = 0, \tag{7.31}$$

on the static and spherical surface.

To lowest order in α_c the gluon self-coupling may be ignored and the colored vector gluon fields behave as Abelian vector fields. They satisfy Maxwell's equations inside the static bag subject to the boundary conditions (7.30) and (7.31).

Similarly to spherical cavity resonators, two types of states are found for each value of the total angular momentum $J (J \geq 1)$:

mode	notation	parity (Π)
transverse electric	TE	$(-1)^{J+1}$
transverse magnetic	TM	$(-1)^{J}$

For each value of J and Π there is an infinite sequence of modes with increasing number of radial nodes. This feature of the spectrum is similar to the radial modes of quark orbitals as determined from the eigenfrequency equation (6.17). The analogous equation for the eigenfrequencies of gluon orbitals yields the following lowest modes:

mode	frequency	J^{Π}	energy
TE	2.74	1^+	$2.74/\rho$
TM	4.49	1^-	$4.49/\rho$

These modes when populated with gluons must form overall color singlets. Color singlet states of two gluons may be constructed with δ_{ik} coupling, the charge conjugation quantum number C is $+1$ then. Color singlet states of three gluons may be constructed by $d_{ikl}(C=+1)$ or $f_{ikl}(C=-1)$ couplings.

The calculation of the masses follows the method developed in section 6. Since the gluon states of non-zero total angular momentum are not spherical at the semi-classical level, their masses cannot be reliably estimated in the static bag approximation to a spherical shape. However, the predictions for zero total angular momentum of all-glue hadrons are on the same level of reliability as the mass predictions of subsection 6.3.

The most interesting result from the above considerations of Jaffe and Johnson is that the quark bag model predicts a new form of hadronic matter – glueballs – in the 1–2 GeV energy region following the same approximation procedures which yielded a qualitatively acceptable description of ordinary light mesons and baryons. The lowest masses are given by

occupied modes	J^{PC}	mass (MeV)
TE TE	0^{++}	960
TE TM	0^{-+}	1290
TE TE TE	0^{+-}	1460
TM TM	0^{++}	1590
TE TE TM	1^{--}	1640
TE TE	2^{++}	960

All states are flavor and color singlets in the above table. The last two states of the table are not well described in spherical approximation, they are included for later reference.

The high angular momentum excitations of glueballs become elongated string-like objects on approximately straight-line Regge trajectories. This description is motivated by the discussion of subsection 7.4. Here we only recall that the slope of the Regge trajectories associated with "fat" gluon strings is given by (7.27a),

$$\alpha'_{\text{glue}}(0) = \tfrac{2}{3}\alpha'(0), \tag{7.32}$$

where $\alpha'(0) = 0.9\,\text{GeV}^{-2}$ is the slope of ordinary Regge trajectories. The factor $\frac{2}{3}$ in (7.32) is a consequence of color octet charge separation at the ends of the string due to the centrifugal force exerted on the gluons in large angular momentum states. Ordinary elongated hadrons as "fat" strings carry a color triplet charge at the ends, hence the different slope of the trajectories.

If the pomeron with an intercept of one is identified with a spinning string of two gluons in color singlet and flavor singlet state (see section 9), the slope $\alpha'_{\text{glue}}(0) = 0.6\,\text{GeV}^{-2}$ from (7.32) predicts 1.3 GeV for the mass of the first physical state (2^{++}) on the trajectory. Some curvature in the pomeron trajectory may shift the mass 1.3 GeV upward.

The spherical cavity state 2^{++} in TE^2 mode whose mass was given at 960 MeV in the glueball table may become the 2^{++} particle on the pomeron trajectory when the hadron deformation from the non-spherical pressure is included in the calculations.

One finds motivation for the existence of all-glue hadron states outside the quark bag model, too. Quantum chromodynamics makes their existence conceivable, whereas Freund and Nambu predicted this new form of hadronic matter in the string model, in close association with the dual resonance model. They identified the pomeron and its daughters with closed quarkless strings whose slope is one-half of the ordinary slope $\alpha'_{\text{Pom}} = \frac{1}{2}\alpha'$.

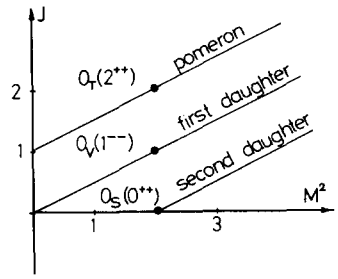

Fig. 7.10. The pomeron trajectory and its daughters in the string model. The pomeron intercept is set to $\alpha_p(0) = 1$ in an arbitrary manner. The tensor, vector, and scalar glueball states are indicated.

The leading pomeron trajectory and some daughters of the closed string are shown in fig. 7.10 where the intercept of the pomeron is set to one arbitrarily.

Glueball phenomenology

One way to produce quarkless states in any of the above mentioned models is to annihilate quarks with antiquarks. Some authors have explored the possibility that when such annihilations occur, as in Zweig-rule violating meson decays, the intermediate quarkless resonances (glueballs) dominate the dynamics. Unfortunately, the discussions remain on the level of a gross form of phenomenology. Nevertheless, we hope that a first qualitative insight into the problem may be useful and stimulating for an experimental search, and it may lead to the construction of a genuine theory of all-glue hadron states.

Let us consider first the vector glueball O_V with quantum numbers $J^{PC} = 1^{--}$. In the string model O_V is the lowest physical state on the first daughter of the pomeron trajectory. Its mass may be estimated from fig. 7.10 where the parallel and equidistant trajectories yield the mass $m_{O_V} = 1.34\,\text{GeV}$, if $\alpha'_{Pom}(0) = \frac{1}{2}\alpha'(0)$ is taken.

The lowest lying 1^{--} state has a mass of 1640 MeV in the glueball table of the bag model which is subject to modifications due to deformations by the non-spherical pressure. If we accept the trajectory structure for all-glue string-like bags where the pomeron has intercept one and its daughters are integer spaced below, the mass of the vector glueball should be $m_{O_V} = 1.3\,\text{GeV}$ with the slope $\alpha'_{glue}(0) = 0.6\,\text{GeV}^{-2}$.

Given the uncertainties we expect the mass of the particle to be somewhere between 1.3 GeV and 1.6 GeV.

Recently Robson has suggested that the vector glueball might have already been found in a DESY–Frascati experiment at 1.11 GeV. He argues that the main decay properties of the recent DESY–Frascati resonance are certainly consistent with a vector glueball, if the basic assumption of Freund and Nambu is accepted: the only poles needed in the Zweig forbidden decays are the O_V, ω, ϕ and ψ, as shown in fig. 7.11 for some sequential pole model diagrams.

In the experiment the reaction $\gamma + p \to V^0 + p$, $V^0 \to e^+e^-$ was studied by the interference between the Compton and Bethe–Heitler processes and a resonance-like structure of mass 1110 MeV was found. The observed width was consistent with the experimental resolution of 30 MeV and it was parametrized as a resonance of width 20 MeV, and B.R. $(d\sigma/dt)|_{t=0} = 4.9 \times 10^{-5}\,\mu\text{b GeV}^{-2}$, a factor of twenty smaller than for ω production.

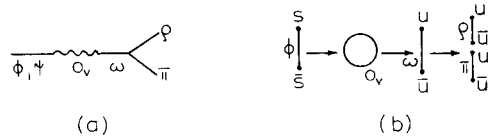

Fig. 7.11. Zweig-rule violating decay modes of the ϕ and ψ meson are given in (a). The corresponding string picture for the ϕ meson is shown in (b).

If one assumes the SU(4) broken couplings of the O_V to the known vector mesons,

$$\frac{f_{O_V\psi}}{m_{O_V}+m_\psi}=\frac{f_{O_V\phi}}{m_{O_V}+m_\phi}=\frac{1}{\sqrt{2}}\frac{f_{O_V\omega}}{m_{O_V}+m_\omega}=S, \tag{7.33}$$

and $m_{O_V}=1.11\,\text{GeV}$, $\Gamma_{O_V}=20\,\text{MeV}$ are accepted for input, then

$$\Gamma(\psi\to\rho\pi)=1.6\,\text{keV}$$

is obtained from the sequential pole model of fig. 7.11, only a factor of two above experiment. This is taken by Robson as an encouragement for ignoring the contribution of higher mass vector glueballs in the sequential pole model. Their inclusion would not be an appealing possibility, anyway.

Using the mass 1.11 GeV and eq. (7.33) as input, the width may also be predicted from the sequential pole model of Freund and Nambu, together with the following results

$$S=0.032\,\text{GeV}^{-1},$$
$$\Gamma(\psi\to K^+K^-)=0.12\,\text{eV}\ (9.8\pm 9.8\,\text{eV experimentally}),$$
$$\Gamma(O_V\to\rho\pi)=7.8\,\text{MeV},$$
$$\Gamma(O_V\to K^+K^-)=0.81\,\text{MeV}\simeq\Gamma(O_V\to K_0\bar{K}_0),$$
$$\Gamma(O_V\to e^+e^-)=85\,\text{eV}.$$

The dominant decay mode is $O_V\to\rho\pi$ evolving into a $\pi^+\pi^-\pi^0$ final state, and the decay into two kaons is suppressed.

The tensor glueball O_T as the lowest physical state on the pomeron trajectory, and the scalar glueball O_S as the second daughter are also expected in the mass region of 1.–1.5 GeV. Their phenomenology is most interesting and given elsewhere.

8. Hadron spectroscopy, II (exotic states)

In this section we shall briefly discuss the low-lying multiquark hadrons, baryonium, and quark bag star as the most spectacular exotic objects within the framework of the quark bag model.

8.1. Multiquark hadrons

The quark bag model may shed some light on the old problem of exotics. In this model the mass of a hadron increases roughly in proportion to the total number of quarks inside the bag. This is due to the fact that the quark kinetic energy dominates the total energy of the bag, about $\frac{3}{4}$ of the mass of a typical hadron arises from the motion of the quarks.

It has been known for a long time that the Coulomb-like color electric forces saturate inside hadrons supporting rather strong evidence against low-lying exotic states in quantum chromodynamics. It means that there are no strong forces between color singlet mesons and baryons which might be related to confinement structure. With this argument a low-lying $qq\bar{q}\bar{q}$ state, say, would be rather like a loosely bound molecule with color singlet $q\bar{q}$ "atoms", if such a molecule may exist at all.

Recently Jaffe has called attention to the presence of color-magnetic forces, however. Two color singlet hadrons sitting close to each other are not an eigenstate of the magnetic gluon exchange operator of eq. (7.9). They can exchange a gluon becoming color octets still forming an over-all color singlet state. This force mixes and splits multiquark states.

Since the spin splittings among qqq baryons and $q\bar{q}$ mesons are a significant fraction of their masses, it may happen that a multiquark state $qq\bar{q}\bar{q}$ or $qqqq\bar{q}$ may lose so much energy in color-spin interaction that it becomes bound, relative to the decay into normal $q\bar{q}$ or qqq hadrons.

Jaffe proceeds now exactly as we did in the $q\bar{q}$ and qqq sectors in subsection 7.1. There are no new parameters or approximations. However much we like this, the critical remarks of subsection 7.1 are also carried over here without new parameters, and the shortcomings may hurt here even more than for ordinary hadrons. Nevertheless, Jaffe's calculation is the first and very interesting insight into the problem with surprising and encouraging results.

Jaffe approximates ΔE_M by replacing m_i by the average quark mass of the state. ΔE_M may be rewritten then in terms of Casimir operators of color $SU(3)_c$, spin SU(2) and color-spin $SU(6)_{cs}$, which is the SU(6) generated by $SU(3)_c \times SU(2)$:

$$\Delta E_M \sim 8N + \tfrac{1}{2}C_6(\text{tot}) - \tfrac{4}{3}S_{\text{tot}}(S_{\text{tot}}+1) + C_3(q) + C_3(\bar{q}) + \tfrac{8}{3}S_q(S_q+1) + \tfrac{8}{3}S_{\bar{q}}(S_{\bar{q}}+1) - C_6(q) - C_6(\bar{q}) \tag{8.1}$$

where C_3 and C_6 are the quadratic Casimir operators of SU(3) and SU(6), respectively. We refer to the SU(2) of S-wave $J = \frac{1}{2}$ quarks from eqs. (6.15) and (6.16) loosely as spin. The 35 generators of color-spin are

$$\{\alpha\} = \{\sqrt{\tfrac{2}{3}}\sigma^k;\ \lambda^a;\ \sigma^k\lambda^a;\ k = 1, 2, 3;\ a = 1, 2, \ldots, 8\}.$$

The Casimir operators are defined by

$$C_3(q) = \sum_{a=1}^{8}\left(\sum_{i=1}^{N_q}\lambda_i^a\right)^2; \qquad C_6(q) = \sum_{\mu=1}^{35}\left(\sum_{i=1}^{N_q}\alpha_i^\mu\right)^2; \qquad 4S_q(S_q+1) = \sum_{k=1}^{3}\left(\sum_{i=1}^{N_q}\sigma_i^k\right)^2.$$

Now, the Casimir operators of color-spin dominate eq. (8.1), as Jaffe pointed out. They are generally much larger than those of spin or color. For a given number of quarks and antiquarks $q \ldots q\bar{q} \ldots \bar{q}$ the lowest lying multiplet follows the rules:

1. The quarks and antiquarks are separately coupled to the largest allowed representation of color-spin.

2. The color-spin Casimir operator of the system including quarks and antiquarks is minimized.

On the basis of these rules it can be shown that the ground states of $qq\bar{q}\bar{q}$ and $qqqq\bar{q}$ are not exotic, they are nonets. Therefore, they may be misclassified as conventional $q\bar{q}$ or qqq states. The weight diagrams and quark content of these multiplets are shown in fig. 8.1.

The exotic states turn out to be heavier in Jaffe's calculation, far above the threshold for decaying into $(q\bar{q})(q\bar{q})$ or $(qqq)(q\bar{q})$, so that they must be broad if resonant at all.

A more detailed discussion about the phenomenological aspects of the multiquark states in the bag

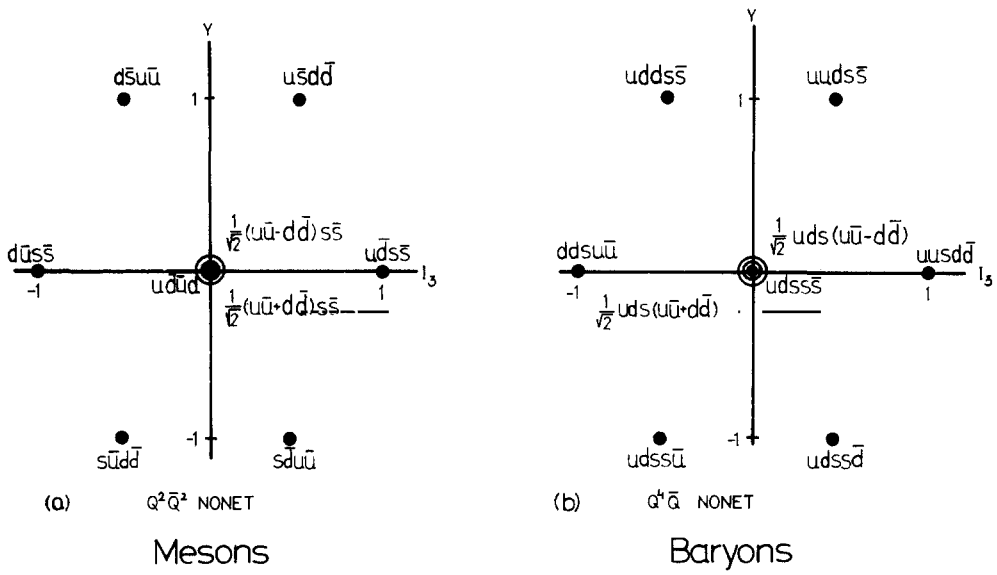

Fig. 8.1. The quark content of $qq\bar{q}\bar{q}$ and $qqqq\bar{q}$ nonets: (a) for the lowest meson nonet; (b) for the lowest baryon nonet.

model is found in Jaffe's papers. We turn now to the very interesting problem of high angular momentum excitations of $qq\bar{q}\bar{q}$ states.

8.2. Baryonium

The quark bag model accommodates a family of mesons which are probably dominantly coupled to baryon–antibaryon channels. Experimental results support the existence of these peculiar mesons, often characterized as states of baryonium.

The baryonium is pictured in the quark bag model as a fat string-like spinning object with a diquark and anti-diquark pair at the two ends. The dominant decay mode of the spinning string is to create a $q\bar{q}$ pair in the color-electric field of the elongated bag, where the quark joins the diquark, the antiquark joins the anti-diquark and the string breaks into a baryon–antibaryon pair.

We have seen in subsection 7.4 that the slopes of Regge trajectories associated with rotating string-like objects in the quark bag model depend on the color charge separation at the two ends. The slope formula (7.27a) depends on the value C of the Casimir operator. We may have color charges in triplet, sextet, or octet representation at the ends of the spinning bag.

The triplet separation occurs in the large angular momentum excitations of ordinary mesons or baryons. Octet separation is characteristic of the excitations of glueballs into spinning objects with gluons at the ends. In baryonium the diquark qq may be in color triplet or color sextet representation. The slopes of the corresponding trajectories are given in the following table:

	triplet	sextet	octet
$C=\sum_{i=1}^{\infty}(\frac{1}{2}\lambda_i)^2$	$\frac{4}{3}$	$\frac{10}{3}$	3
slope	$\alpha'(0)$	$\sqrt{\frac{2}{5}}\alpha'(0)$	$\frac{2}{3}\alpha'(0)$

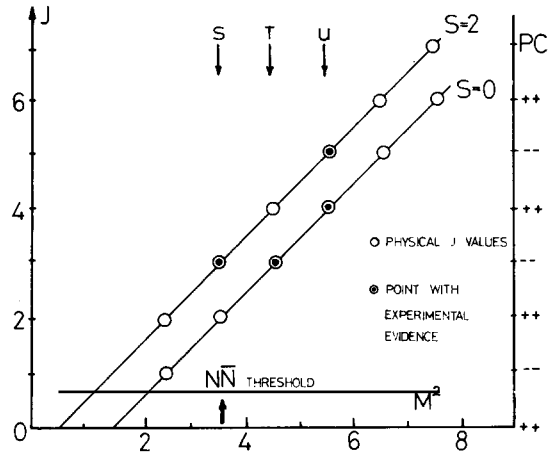

Fig. 8.2. The two leading natural-parity baryonium trajectories proposed by G.F. Chew.

Therefore, we expect baryonium trajectories with ordinary slope $\alpha'(0)$ when the diquark is in color triplet representation, with a slope $\frac{2}{5}\alpha'(0)$ in the sextet representation of the diquark. The latter states are very difficult to excite from ordinary hadrons since this 6–$\bar{6}$ string can only be produced in higher order requiring an extra gluon exchange in comparison with ordinary processes. If, however, such a state is produced somehow, it remains quite stable since its decay is also of higher order in the quark–gluon coupling.

The quark bag model therefore predicts the existence of extremely narrow spinning states with large angular momentum which predominantly decay into baryon–antibaryon channels.

Recently Chew suggested that two natural-parity trajectories, with isospin degeneracy as well as exchange degeneracy are able to account for most of the available evidence concerning meson states that communicate preferentially with baryon–antibaryon channels. The two baryonium trajectories are shown in fig. 8.2. They have ordinary slopes $\alpha'(0)$ corresponding to diquarks in color triplet representation.

Further search for baryonium states remains one of the most exciting projects in hadron spectroscopy.

8.3. Quark bag star

There is a general belief that pulsars are neutron stars compressed to densities greater than the density of atomic nuclei. We may guess that when the density of matter is further increased and becomes so large that the mean distance between quarks in different baryons is much less than one fermi the description of matter as nucleons interacting via potentials does not remain valid. A new description of matter composed of quarks may become relevant then. It is conjectured that at sufficiently high densities matter will behave as a relativistic gas of free quarks with $p \to \frac{1}{3}\rho$, where p is the pressure and ρ is the density of matter.

We shall bring now some qualitative arguments that the vacuum pressure (or surface tension) in the quark bag model may be large enough to compress the neutron phase of pulsars into quark phase.

The normal density of nuclear matter is

$$n_0 = 0.16 \text{ nucleon/fermi}^3,$$

or

$$\rho_0 = 2.4 \times 10^{14}\ \mathrm{g/cm^3}.$$

In highly compressed nuclear matter experts estimate the density to be about

$$\rho = 10^{15}\ \mathrm{g/cm^3},$$

and the corresponding pressure in neutron stars may be about

$$p = 5 \times 10^{34}\ \mathrm{dynes/cm^2}.$$

Now we recall from subsection 7.1 that a fit to the lowest meson and baryon states yielded the value $B^{1/4} = 146$ MeV as shown in fig. 7.2. This value of the vacuum pressure in c.g.s. units is

$$B = 9.5 \times 10^{34}\ \mathrm{dynes/cm^2},$$

so that the possibility for the formation of quark bag stars is there.

Following Chaplin and Nauenberg we shall apply Gibbs' criterion for a phase transition to calculate the density where the baryon matter changes to quark matter at zero temperature. At a fixed pressure p and zero temperature the stable phase of matter is the one which has the lowest Gibbs energy

$$\mu = (p + \rho)/n, \tag{8.2}$$

where ρ is the energy density and n is the conserved baryon number density. Equating the Gibbs energy for quark matter and for baryon matter at the same pressure,

$$\mu_{\text{baryon phase}} = \mu_{\text{quark phase}} \tag{8.3}$$

determines then the transition point.

First, we calculate the chemical potential in the quark phase of matter. The ground state of quark matter inside a gigantic quark bag star under vacuum pressure from outside is a fermi gas with all color states occupied for each eigenmode up to the fermi level.

When the quark masses may be neglected in comparison with the fermi energy of quarks, one can write for the energy density ρ at zero temperature

$$\rho = An^{4/3} + B \tag{8.4}$$

on dimensional grounds. Here A is a constant proportional to $\hbar c$, and n is the baryon number density which is conserved even when baryons do not exist any more individually.

The constant A was calculated by Chaplin and Nauenberg to second order in the quark–gluon coupling constant g,

$$A = \frac{9}{4}\left(\frac{3\pi^2}{\kappa}\right)^{1/3}\left(1 + \frac{8g^2}{3\pi}\right)\hbar c, \tag{8.5}$$

where κ is the number of quark flavors contributing to the energy density ρ.

From eqs. (8.2), (8.4) and (8.5) we can express the chemical potential (Gibbs energy per unit baryon number) as a function of the pressure p for zero temperature

$$\mu = 4(\tfrac{1}{3}A)^{3/4}(p + B)^{1/4}.$$

From the condition (8.3) we may calculate the critical baryon energy density where baryons begin to disappear and a new quark phase develops. The following table shows the critical baryon density ρ_c

in units of 10^{15} g/cm^3 in three different models of nuclear matter at high densities

model	ρ_c
Pandharipande–Smith	2.7
Bethe–Johnson I	6.5
Bethe–Johnson II	13

In these calculations the values of subsection 7.1 were used for α_c and B.

From the table it turns out that the phase transition occurs at baryon energy densities which are 10–50 times the baryon energy density in normal nuclei. Now Chaplin and Nauenberg argue that the maximum allowed energy density for stable quark stars as derived from general relativity is

$$\rho_{max} \approx 8.3B, \qquad B = (55\ \text{MeV/fermi}^3). \tag{8.6}$$

The value of ρ_{max} in (8.6) seems to be smaller than ρ_c in the table by a factor of three to five. Therefore the existence of stable quark bag stars remains under question. Since we are in a very sensitive energy region both in baryon phase and quark phase, the results are far from being conclusive in either direction. We seem to be on the border line of being capable of determining the possible existence of this incredible object. There is certainly more to come in the theoretical development of the quark bag model and nuclear matter calculations at extreme densities before the question becomes settled satisfactorily.

9. High energy scattering processes

In this section we shall study the qualitative description of hadronic final states associated with high energy processes within the framework of the quark bag model. It will be shown that color separation above one fermi is the governing mechanism to generate the final state in high energy collisions. This mechanism may explain the great similarity of final states in hadron–hadron and lepton–hadron reactions, as well as in e^+e^- annihilation. Scaling in deep inelastic lepton–nucleon scattering is discussed in subsection 9.2.

9.1. Low's model of the bare pomeron

A remarkable feature of total hadronic cross sections is that they are approximately constant over a broad energy range, between 10 GeV and 300 GeV laboratory energy. Low presents an attractive and simple model for the bare pomeron with sufficiently weak coupling, so that the problem of rising cross sections and the related logarithmic energy dependence may be viewed as higher order corrections (ignored here).

The constancy of the total cross sections is usually associated with the following experimental observations:

1. Elastic cross sections are also approximately constant over the same energy range, though they are much smaller than the corresponding total cross sections. The elastic amplitudes mainly appear as the diffraction due to multi-particle production processes. The elastic processes themselves are only secondarily reflected in the elastic amplitudes.

2. The real parts of forward scattering amplitudes are small compared to imaginary parts. The real part associated via dispersion relations with a constant σ_{tot} is zero, so that its presence is a measure of the non-constancy of σ_{tot}.

3. There is a diffraction peak which is approximately Gaussian in the momentum transfer.

4. There is an approximate factorization of diffraction amplitudes and total cross sections.

5. Approximate factorization and Feynman scaling (or limiting fragmentation) are observed in inclusive processes. In the fragmentation region of b the inclusive cross section for a fragment c is

$$\frac{E_c}{\sigma_{ab}}\frac{d\sigma_{ab}}{d^3q_c} = F_{bc}(t_{bc}, x_c),$$

demonstrating the independence from the projectile a. t_{bc} is the momentum transfer from b to c and $x = 1-(M^2/s)$ is Feynman's scaling variable with M the missing mass, and s the center of mass energy squared.

6. A universal plateau is observed in the central region in rapidity space. This plateau seems to be independent of the initial state of the reaction in which it is created.

Low's model to be described in this subsection seems to account qualitatively for all the above mentioned observations, together with the constancy of σ_{tot}. The only exception is factorization which is accidental in the model.

Bags in interaction

Following Low we describe the collision process of two hadrons qualitatively as the specific interaction of the associated bags with color gluon exchange. Let us consider two bags approaching each other in the c.m. system with a definite impact parameter b as shown in fig. 9.1. We assume the same radius and mass for the two bags. In a classical picture with sharp bag boundaries the bags will pass each other without interaction for $b > 2R$. They cannot interact, since the colored vector gluon fields are confined to the interior of the bags. In the quantum theory the surface of the bag becomes fuzzy, but a well-defined meaning is maintained for the impact parameter b.

When $b < 2R$ the two bags will touch in some point, and evolve for intermediate times as a fused single bag in highly excited state. The most probable interaction which may occur is the exchange of a soft colored gluon between the two parts of the intermediate bag running away with a relative velocity $2v \sim 2c$. The two color singlet parts become color octets due to the exchange of the soft gluon. Since the color flux lines are confined, the intermediate bag stretches and a color-electric vortex develops between the two color octet parts, as shown in fig. 9.2.

The overlap of the initial configuration with the stretched intermediate bag is negligible, so that the lowest order real part of the elastic scattering amplitude $f(b)$ vanishes. Elastic scattering requires the exchange of two colored gluons which is a higher order process in α_c.

One notes that a similar color-electric vortex develops in deep inelastic lepton–nucleon scattering when a colored quark inside the nucleon receives enormous momentum transfer by, say, a very

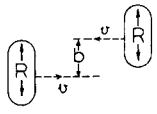

Fig. 9.1. Two bags colliding in the center of mass frame with impact parameter b.

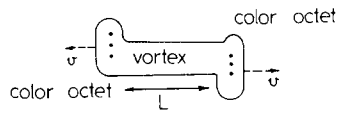

Fig. 9.2. The color-electric vortex tube after gluon exchange.

energetic electron. As a result, the kicked out quark carrying color charge is running away from the rest of the nucleon approximately with light velocity. Since the diquark left behind must be in color triplet state, the bag stretches and a color-electric vortex appears between the escaping quark and the rest of the nucleon.

In electron–positron annihilation at very large energies when a $q\bar{q}$-pair is created inside a "hadronic domain" of the physical vacuum, the pair is running away in back-to-back configuration with a relative velocity $2v \sim 2c$. Again, a color-electric vortex develops with color triplets at the two ends.

We have seen that three different reactions with different initial states have led to very similar intermediate states (stretched color-electric vortex) before decaying into the final state. This observation may serve as an explanation for the experimental fact that the three reactions have very similar multi-particle distributions in the hadronic final states.

Fragmentation in the bag model

For the sake of definiteness, we shall describe first the decay of the elongated intermediate bag of the e^+e^- annihilation process.

From Gauss's theorem the effective color-electric field strength inside the vortex is

$$E = \sqrt{\tfrac{4}{3}} g / R^2 \pi, \tag{9.1}$$

where R stands for the radius, and g is the fundamental quark–gluon coupling. The factor $\sqrt{\frac{4}{3}}$ in (9.1) comes from the triplet representation of color at the two ends.

Since the bag surface is classical throughout this section, we shall apply vacuum pressure for confinement to stay close to the original work of Low. The conclusions remain the same with surface tension.

The energy of a vortex of length L is

$$\epsilon = \tfrac{1}{2} E^2 R^2 \pi \cdot L + B R^2 \pi L,$$

where the second term comes from the volume energy. From the minimum of ϵ for a given L, we find the radius

$$R^4 = \tfrac{2}{3} g^2 / \pi^2 B,$$

and

$$\epsilon = \sqrt{\tfrac{8}{3} g^2 B} \cdot L.$$

When the vortex tube is long enough, a new $q\bar{q}$-pair may be created inside. Pair creation may occur through tunneling. For the balance of energy it is necessary that

$$\epsilon \geqslant 2m,$$

where m is the minimum quark energy allowed by the momentum uncertainty due to the transverse dimension R:

$$m \sim \pi / R \sim 1 \text{ GeV}.$$

Since the flux lines become abrupted between the newly created q and $\bar{q}$, the bag may break there producing two colorless objects. The newly born and longitudinally excited objects are similar to the elongated intermediate bag, so that they split again. After n splitting we get 2^n similar objects. The

decay continues until the longitudinal excitation of the new objects becomes comparable to their transverse excitation. These are not stable hadrons yet, though they decay into the final state as ordinary resonances (fireballs).

Let us consider the above process in the rapidity variable. Initially, the rapidity of the back-to-back $q\bar{q}$-pair is $-\ln 2p$ and $\ln 2p$, respectively:

The pair creation energy somewhat decreases the momentum of the quark and antiquark, from p to $p - m$. The rapidity, on the other hand, remains almost the same:

$$\ln 2(p - m) \approx \ln 2p - (m/p) \approx \ln 2p, \qquad \text{if } m \ll p.$$

In other words, if the quark and antiquark of the longitudinally excited bag are sufficiently separated in rapidity space ($\Delta y \geq 3$), then pair creation does not change their rapidity.

After splitting the bag, we find the following rapidity diagram:

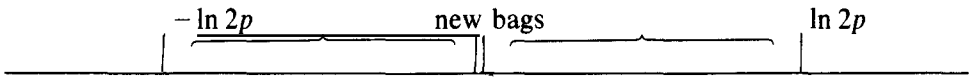

This simple picture already yields the important properties of fragmentation.

Indeed, the multiplicity of hadrons from the elongated bag is the same as the sum of hadron multiplicities of two newly created bags. The extension of bags in rapidity space is also additive,

$$\Delta y = \Delta y_1 + \Delta y_2,$$

so that the multiplicity is proportional to the length of the rapidity interval

$$n \sim \text{const} \cdot 2 \ln 2p,$$

or

$$n \sim c \cdot \ln s.$$

The above picture is valid, if the mass of the splitting bags is sufficiently large, $\sqrt{s} \geq 2$–3 GeV. Such a fireball may radiate about five pions on the average, therefore we may set the value of c at $c \sim 3$, in accordance with experiments.

The existence of the universal plateau and the fragmentation regions is a natural consequence of the model. Since the color-electric field is invariant under flavor SU(3), the flavor of the created pair in the middle of the expanding bag does not depend on the type of the originally incoming particles. Therefore, the rapidity space becomes populated uniformly by fireballs of 2–3 GeV, and only the ones at the end of the rapidity distribution remember the specific properties of the original quarks.

Fireballs from the interior of the rapidity distribution decay into the final particles of the universal plateau, whereas the two fireballs at the end of the rapidity distribution populate the fragmentation region of the target and projectile. It follows then that the width of a fragmentation region is the same as the extension of a fireball's decay products in rapidity space, $\Delta y \sim 2$.

At higher center of mass energy the only change is that the distance between the two fragmentation regions becomes larger, so that the distribution depends only on $y_{\max} - y$ and $y_{\min} - y$, respectively. In other words, Feynman's limiting fragmentation hypothesis is a natural consequence of the model.

The pomeron

The mechanism of multi-particle production is the same in e^+e^- collision as in, say, proton–proton scattering. The fragmentation regions are, of course, different.

In pp collision at least two $q\bar{q}$ pair must be created to neutralize the color octet content of the fragmenting parts. The central plateau develops in the above described manner, though its height may depend on the different pair creation in the middle, and the different strength of the color-electric field generated by the octet charges at the ends of the elongated bag.

If the length of the initial system before breakup is L_0 in the c.m. system in pp collision, then the corresponding time for which the combined system holds together is $\tau_0 \approx L_0$ since $v \sim c = 1$. In the lab system, the corresponding event happens at a time after collision

$$t_L = \tau_0/\sqrt{1 - v_L^2},$$

and distance from the collision point

$$x_L = v_0\tau_0/\sqrt{1 - v_L^2},$$

where $-v_L$ is the velocity of the transformation from the c.m. system to the laboratory system,

$$v_L = p_L/(m + E_L),$$

and

$$1/\sqrt{1 - v_L^2} \approx \sqrt{E_L/2m}.$$

At 300 GeV, for example, $1/\sqrt{1 - v_L^2} \sim 12$ so that the combined state holds together for a long time before breakup. This property may give a natural explanation for the Gottfried model of particle production in nuclei.

The exchange of a soft gluon in pp collision leads automatically to a constant cross section which is mainly inelastic due to color separation. Low estimates $\alpha_c \sim \frac{4}{3}$ for the quark–gluon coupling from the value of the total cross section, $\sigma_t^{pp} \sim 40$ mb. He also calculates an approximate Gaussian shape for the diffractive peak in elastic pp scattering.

A similar qualitative description may be developed for non-diffractive scattering processes where color separation occurs via quark–antiquark annihilation [7.7].

9.2. Deep inelastic scattering

Deep inelastic scattering has suggested point-like quark constituents inside the nucleon. Considered from a reference frame with infinite momentum the nucleon can be envisaged as an assemble of quark partons sharing the nucleon's momentum and almost free. This picture is to be contrasted with the indications that hadrons are impossible to break into their constituents.

It seems natural to believe that the quark bag model comprises these aspects of deep inelastic scattering processes. Actually these requirements were basic in motivating the MIT bag model.

Inside the bag the quark fields are coupled to the non-Abelian gluon fields with a coupling constant which is assumed to be small. So apart from a region close to the boundary the quarks are moving relatively freely and it is natural to assume that a highly virtual photon will see a free field short distance structure.

Unfortunately our present knowledge is not very far from these qualitative arguments. The problem is extremely interesting but difficult. The virtual photon kicks the quark into a highly excited

state with large angular momentum, where the surface is centered about a strongly deformed shape. In configuration space large distances are involved before the asymptotic state of all produced hadrons is reached. There is a quark parton propagation over a distance $\sim \omega/M \approx 0.2\,\omega$ fermi ($\omega = 1/\xi = 2M\nu/(-q^2)$), leading to the qualitative picture of a color electric vortex discussed previously. For a better understanding it is basically important to get a closer insight into the surface dynamics, to handle the motion of highly deformed shapes and so on.

To get a first insight Jaffe has approached this problem in the spherical cavity approximation. Here the quantum modes of the cavity are populated with colored quarks, and the forward Compton scattering amplitude is calculated.

Of course, if the average quark propagation distance is larger than the bag radius R, the picture does not make sense. So we must restrict ourselves to the region

$$\omega \ll R/0.2 \leqslant 10.$$

Not only the hadron, but the currents and so the propagator are also built up from the eigen-modes of the spherical cavity. They usually do not satisfy the non-linear boundary condition, so there is no momentum conservation in this approximation. What we essentially have here is a potential picture: there is a nailed down spherical box with an infinitely high potential wall.

To keep the formulae transparent, consider the $1+1$ dimensional case. In order to get scaling in $1+1$ dimension we shall study the scattering of virtual scalar mesons coupled to the quarks via the scalar current

$$J^i(x,t) = \sum_a \bar{q}_a(x,t)\tfrac{1}{2}\lambda_i q_a(x,t),$$

where $q(x,t)$ is the quark field confined to the static bag of length $2l$ centered at the origin, $a = 1, 2, 3$ is the color index, the matrices $\frac{1}{2}\lambda_i$ act in the flavor space.

The graphs contributing in lowest order to the imaginary part of the forward Compton amplitude are given in fig. 9.3. The wall of the cavity could absorb momentum and so the last two graphs persist even for $q^2 < 0$. Jaffe has discarded the contribution of the cavity vacuum bubbles (last graph) on the ground that they require a better understanding of the vacuum state which is beyond the scope of the approximation. If we take the potential picture seriously, the last graph is there and describes the physical process of a pair creation in an external field.

The quark fields can be expanded in terms of the cavity eigenfunctions satisfying the linear boundary conditions eq. (4.1):

$$q_\alpha(x,t) = \frac{1}{2\sqrt{l}} \sum_{n \geqslant 0} b_\alpha(n) \begin{pmatrix} \exp\{-in'\pi(t-x)/2l\} \\ (-1)^n \exp\{-in'\pi(t+x)/2l\} \end{pmatrix} + d_\alpha^+(n) \begin{pmatrix} \exp\{in'\pi(t-x)/2l\} \\ (-1)^n \exp\{in'\pi(t+x)/2l\} \end{pmatrix},$$

where $n' = n + \frac{1}{2}$ and α is a shorthand notation for all the necessary indices. The operators b_α and d_α obey canonical anticommutation relations

$$\{b_\alpha(n_1), b_\alpha^+(n_2)\}_+ = \{d_\alpha(n_1), d_\alpha^+(n_2)\}_+ = \delta_{\alpha\alpha'}\delta_{n_1 n_2}.$$

Fig. 9.3. The diagrams of the virtual forward Compton scattering amplitude in the bag model.

The bag as a nailed down line segment is not translationally invariant and accordingly the structure functions are defined as

$$W^{ij} = \frac{M}{2\pi} \int_{-\infty}^{\infty} \mathrm{d}t \int_{-l}^{l} \mathrm{d}x_1 \int_{-l}^{l} \mathrm{d}x_2 \exp\{\mathrm{i}q^0 t - \mathrm{i}q^1(x_1 - x_2)\}\langle \mathrm{T}|[J^i(x_1, t), J^j(x_2, 0)]|\mathrm{T}\rangle,$$

where M is the mass of the state $|\mathrm{T}\rangle$.

The current commutator can be expressed in terms of the anticommutator $S_{\mathrm{cav}}(x_1, x_2, t)$ of the quark fields:

$$[J_i(x_1, t), J_j(x_2, t)] = \sum_a \bar{q}_a(x_1, t)\tfrac{1}{2}\lambda_i S_{\mathrm{cav}}(x_1, x_2, t)\tfrac{1}{2}\lambda_j q_a(x_2, 0) - \bar{q}_a(x_2, 0)\tfrac{1}{2}\lambda_j S_{\mathrm{cav}}(x_2, x_1, -t)\tfrac{1}{2}\lambda_i q_a(x_1, t).$$

$S_{\mathrm{cav}}(x_1, x_2, t)$ is given by

$$S_{\mathrm{cav}}(x_1, x_2, t) \equiv \{q(x_1, t), \bar{q}(x_2, 0)\}$$
$$= \frac{1}{4l} \sum_n \begin{bmatrix} (-1)^n \exp\{-\mathrm{i}n'\pi(t - x_1 - x_2)/2l\} & \exp\{-\mathrm{i}n'\pi(t - x_1 + x_2)/2l\} \\ \exp\{-\mathrm{i}n'\pi(t + x_1 - x_2)/2l\} & (-1)^n \exp\{-\mathrm{i}n'\pi(t + x_1 + x_2)/2l\} \end{bmatrix}.$$

Using these ingredients the Bjorken limit of the structure functions can be evaluated. Due to the permanent confinement the quark spectrum is discrete and correspondingly the structure function is a sum of terms proportional to delta functions enforcing energy conservation.

The smeared structure function $\bar{W}$ is defined by averaging W over a Gaussian

$$\bar{W}(\bar{q}^0, \xi) = \int \frac{\mathrm{d}q^0}{\Delta\sqrt{\pi}} \exp\{-(q^0 - \bar{q}^0)^2/\Delta^2\} W(q^0, \xi),$$

and is given by the expression:

$$\lim_{B_j} \bar{W}^{ij}(\xi, \bar{q}^0) = \bar{F}^{ij}(\xi) = \frac{Ml}{2\pi} \sum_{a,m} \left\{ \frac{\sin^2 \pi(m + \frac{1}{2} - (Ml/\pi)\xi)}{\pi^2(m + \frac{1}{2} - (Ml/\pi)\xi)^2} \langle \mathrm{T}|b_a^+(m)\tfrac{1}{2}\lambda_i \tfrac{1}{2}\lambda_j b_a(m)|\mathrm{T}\rangle \right.$$
$$\left. - \frac{\sin^2 \pi(m + \frac{1}{2} + (Ml/\pi)\xi)}{\pi^2(m + \frac{1}{2} + (Ml/\pi)\xi)^2} \langle \mathrm{T}|b_a^+(m)\tfrac{1}{2}\lambda_j \tfrac{1}{2}\lambda_i b_a(m)|\mathrm{T}\rangle \right\}. \tag{9.2}$$

Equation (9.2) displays Bjorken scaling and crossing explicitly.

The lack of momentum conservation is reflected in the structure functions being non-zero for $\xi > 1$. The second term occurs with a negative sign which causes $F^{ij}(\xi)$ to be negative for certain choices of the indices i, j, in violation of the positivity restrictions on $F^{ij}(\xi)$. This defect is due to the negligence of the vacuum bubbles.

A similar calculation can be repeated in $3+1$ dimension. As Jaffe and Patrascioiu have shown the cavity propagator can be replaced by a free field propagator in the Bjorken limit. Exact scaling is obtained, W_1, νW_2 and $\nu W_L/M^2$ depend only on ξ. There is a parton interpretation and different sum rules can be written down explicitly. However it is difficult to judge on the approximations and we think the question of scaling and related problems are open in the bag model.

Just as the original MIT bag model was motivated by the requirements of deep inelastic scattering phenomena, the introduction of surface tension was partly motivated by an apparent puzzle there: there is about fifty percent missing momentum of the nucleon's parton momentum spectrum. There

must be some component within the nucleon not taking part in electromagnetic and weak interactions, which carries a large part of the nucleon's total momentum.

If the missing momentum is associated with colored gluon fields, they must be fairly strong fields somehow and many pairs are expected from vacuum polarization. Those pairs are just not there, at least not in the momentum region $0.1 < \xi < 1$ where ξ is the parton momentum with the nucleon's momentum chosen to be unity.

It is suggestive that the quark gluon coupling constant is fairly weak so that there is little vacuum polarization present in the ground state wave function of the nucleon. If that implies that gluons carry little momentum in parton language, a large fraction of it must be carried by as yet unidentified component of the nucleon.

The volume term in the stress tensor is purely diagonal ($g^{\mu\nu}B$) in any frame and never carries momentum. A significant part of the fast moving nucleon's momentum may be carried by the membranous surface however, and the puzzle may have a trivial solution in this model.

10. Conclusion

The quark bag model as a clever phenomenological device to the hadron structure is the invention of a theoretical group at the Massachusetts Institute of Technology. The pioneers and the authors of the first two papers on the model [1.1, 1.2] are A. Chodos, R.L. Jaffe, K. Johnson, C.B. Thorn and V.F. Weisskopf. In later investigations T. De Grand, C. DeTar, J. Kiskis, C. Rebbi, and D. Shalloway also made a useful impression on our way of thinking about the model.

The physical picture of the bag model is associated with a two-phase description of the physical vacuum which in "normal" phase outside hadrons cannot support the propagation of quark and gluon fields. By concentration of energy, a small domain of a new phase (hadron phase) may be created in the medium of the physical vacuum inside which quark and gluon fields can propagate in the ordinary manner. This is the bag.

There is now a vague hope that a similar picture might emerge from the detailed study of the vacuum structure in quantum chromodynamics [1.27]. We find it unlikely that in developing a phenomenological model from the detailed microscopic calculations, volume energy will play a distinguished role in comparison with surface energy when a bubble is created in the "wrong" phase. We have treated both binding terms on an equal footing in our report.

With due credit to the original work of the M.I.T. group who have introduced volume energy (or vacuum pressure) to bind quarks and gluons inside hadrons, we find slightly advantageous to keep the surface energy for later dynamical calculations. We do not want to overemphasize the possible significance of the latter term and only more refined calculations and results will decide whether it really should be kept.

The applications of the quark bag model are very stimulating, though far from complete or convincing. Even if the description of light mesons and baryons turns out to be successful, the model faces its fate in predicting an enormously rich spectrum of excitations. In our opinion real hard work is necessary in the coming years to sharpen the reliability of these predictions and confront them with the experimental situation.

The model predicts relatively narrow exotic states in high angular momentum states (baryonium) and all-glue hadron states. Both are qualitative predictions subject to future experimental tests. It remains a remote though extremely interesting possibility to explore the possible astrophysical

consequences of the formation of a quark phase of matter in neutron stars, or self-supporting quark stars. The bag model proved to be very helpful in the first preliminary investigations of this phase transition from baryon matter to quark matter.

Obviously there are two important tasks of high priority in the near future. The first one is to finish the job of the cavity approximation by a systematic treatment of the confined gluon propagator in perturbative manner and calculating the spectrum with a quantum mechanically blurred surface. Secondly, and not completely independently, there is an urgent need for developing systematic methods for calculating departures from the spherical approximation in large angular momentum states.

In the meantime it would be very interesting to derive a bag-like structure from the microscopic investigation of the physical vacuum in quantum chromodynamics.

Acknowledgements

We are indebted to our colleagues of the Particle Theory Group in Budapest for very useful discussions and interesting conversations.

References

For some introductory papers on the quark bag model with pure volume tension, see

[1.1] A. Chodos, R.L. Jaffe, K. Johnson, C.B. Thorn and V.F. Weisskopf, Phys. Rev. D9 (1974) 3471.
[1.2] A. Chodos, R.L. Jaffe, K. Johnson and C.B. Thorn, Phys. Rev. D10 (1974) 2599.
[1.3] T. DeGrand, R.L. Jaffe, K. Johnson and J. Kiskis, Phys. Rev. D12 (1975) 2060.
[1.4] K. Johnson, Acta Phys. Polonica B6 (1975) 865.
[1.5] V.F. Weisskopf, CERN-Th 2068 (1975).
[1.6] K. Johnson, Lectures presented at Scottish Universities Summer School, August 1976, St. Andrews, Scotland.

For the discussion of surface dynamics, see

[1.7] P. Gnädig, P. Hasenfratz, J. Kuti and A.S. Szalay, Proc. of the Neutrino 75 IUPAP Conference, Vol. 2 (1975) p. 251.
[1.8] P. Gnädig, P. Hasenfratz, J. Kuti and A.S. Szalay, Phys. Letters 64B (1976) 62.
[1.9] J. Kuti, Mini-rapporteur talk in: Proc. XVIII. Intern. Conf. on High Energy Physics, Tbilisi, Vol. 1 (1976) C101;
P. Gnädig, P. Hasenfratz, J. Kuti and A. S. Szalay, paper 994, submitted to the XVIII. Intern. Conf. on High Energy Physics, Tbilisi, July 1976.
[1.10] P.A. Collins and R.W. Tucker, Nucl. Phys. B112 (1976) 150.

Soft bags in field theory are discussed in

[1.11] G.'t Hooft. CERN preprint (1974).
[1.12] J. Kogut and L. Susskind, Phys. Rev. D9 (1974) 3501.
[1.13] M. Creutz and K.S. Soh, Phys. Rev. D12 (1975) 443;
P. Vinciarelli, Lectures given at the XV. Intern. Universitätswochen für Kernphysik, Schladming, February 1976.

For an introduction to the SLAC bag model, see

[1.14] W.A. Bardeen, M.S. Chanowitz, S.D. Drell, M. Weinstein and T.M. Yan, Phys. Rev. D11 (1975) 1094.
[1.15] R.C. Giles, Phys. Rev. D13 (1976) 1670.

The confinement of magnetic charges through magnetic vortices is discussed in

[1.16] H.B. Nielsen and P. Olesen, Nucl. Phys. B61 (1973) 45.
[1.17] Y. Nambu, Phys. Rev. D10 (1974) 4262.
[1.18] G. Parisi, Phys. Rev. D11 (1975) 970;
A. Patkós, Nucl. Phys. B97 (1975) 352.

For some pioneering papers on quantum chromodynamics, see
[1.19] H. Fritzsch and M. Gell-Mann, Proc. XVI Intern. Conf. On High Energy Physics, Chicago 1972, Vol. 2.
[1.20] H. Fritzsch, M. Gell-Mann and H. Leutwyler, Phys. Letters 47B (1973) 365.
[1.21] D. Gross and F. Wilczek, Phys. Rev. Letters 30 (1973) 1343.
[1.22] H.D. Politzer, Phys. Rev. Letters 30 (1973) 1346.
[1.23] G.'t Hooft, Marseille Conf. on Renormalization, June 1972, unpublished comments.
[1.24] K.G. Wilson, Phys. Reports 23C (1976) 331.

The vacuum structure of gauge theories and instantons are discussed in
[1.25] A. Polyakov, Phys. Letters 59B (1975) 82.
[1.26] A. Belavin, A. Polyakov, A. Schwartz and Y. Tyupkin, Phys. Letters 59B (1975) 85.
[1.27] C.G. Callan Jr., R.F. Dashen and D.J. Gross, Phys. Letters 63B (1976) 334; 66B (1977) 375.
[1.28] G.'t Hooft, Phys. Rev. Letters 37 (1976) 8.
[1.29] A. Polyakov, Nordita Pub. 76/33, Nucl. Phys. B120 (1977) 429.

For collective and single particle phenomena in nuclear physics, see
[1.30] J. Rainwater, Phys. Rev. 79 (1951) 432.
[1.31] A. Bohr, Kgl. Danske Videnskab. Selskab Mat.-Fys. Medd. 26, no. 14 (1951).
[1.32] J.M. Eisenberg and W. Greiner, Nuclear Theory, Vol. 1 (North-Holland Publ. Co. 1970).

[2.1] P.A.M. Dirac, Proc. Roy. Soc. 268A (1962) 57.

For the discussion of a relativistic membrane, see
[2.2] References [1.7–1.10] on surface dynamics.
[2.3] The instability of Dirac's extended electron was recognized by P. Gnädig and Z. Kunszt. We are indebted to them for using their unpublished results;
P. Grädig, Z. Kunszt, P. Hasenfratz and J. Kuti, KFKI preprint 78/1 (1978).

For references for sections 3 and 4, see references [1.1–1.32].

For an excellent introduction to the Hamiltonian formulation of singular Lagrangian systems, see
[5.1] P.A.M. Dirac, Lectures on Quantum Mechanics, Belfer Graduate School of Science, Yeshiva University 1964.

For the quantization of the bag model with pure volume tension, see
[5.2] D. Shalloway, Phys. Rev. D11 (1975) 3545.
[5.3] D. Shalloway, Phys. Rev. D14 (1976) 1032.
[5.4] C. Rebbi, Phys. Rev. D12 (1975) 2407.
[5.5] C. Rebbi, Phys. Rev. D14 (1976) 2362.
[5.6] K. Johnson [1.6].

For the quantization of the bag model with surface tension, see
[5.7] References [1.7–1.10].

For references in the early calculation of the charmonium spectrum in the spirit of the adiabatic approximation, see
[6.1] T. Appelquist, A. De Rujula, H.D. Politzer and S. L. Glashow, Phys. Rev. Letters 34 (1975) 365.
[6.2] E. Eichten, K. Gottfried, T. Kinoshita, J. Kogut, K.D. Lane and T.M. Yan, Phys. Rev. Letters 34 (1975) 369.
[6.3] J. Kogut and L. Susskind, Phys. Rev. Letters 34 (1975) 767.
[6.4] P. Hasenfratz, J. Kuti and A.S. Szalay, Proc. Xth Rencontre de Moriond, Meribel, March 1975, Vol. 2, p. 209.

For the adiabatic approximation of the nucleon's bag model, see
[6.5] Reference [1.2].
[6.6] Several years ago P.N. Bogoliubov, Ann. Inst. Henri Poincaré 8 (1967) 163 developed a quark model with the quark bound in an infinite, scalar "square-well" potential.

On the Casimir effect:
[6.7] H.B.G. Casimir, Koninkl. Ned. Akad. Wetenschap, Proc. 51 (1948) 793.
[6.8] T.H. Boyer, Ann. of Physics (New York) 56 (1970) 474.
[6.9] R. Balian and C. Bloch, Ann. of Physics (New York) 60 (1970) 401; 64 (1971) 271.
[6.10] C.M. Bender and P. Hays, M.I.T. CTP preprint #554 (1976).

For quark orbitals in the bag model with quarks of non-vanishing mass, see
[7.1] E. Golowich, Phys. Rev. D12 (1975) 2108.
[7.2] T. Barnes, Nucl. Phys. B96 (1975) 353.

For the calculation of the light hadron spectrum, see
[7.3] Reference [1.3].

The electromagnetic self-energy of confined massless quarks is discussed in
[7.4] A. Chodos and C.B. Thorn, Phys. Letters 53B (1974) 359; Nucl. Phys. B104 (1976) 21.

For the calculation of the charmonium spectrum and the charmonium molecule in the string limit, see
[7.5] References [1.7–1.9.]

Calculation of the hadronic deformations in the bag model is found in
[7.6] C. DeTar, M.I.T. CTP preprint # 546 (1976).

The string-like excitations of light hadrons are discussed in
[7.7] K. Johnson and C.B. Thorn, Phys. Rev. D13 (1976) 1934.
[7.8] T. Eguchi, Phys. Lett. 59B (1975) 475.

For some recent papers on all-glue hadrons, see
[7.9] P.G.O. Freund and Y. Nambu, Phys. Rev. Letters 34 (1975) 1645.
[7.10] J.F. Willemsen, Phys. Rev. D13 (1976) 1327.
[7.11] D. Robson, Phys. Letters 66B (1977) 267.

For the discussion of low-lying exotic states in the bag model, see
[8.1] R.L. Jaffe and K. Johnson, Phys. Lett. 60B (1976) 201.
[8.2] R.L. Jaffe, Phys. Rev. D15 (1977) 267; D15 (1977) 281.

The baryonium states are discussed in
[8.3] G.F. Chew, LBL-5291 preprint (1976).

A partial list of references on the possible existence of a quark phase inside neutron stars, or on the formation of a quark star is:
[8.4] J.C. Collins and M.J. Perry, Phys. Rev. Letters 34 (1975) 1353.
[8.5] J.R. Ipser, M.B. Kislinger and P.D. Morley, University of Chicago preprint EFI-75-38 (1975).
[8.6] G. Chapline and M. Nauenberg, University of California (Santa Cruz) preprint (1976).
[8.7] K. Brecher and G. Caporaso, Nature 259 (1976) 377.
[8.8] B.D. Keister and L.S. Kisslinger, Phys. Letters 64B (1976) 117.

For the corresponding nuclear matter calculations, see
[8.9] H.A. Bethe and M.B. Johnson, Nucl. Phys. A230 (1974) 1.
[8.10] R.C. Malone, M.B. Johnson and H.A. Bethe, Astrophys. Journal 199 (1975) 741.
[8.11] V.R. Pandharipande and R. A. Smith, Nucl. Phys. A237 (1975) 507.

For the pomeron model, see
[9.1] F.E. Low, Phys. Rev. D12 (1975) 163.
[9.2] S. Nussinov, Phys. Rev. Letters 34 (1975) 1286.

For a discussion on non-diffractive scattering amplitudes in the bag model, see
[9.3] C.B. Thorn and M.V.K. Ulehla, Phys. Rev. D11 (1975) 3531.
[9.4] Reference [7.7].
[9.5] T.T. Wu, B. McCoy and H. Cheng, Phys. Rev. D9 (1974) 3495.

Deep inelastic processes in the bag model are discussed in
[9.6] R.L. Jaffe, Phys. Rev. D11 (1975) 1953.
[9.7] R.L. Jaffe and A. Patrascioiu, Phys. Rev. D12 (1975) 1314.